Journal
of
The Franklin Institute

EDITOR, HENRY BUTLER ALLEN, MET.E., D.SC.
ASSISTANT EDITOR, JOHN FRAZER, PH.D.

Associate Editors:

WILDER D. BANCROFT, PH.D. — A. S. EVE, F.R.S. — HENRY C. SHERMAN, SC.D.
C. B. BAZZONI, PH.D. — PAUL D. FOOTE, PH.D. — W. F. G. SWANN, D.SC.
E. G. COKER, F.R.S. — W. J. HUMPHREYS, PH.D. — HUGH S. TAYLOR, D.SC.
ARTHUR L. DAY, SC.D. — C. E. K. MEES, D.SC. — A. F. ZAHM, PH.D.
R. EKSERGIAN, PH.D. — WILLIAM B. MELDRUM, PH.D. — JOHN ZELENY, PH.D.

Committee on Publications:

G. H. CLAMER, CHAIRMAN — LIONEL F. LEVY — HIRAM S. LUKENS
RICHARD HOWSON — MALCOLM LLOYD, JR. — RICHARD H. OPPERMAN N
C. L. JORDAN — WINTHROP R. WRIGHT

Vol. 236 **JULY, 1943** **No. 1**

CONTENTS

The Variation of Mesotron Intensity with Altitude and Latitude, Together with Allied Phenomena, and the Bearing of These Matters on the Nature of the Primary Particles ..... W. F. G. SWANN 1

On the Absorption of the Hard Component of the Cosmic Radiation .... M. E. ROSE 9

A Quantitative Evaluation of the Influence of the Lithosphere on the Anomalies of Gravity ..... ROSS GUNN 47

The Horizontal Path along the Earth's Surface of a Projectile or Plane under Constant Tangential Acceleration ..... W. S. KIMBALL 67

Notes from the National Bureau of Standards 81

The Franklin Institute Notes 87

Notes from the Bartol Research Foundation 96

Notes from the Biochemical Research Foundation 99

Book Reviews 101

Publications Received 106

Current Topics 8, 46, 66, 80, 107

Published by

THE FRANKLIN INSTITUTE OF THE STATE OF PENNSYLVANIA
Prince and Lemon Streets, Lancaster, Penna., and
Benjamin Franklin Parkway at Twentieth St., Philadelphia, Penna.

SIX DOLLARS PER YEAR (Foreign Postage Additional) **SINGLE NUMBERS, SIXTY CENTS**

Indexes to the semi-annual volumes of the JOURNAL are published with the June and December numbers. The contents are also indexed in *The Industrial Arts Index.*

★ ★ ★

The Harvard Books on Astronomy

Edited by Harlow Shapley and Bart J. Bok
Harvard College Observatory

GOLDBERG & ALLER—Atoms, Stars and Nebulae

This, the latest, volume in the Harvard Series on Astronomy gives the reader a thrill of discovery as he probes into the seething atmosphere of the stars and even digs into their interiors. It discusses single stars, double stars, multiple, dwarf and giant stars, cool and hot stars, stars that pulsate, and some whose surface layers are suddenly wrenched away in cataclysmic stellar explosions. There is a fascinating discussion of stellar rainbows, atoms and molecules.

By Leo Goldberg, McMath-Hulbert Observatory, University of Michigan, and Lawrence H. Aller, Harvard College Observatory.

150 Illus. 323 Pages. $2.50 (1943)

BOK & BOK—The Milky Way

This book presents for the first time in semi-popular form, a summary of our present knowledge of the Milky Way and explains some of the problems which remain to be solved. The dust and gas in the vast spaces between the stars, the compositions and dimensions of star clusters, the appearance of our galaxy to an observer in the Andromeda nebula, and the problems related to the past and future of our galaxy are discussed.

By Bart J. Bok and Priscilla F. Bok, Harvard College Observatory.

96 Illus. 204 Pages. $2.50 (1941)

WATSON—Between the Planets

In summarizing our knowledge of comets, meteors, asteroids and meteorites, this book includes a description of the latest discoveries and considers the multitude of vexing problems yet unexplained. Interrelationships between several varieties of bodies are stressed and the ways in which they might have been formed are discussed critically in relation to the formation of the planetary system.

By Fletcher G. Watson, Harvard College Observatory.

106 Illus. 222 Pages. $2.50 (1941)

WHIPPLE—Earth, Moon and Planets

A concise, well illustrated account of the planets, their atmospheres with a discussion of the possibilities of life outside the earth is presented in non-technical language. The reader is carried in his imagination below the clouds on Venus, Mars and the giant red planets, into the depths of the Earth and to the rough and airless surfaces on the Moon, Mercury and Pluto. Particular attention is given to the study of the origin of lunar craters and the evolution of the planets. A Planet Finder and Star Chart is included.

By Fred L. Whipple, Harvard College Observatory.

140 Illus. 293 Pages. $2.50 (1941)

CAMPBELL & JACCHIA—The Story of Variable Stars

This book introduces the reader to the technique of observation and then proceeds to analyze the present state of our knowledge of variable stars. Among the types of variable stars discussed are the explosive star or Nova, the giant red variables, erratic stars and eclipsing stars. The principles of spectroscopy and a few technical aspects of variable star astronomy are explained in the appendix. A list of brighter variables, a Julian calendar, and other useful tables are included.

By Leon Campbell and Luigi Jacchia, Harvard College Observatory.

82 Illus. 226 Pages. $2.50 (1941)

THE BLAKISTON COMPANY, Philadelphia

PROFILE OF GENIUS

POOR RICHARD PAMPHLETS

A SERIES OF NINE BROCHURES CONTAINING SELECTIONS FROM THE WRITINGS OF BENJAMIN FRANKLIN

compiled and edited by

Nathan G. Goodman

with introductions by

Nicholas Murray Butler, Thomas S. Gates, Carter Glass, George Wharton Pepper, Charles Franklin Kettering, William Allen White, Roland S. Morris, Douglas Southall Freeman, and John R. Mott

TITLES

I Life of Benjamin Franklin, Year by Year—1706–1790

II Benjamin Franklin on Honesty

III The Way to Wealth, and Words of Wisdom from Benjamin Franklin's "Poor Richard's Almanack"

IV Benjamin Franklin on Peace

V The Practical Dr. Franklin

VI Benjamin Franklin on Industry, Frugality, and Thrift

VII Benjamin Franklin on Citizenship

VIII Benjamin Franklin on the Art of Virtue

IX Benjamin Franklin on Religion

A complete set in an attractive slip case $2.25, postpaid

Individual pamphlets 25c, postpaid

Make checks payable to The Franklin Institute

Benjamin Franklin Parkway at 20th Street

Philadelphia

YARWAY RESEARCH

SOME YEARS AGO Yarway added to its facilities a completely equipped steam laboratory employing one of the highest pressure (2500 psi) water line boilers ever built. This was in line with the Yarway policy of keeping pace with the times, of constantly forging ahead with new developments in anticipation of mounting pressures and temperatures, of meeting every new and more strenuous service requirement with tried and proved equipment.

This laboratory serves as a proving ground for testing of Yarway products under conditions duplicating actual service requirements. In addition it has provided means for invaluable research and further improvement of existing Yarway equipment.

YARNALL-WARING COMPANY

131 MERMAID STREET PHILADELPHIA, PA.

•

Blow-Off Valves • Water Columns & Gages • Expansion Joints • Steam Traps • Strainers • Spray Nozzles

"MEGGER"
TRADE MARK REGISTERED U S PAT OFF.

ELECTRICAL TESTING INSTRUMENTS

- "Megger" Insulation Testers
- "Megger" Ground Testers
- "Megger" Direct-Reading Ohmmeters

ALSO

- "Frahm" Vibrating-Reed Tachometers
- "Frahm" Vibrating-Reed Frequency Meters
- Jones Indicating Hand Tachometers
- Jagabi "Lubri-tact" Laboratory Rheostats

Send for Literature

JAMES G. BIDDLE CO.

1211-13 ARCH ST. • PHILADELPHIA, PA.

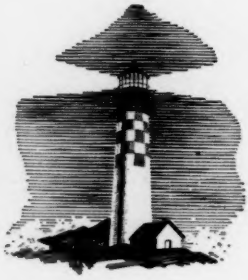

PROTECTION is usually the result of careful planning. We built our vaults on solid rock—with massive walls of steel and concrete—with the latest protective devices. A safe deposit box within them will cost you little.

WE INVITE YOUR INSPECTION

FIDELITY-PHILADELPHIA TRUST COMPANY

135 SO. BROAD STREET

Journal
of
The Franklin Institute
Devoted to Science and the Mechanic Arts

Vol. 236 **JULY, 1943** **No. 1**

THE VARIATION OF MESOTRON INTENSITY [1] WITH ALTITUDE AND LATITUDE, TOGETHER WITH ALLIED PHENOMENA, AND THE BEARING OF THESE MATTERS ON THE NATURE OF THE PRIMARY PARTICLES.

BY

W. F. G. SWANN,

Director, Bartol Research Foundation of The Franklin Institute, Swarthmore, Pa.

PART I.

1. For convenience of publication, and limitation of space, the present paper is divided into two parts, the second of which will be published in the following issue. Part I will contain a statement of the problem, an outline of the procedure, and a summary of the conclusions. For convenience in correlating the two parts, an outline of the individual sections of Part II will be given in the present Part I.

In several former communications [2] the writer has had occasion to invoke the assumption of an incoming heavy

[1] Several of the results established in this paper have been given by the writer in condensed form in former publications. Part II of the present paper is devoted in part to the detailed proof of some of the formulæ formerly cited.

[2] W. F. G. Swann, *Phys. Rev.*, **56**, 209 (1939); *Rev. Mod. Phys.*, **11**, 242 (1939) (see in particular pp. 251–254). *Phys. Rev.*, **58**, 200 (1940). JOUR. FRANK. INST., **226**, 757 (1938). (See, in particular, pp. 780 and 792.) *Phys. Rev.*, **63**, 210 (1943).

(Note—The Franklin Institute is not responsible for the statements and opinions advanced by contributors in the JOURNAL.)

particle which, on collision with the atoms of the air, breaks up into smaller particles, now regarded as mesotrons, which mesotrons travel through the atmosphere and finally disappear, either by completing their range through loss by ionization or by more sudden disappearance resulting from the finite extent of the mesotron life.

The mesotrons give birth to electrons either by knock-on processes closely related to ionization or during their disintegration, in which each mesotron that dies gives birth to an electron and a neutrino. The writer has, moreover, given reasons for supposing that the aforesaid processes are the only processes which are responsible for the appearance of electrons in the atmosphere, and that the direct contribution of outer space to the electron intensity is negligible.

2. If we consider a spectral distribution of energies for the mesotrons produced at any altitude, the mesotrons of different energies will die at different rates on account of the fact that the mean life τ is given by

$$\tau = \tau_o/(1 - \beta^2)^{1/2}, \qquad (1)$$

where τ_o is the mean life for a stationary mesotron, and $\beta = v/c$. Here v is the mesotron velocity and c is the velocity of light. Thus the spectral distribution will change with depth of penetration into the atmosphere; and the matter is further complicated by the fact that on account of energy loss by ionization, even the mean life of a mesotron will change as it progresses through the atmosphere.[3]

3. We shall take all of the foregoing considerations into account [4] and in Part II, Section I, we shall consider the

[3] The term "mean life," as applied to a mean life which is changing, presents an apparent confusion of terms, which confusion is only temporary, however. It is always possible to write for the number of mesotrons n_e in a beam of mesotrons of energy e,

$$-\frac{dn_e}{dt} = \frac{1}{\tau_e} n_e,$$

and this equation may be taken to define the "instantaneous mean life" for the energy e.

[4] However, we shall consider the ionization loss per unit of path at constant pressure to be independent of the energy of the mesotrons. Following the development of the formula deduced in Part II, Section I, for the variation of intensity with altitude, Dr. M. E. Rose carried out the corresponding calculations using the Bethe-Bloch expression for the energy loss. Dr. Rose's paper,

problem of the vertical mesotron intensity at an altitude h above sea-level [5] resulting from production of mesotrons with energy distribution defined by the function $F(E)dE$ for the range dE, the mesotrons being produced at an altitude where the density is $\rho_o D_a$, where D_a is the sea-level density.[6] It will be shown that the aforesaid vertical intensity is obtained by integrating with respect to E the expression

$$(\Delta n)_h = \left\{\left[1 + \left\{\frac{G_o - G_h}{\gamma + 1}\right\}\right]^{[\lambda c\tau_o(\gamma+1+G_o)]^{-1}}\right\} \times \{e^{-x_o/c\tau_o(\gamma+1+G_o)} e^{h/c\tau_o(\gamma+1+G_o)} F(E)dE\} \quad (2)$$

where m_o is the rest mass of the mesotron, x_o is the altitude of production, λ is the constant defined by the atmospheric density formula $D_h = D_a \exp[-\lambda h]$, α is the ionization energy loss per centimeter of path at sea-level, and

$$G_o \equiv \alpha\rho_o/\lambda m_o c^2; \qquad G_h \equiv \alpha\rho_h/\lambda m_o c^2 \qquad \text{and} \qquad \gamma \equiv E/m_o c^2.$$

In integrating this equation over the range of E involved, we must observe that for any depth x below the altitude of production we are concerned only with values of E (at $x = 0$) greater than $\bar{E}_x$, the loss of energy over the range o to x. In other words, our lower limit of E is

$$E_m = \bar{E}_x = \frac{\alpha\rho_o}{\lambda}(e^{\lambda x} - 1) = \frac{\alpha}{\lambda}(\rho_x - \rho_o)$$

unless the earth's magnetic field, through its action on the primaries, has imposed a greater lower limit. Thus, if E_{MP} is the limit for entry of the primaries, and if the primaries split into N mesotrons under the condition that the mesotrons are born at rest in the system of axes in which the primary moved, then the lower limit of the kinetic energy for the mesotrons will be E_{MP}/N. Strictly speaking, it will be even lower than this by $(1/N)$ times the energy lost by the primary by ionization in

which is published in the present issue of the JOURNAL OF THE FRANKLIN INSTITUTE, covers in general a field of application different from that involved in the present paper.

[5] This altitude is supposed expressed in actual distance and not in water equivalent distance.

[6] The analytical equivalent of this formula was quoted by the writer, without proof, in *Phys. Rev.*, **60**, 470 (1941).

descending to the level of production. This correction would be negligible for altitudes of production sufficiently high to have significance in the present theory, particularly on account of the factor $(1/N)$ in the correction.

In Part II, Section I, we shall also deduce the formula for the spectral distribution at sea-level in terms of the spectral distribution at the level of production.

4. In Part II, Section II, we shall extend the formula of Section I to the case where there is an assigned rate of production of mesotrons at all altitudes.

5. In Part II, Section III, we shall revert to the formula deduced in Part II, Section I, with a view to seeing how far the facts may be invoked as a test of the hypothesis of mesotron production by the disintegration of heavy primaries. Our calculations will involve an assumption of the spectral distribution formula for the mesotrons, and we shall obtain this distribution by supposing that the mesotrons have a spectral distribution defined by an $F(E)$ proportional to $1/E^3$. Such a conclusion would result from the assumption that the true primaries are particles heavier than mesotrons,[7] with an inverse cube spectral distribution, and that on entering the atmosphere they split up into mesotrons in such fashion that the mesotrons born from any primary are *born at rest in the system of axes in which the primary was moving.* Indeed, this last assumption results, firstly, in the mesotrons perpetuating everywhere the direction of motion of the primary particles, and secondly, in the expression $K'dE/E^3$ applicable to the primaries being replaced by the expression $K'dE/N^2E^3$ for the mesotrons, where N is the number of mesotrons produced from a primary, and where the lower limit of the spectral distribution for the mesotrons is $1/N$ times the lower limit for the primaries. The value of $\beta(=v/c)$ for a mesotron produced as above is obviously the same as that for the parent primary.

[7] In addition to the citations from the present writer's former publications, the postulation of protons as primary particles has also been made by A. H. Compton and H. Bethe, *Nature*, **134**, 734 (1934), by A. H. Compton, *Rev. Sci. Instr.*, **7**, 71 (1936), by T. H. Johnson, *Phys. Rev.*, **45**, 569 (1934), and by M. Schein, W. P. Jesse and E. O. Wollan, *Phys. Rev.*, **59**, 615 (1941). In most of these cases the protons were regarded as responsible for only a part of the incoming radiation, electrons being invoked in addition.

6. As regards experimental data for the purposes of test, we have the observations of Schein, Jesse, and Wollan [8] on the variation of vertical mesotron intensity with altitude. Then we have a certain amount of data on the sea-level latitude effect. We shall endeavor to utilize this data to fix the unknown quantities, altitude of mesotron production and lower limit of energy and so of β in the mesotron spectral energy distribution. On the basis of the hypothesis of mesotron formation cited above, this value of β is also the lower limit of β for the primaries. Now the lower limit of the *momentum* of the primaries for vertical entry is known from the magnetic field data for any latitude, and so the mass of the primary becomes determined. It turns out that, within the limits of accuracy of the experimental data, the primary may be taken as a proton, or at least that the primaries responsible for the mesotrons observed from sea-level up to semi-high altitudes (Pike's Peak, for example) are protons.

7. In Part II, Section III, we shall also make a comparison of the experimental data for the spectral energy distribution at sea-level and at magnetic latitude 50°, with the results predicted by the theoretical formula deduced in Section I, using for that purpose the altitude of production assigned by the considerations cited above. It may be remarked that the lower limit for β does not become involved in these calculations since mesotrons with that lower limit could not reach down to sea-level.

8. In Part II, Section IV, we consider a matter in a category to some extent different from those discussed in Sections I–III. It concerns the angular distribution of the electrons emitted by the mesotrons at death. In the system of axes which travels with a moving mesotron, the electrons are emitted, on the average, symmetrically in all directions. When viewed from stationary axes, however, the emission favors the direction of propagation of the mesotron just prior to death. In Part II, Section IV, the general problem of electron emission at different angles is discussed and, in particular, expressions are derived for the horizontal and vertical *electron* intensities resulting from the death of vertically directed mesotrons.

---

[8] M. Schein, W. P. Jesse, and E. O. Wollan, *Phys. Rev.*, **59**, 615 (1941).

Now at high altitudes the horizontal intensity (presumably an electron intensity) is so great [9] as to imply a considerable symmetry in electron emission at mesotron death when measurements are made from fixed axes. Indeed, it was the large horizontal intensity which caused the writer [2] to propose the view that the electrons in the upper atmosphere come mainly from the death of mesotrons, and that only a negligible fraction can be attributed to incoming primary electrons. However, it turns out that the lower limit of the mesotron velocities necessary to account for the sea-level latitude ratio and the intensity-altitude data is too high to permit sufficient symmetry in electron emission at mesotron death to provide for the observed horizontal intensity at high altitudes in the case of proton born mesotrons. In order to obtain a sufficiently low mesotron velocity to provide for the observed symmetry, it is necessary to provide for a correspondingly low velocity in the incoming primaries which give rise to the mesotrons, and such a low velocity demands a mass larger than the proton mass for these primaries in order that they may enter through the earth's magnetic field. It is shown that the conditions are satisfactorily provided for if singly charged helium atoms are invoked for the primaries. It is inferred, therefore, that in addition to the protons already invoked to explain, through their progeny, phenomena at low altitudes and at semi-high altitudes (Pike's Peak, for example)

[9] It has come to the writer's attention that some doubt has been expressed (not in writing, but in conversations) as to the validity of these results, the criticism being to the effect that the observations may have resulted from shower rays passing simultaneously through the coincidence counters. It is, therefore, worth while to point out that, in addition to using triple coincidence counter telescopes, the individual units of the triplet sets were protected from showers such as the above by a wall of anti-coincidence counters. This was done in the case of half of the ten telescope assemblies, the other half being unprotected against showers for comparison. A full description of the details is given in published papers on this matter; and in the case of the flight of Explorer II, the intensity-altitude curves are given for the protected and the unprotected sets for various zenith angles ranging from zero to 90°. See W. F. G. Swann and G. L. Locher, Nat. Geog. Soc. Contr. Tech. Pap., Stratosphere Series, No. 1, pp. 7–14 (1935); also, W. F. G. Swann, G. L. Locher, and W. E. Danforth, Nat. Geog. Soc. Contr. Tech. Pap., Stratosphere Series, No. 2, pp. 16–25 (1936); also, W. F. G. Swann, JOUR. FRANK. INST., **222**, 1 (1936) (see, in particular, pp. 45–58).

we may have to invoke singly charged helium primaries in order to account for phenomena observable at high altitudes where the horizontal intensity becomes important. The slowly moving mesotrons born of the helium atoms die, of course, on account of their short mean lives, before they have penetrated far into the atmosphere.

Of course, it must be realized that all of the considerations involved in all but Section II, applicable, as they are, to only a single altitude of mesotron production, are limited in approximation by that circumstance. They tend to validity only in places reasonably far below the region where production is appreciable, and there only to the extent that we can invoke a kind of "center of gravity" of production as an adequate representative of the facts. Naturally they do not contain the story of the maximum of mesotron intensity to be expected at some altitude in the region of production, since that phenomenon involves in its representation the law of disappearance of primaries with penetration into the atmosphere.

(To be continued in August issue.)

Crystals Used to Measure High Accelerations. (*Westinghouse Engineer*, Vol. 3, No. 1.) The use of quartz spans the entire history of mankind. Among the few remaining artifacts of earliest man are arrowheads of flint, a hard form of quartz. The frequencies of radio broadcast stations are controlled by quartz crystals. And now an ultra-modern use—the measurement of acceleration—has been made of their fascinating physical and electrical properties. Quartz has a mysterious ability. When an alternating voltage is applied between the faces of a quartz crystal, properly cut, the crystal vibrates mechanically at the frequency of the applied voltage. This is the property utilized in radio frequency control. But this action can be worked in reverse. Vibrate the crystal mechanically, and an alternating voltage of the same frequency appears across the faces. This fact has been put to work at the Westinghouse Research Laboratories as a new kind of accelerometer. This device is intended to measure high rates of accelerations. It consists of a steel case bolted solidly to the object whose acceleration is being measured. On the inside, stacked in line in the direction of motion, are a quartz crystal, a thin layer of copper, another quartz crystal and a small mass all held against the case by a soft spring. When the acceleration occurs, this mass, because of its inertia, exerts a force on the quartz crystals. Because of their peculiar ability the crystals translate this force into a charge proportional to the acceleration. This charge is taken off at the copper leaf, led to an amplifying system, and thence to a cathode ray oscillograph, where it is photographed on a moving film. The film speed is such that the events of one thousandth of an inch are spread over an inch of film. The quartz accelerometer faithfully records accelerations of high order occurring at frequencies up to 10,000 per second, which is well below its own natural frequency. The accelerometer itself is small enough to be carried in a coat pocket, being about $1\frac{1}{8}$ inches square by 3 inches long. Its special merit is ruggedness. While the output of quartz is not as high as some other crystals, it is able to withstand without injury the high forces associated with high accelerations.

R. H. O.

ON THE ABSORPTION OF THE HARD COMPONENT OF THE COSMIC RADIATION.

BY

M. E. ROSE,

Bartol Research Foundation of The Franklin Institute, Swarthmore, Pa.*

ABSTRACT.

A phenomenological theory of absorption of mesotrons in the atmosphere and in dense materials at and below sea-level is given. The calculations are based on the following assumptions: (1) absorption due entirely to energy loss caused by electric interactions of charged particles and to spontaneous decay, (2) the localization of mesotron production in an equivalent layer 10 per cent. below the top of the homogeneous atmosphere, and (3) neglect of scattering. From the absorption of vertically incident mesotrons in thick layers of rock the energy distribution in the formation layer is deduced. The energy distribution at sea-level is then determined, without approximations in the analysis, and compared with observations. It is shown that fair agreement is obtained for any reasonable value of the proper lifetime but that a value of about 2×10^{-6} sec. allows the most favorable comparison of the calculated results and the data. The integral energy distribution and the angular distribution at sea-level are obtained. For the latter it is assumed, as is plausible, that the initial angular distribution is isotropic and that the primary energy distribution is independent of the original direction of motion. The agreement between calculated and observed angular distributions is very satisfactory. The absorption in lead and in light materials for vertically incident mesotrons at sea-level is considered. The need for a more precise definition of equivalent thicknesses is pointed out and the stopping powers of lead and light substances are compared. The absorption in lead is calculated and comparison with the data indicates a slightly larger absorption

* Now at Princeton University.

than is found theoretically. However, the absorption at large lead thicknesses (over 100 cm.) and the qualitative behavior of the absorption coefficient with increasing depth below sea-level are in accord with experiment. The consideration of absorption above sea-level indicates that there should be appreciable mesotron production at elevations comparable to that of Mt. Evans (4,300 meters). This is borne out by recent observations.

I. INTRODUCTION.

As a result of a considerable number of investigations carried out in recent years the nature of the hard, or penetrating, component of the cosmic radiation is now fairly well established. These radiations are known to consist of charged particles,[1] mesotrons, with a mass of roughly 200 times the mass of the electron. Moreover, it is now quite certain that the mesotrons are unstable and disintegrate spontaneously in their passage through the atmosphere. From this fact alone it follows that these particles are of secondary origin and are produced in the atmosphere—mainly in the stratosphere. Concerning the nature of the primary particle and the mechanism of the production process very little can be stated with certainty, except that the process is probably a nuclear one.[2]

The process of production constitutes one of the principle problems in the analysis of the hard component. A second problem is concerned with the subsequent behavior of the mesotrons once they have been produced. It is clear that these two problems are independent except insofar as the production process determines the initial energy and angular distributions of the mesotrons, and even this information is deducible from experiments on the absorption of the hard component.

---

[1] For the considerations presented here the sign of the charge is immaterial. Actually there is a slight excess of positively charged particles. In addition the existence of neutral mesotrons has been postulated but not as yet confirmed. Our considerations are also independent of the question of the existence of such uncharged particles.

[2] W. F. G. Swann, *Phys. Rev.*, **59**, 770, 836 (1941); T. H. Johnson, *Rev. Mod. Phys.*, **11**, 208 (1939).

Since the mesotrons are charged particles it is to be expected that their behavior in passing through matter is to be described by the well-known collision processes to which such particles are subject; *viz.*, ionization and radiative collisions. These processes, in addition to the aforementioned spontaneous decay should determine the manner in which the particles are absorbed. While it is true that a mechanism of absorption involving nuclear collisions occurs, as is evidenced by the appearance of "stars" on photographic plates,[3] these effects are rare and do not play an essential role in the cosmic-ray phenomena to be discussed here.

Once the mechanisms of absorption and, in particular, that of energy loss have been specified (cf. Section III, below), it becomes possible to determine the energy distribution (and angular distribution) as well as the total number of particles arriving at any given depth below the point of formation of the particles, provided the energy (and angular) distribution as well as the spatial distribution at the moment of formation are known. In the absence of information concerning the mechanism of production, the latter information could be obtained only from direct experimental data. Unfortunately, direct information as to the distribution of the mesotrons at birth is not now available. Therefore one may attempt to solve the converse problem: to obtain information as to the place of origin and the distribution in energy and angle of the produced mesotrons from the existing data on absorption in the atmosphere and below sea-level. Such a program could be carried through if the experimental data were sufficiently complete. While this is not quite the case, the information that is available is sufficient to permit what may be termed a first-order solution of the problem. From the results obtained it will be possible to draw several conclusions of interest. At the same time it is the purpose of the present paper to indicate in what directions the measurements should be extended in order that more complete information concerning the process of mesotron production may be obtained. The extent to which the theory can be carried at present is indicated in the next section.

[3] W. M. Powell, *Phys. Rev.*, **61**, 670 (1942). See also Section III of the article by M. M. Shapiro, *Rev. Mod. Phys.*, **13**, 58 (1941).

II. PRIMARY MESOTRON DISTRIBUTION.

The experimental data thus far obtained are sufficient to determine the energy distribution of the mesotrons at their place of origin.[4] The measurements which provide this information are the following:

(*a*) The energy distribution of vertically incident mesotrons at sea-level.
(*b*) The absorption of mesotrons in rock (or water) up to depths below sea-level equivalent in mass to as much as 1,100 meters of water.
(*c*) The angular distribution of mesotrons of all energies at sea-level.[4]

The manner in which these measurements are to be used is considered in detail in Sections IV and V. An indication of the consistency of the results may then be obtained from the comparison of theoretical results with observations in the case of further experiments. The angular distribution at sea-level is considered in Section VI. In Section VII the results previously obtained are applied to a consideration of the absorption in lead and other materials for the case of vertically incident mesotrons at sea-level. In Section VIII the absorption in the atmosphere is considered.

It may be noted that no conclusions regarding the place of formation, or the spatial distribution of mesotrons at formation, are advanced. In fact, since the intensity of the hard component in the atmosphere or underground depends not only on the distance traversed by the rays but also on the shape of the primary energy distribution, it may appear surprising that one can obtain information concerning the one and not the other. By way of explanation it may be pointed out that the original energy distribution of the particles is determined primarily from the absorption in very thick layers of rock (see (*b*) above). Because of the large thicknesses involved and the extremely large energies required to penetrate such thicknesses it does not matter much where the rays are formed, since a completely negligible energy loss

[4] The angular distribution may also be determined. Alternatively, one can make a plausible assumption for the initial distribution in angle and compare the calculated and observed distributions at sea-level to check the theory.

and absorption takes place in the atmosphere. Hence the energy distribution can be obtained from the differential absorption without assumptions as to the place of formation. It is to be emphasized however, that only the distribution for primary energies greater than about 10^{10} e.v. is fixed in this way because particles of lower energy are not transmitted through the very thick layers of dense material. The energy distribution for lower energies is obtained from the absorption in thinner layers of material and from the energy distribution as observed at sea-level. However, this still leaves the primary distribution undetermined for energies below 2×10^9 e.v., since slower particles, in general, are absorbed before reaching sea-level.

While no detailed information is at hand concerning the *spatial* distribution of the mesotrons at the moment of formation, it appears that production takes place at all elevations throughout the atmospheric layer. However, there is evidence for production with appreciable intensity only above 4,000 meters or thereabouts.[5] Moreover, the intensity of production increases so rapidly with elevation that for most purposes it is sufficient to replace the entire producing region by an equivalent layer. That is, one assumes that all mesotrons are produced in a certain layer of fixed depth below the top of the homogeneous atmosphere.[6] It is customary to take the position of this equivalent layer at 10 per cent. below the top of the homogeneous atmosphere: at an elevation of 9.3 meters water equivalent above sea-level. As a justification for this procedure it may be stated that the energy distribution and/or the total intensity at sea-level and below is insensitive to the choice of position of the equivalent layer as long as this layer is placed near the top of the homogeneous atmosphere. It is obvious that shifting the position of the layer from which the particles start will have virtually no effect on the absorption due to energy loss since this depends on the amount of matter traversed. A somewhat greater effect on absorption due to decay would be

[5] M. Schein, W. P. Jesse and E. O. Wollan, *Phys. Rev.*, **59**, 615 (1941).

[6] That is, the atmospheric layer considered as compressed in such a way that the pressure is uniform and equal to the normal sea-level value of 76 cm. Hg. The height of the homogeneous atmosphere is thus 8.35×10^3 meters.

expected (dependent on distance traversed) but, as will be seen in the following, the effect of decay does not appreciably change the *shape* of the energy distribution nor the *shape* of the absorption curve in dense materials. However, when one attempts to extend the calculations to absorption in the atmosphere and at the same time retaining the assumption of an equivalent producing layer, no agreement between theory and observed results can be obtained (see Sec. VIII). This is to be expected since, for elevations where mesotron production is of some importance, the results are much more sensitive to the assumed position of the equivalent producing layer.

III. ENERGY LOSS AND DISINTEGRATION.

For the absorption of mesotrons in the atmosphere or for the penetration through dense materials of low atomic number the energy loss of the particles is almost entirely determined by the ionizing collisions. Energy loss due to radiative collisions become of equal importance only for very high energies; namely, for energies of the order 2×10^{12} e.v. in light materials such as rock, and for about 3×10^{11} e.v. in lead. In addition, as will be shown below, the intensity of such mesotrons, whose energy is so great as to experience appreciable radiative losses, depends only slightly on the total energy loss. Therefore, radiation energy losses will contribute only a small correction term to the intensity.

The precise form for the rate of energy loss depends on the spin of the mesotron and it is not yet possible to assign a value of the spin with any degree of assurance. However, in the case of energy loss due to ionization the collision probability, and therefore the rate of energy loss, becomes independent of the spin when the energy given to the secondary electron is small compared to the mesotron energy. This will be the case in the vast majority of events since large energy transfers result from very close collisions (scattering through large angles), and such collisions are exceedingly rare due to the long range nature of the Coulomb forces responsible for the scattering.[7] In the case of radiative

[7] Cf., for example, B. Rossi and K. Greisen, *Rev. Mod. Phys.*, **13**, 240 (1941). It is also necessary that the energy transfer be small compared to 2×10^{10} e.v. which will be fulfilled in practically all cases of interest.

losses the question of spin dependence does not concern us in view of the remarks made above.

In the following it will be convenient to measure distances in terms of mass traversed. Thus, if t represents a distance in g/cm.^{2} or cm. of water, and x represents the same distance in conventional units (cm.) we have

$$dt = \rho dx, \tag{1}$$

where ρ is the density of the material under consideration. It is also convenient to introduce the energy of the mesotron in units of the rest energy. Thus if E represents the energy in c.g.s. units we introduce

$$\epsilon = E/\mu c^2, \tag{2}$$

where μ is the rest mass of the mesotron. For $\mu = 200m$ (i.e., $\mu = 1.8 \times 10^{-25}$ g.) the rest energy of the mesotron is just 10^8 e.v. Thus the energy E is given by $10^8\epsilon$ e.v.[8]

The rate of energy loss by ionization is now given by [9]

$$B_i(\epsilon) = -\left(\frac{d\epsilon}{dt}\right)_i = \frac{2\pi r_0^2 Z}{A m_H}\frac{m}{\mu\beta^2}\left[\log\frac{2mc^2\beta^2 W_m}{I^2(Z)(1-\beta^2)} - 2\beta^2\right]. \tag{3}$$

Here $r_0 = e^2/mc^2$ is the classical electronic radius, e and m being the electronic charge and mass; Z and A are the atomic number and mass number respectively; m_H is the mass of the hydrogen atom, 1.66×10^{-24} g., so that Am_H is the atomic weight. $I(Z)$ is the average ionization energy of the atom of atomic number Z. Following Bloch [10] we set

$$I(Z) = 13.5Z \text{ e.v.} \tag{3a}$$

[8] Recent determinations of the mass would indicate that $\mu = 180\,m$ is a more reliable value. Inasmuch as this work was completed before the better mass determinations appeared the value $\mu = 200\,m$ had been adopted. However, the error thereby induced is, in general, unimportant and is certainly smaller than the experimental errors involved in absorption measurements, etc. See also Sec. IV.

[9] Cf., for example, J. A. Wheeler and R. Ladenburg, *Phys. Rev.*, **60**, 754 (1941). We neglect the so-called density effect investigated by Fermi, *Phys. Rev.*, **56**, 1242 (1940); **57**, 485 (1940). See also O. Halpern and H. Hall, *Phys. Rev.*, **57**, 459 (1940), and reference 7, p. 247.

[10] F. Bloch, *Zeits. f. Phys.*, **81**, 363 (1933).

As usual $\beta = v/c$ where v is the mesotron velocity, and we have

$$\beta^2 = \frac{\epsilon(\epsilon + 2)}{(\epsilon + 1)^2}. \tag{3b}$$

W_m is the maximum energy that may be transferred to the secondary electron

$$W_m = \frac{2m\mu^2c^2(\epsilon + 2)}{m^2 + \mu^2 + 2m\mu(\epsilon + 1)}\epsilon. \tag{3c}$$

The rate of energy loss due to radiative collisions is given by [11]

$$B_r(\epsilon) = -\left(\frac{d\epsilon}{dt}\right)_r$$

$$= \frac{Z^2r_0^2}{137Am_H}\left(\frac{m}{\mu}\right)^2(\epsilon + 1)\left[\chi(\xi) + 4\log\frac{\mu}{m}Z^{-1/3}\right] \tag{4}$$

where

$$\xi = Z^{1/3}\left(\frac{m}{\mu}\right)\frac{\epsilon + 1}{2},$$

and $\chi(\xi)$ is a function given in Fig. 2 of reference 11. The total rate of energy loss is then

$$B(\epsilon) = B_i(\epsilon) + B_r(\epsilon). \tag{5}$$

It may be noted that for a given velocity the ionization loss dE/dt is independent of the mesotron mass for all but the very high energies, *viz.*: for $\epsilon \ll \mu/m$ or for energies small compared to 2×10^{10} e.v., W_m and therefore dE/dt depends only on the velocity. $B_i(\epsilon)$ is then inversely proportional to the mesotron mass for a given velocity. This fact has the important consequence that under conditions in which only ionization loss is responsible for absorption, the absorption coefficient depends on the mass in a very simple manner (Sec. IV).

The range of a mesotron with initial energy ϵ_0 is given in terms of the stopping function B by

$$R(\epsilon_0) = \int_0^{\epsilon_0}\frac{d\epsilon}{B(\epsilon)}. \tag{5a}$$

[11] Cf., for example, H. J. Bhabha, *Proc. Roy. Soc.*, **A164**, 257 (1938). Eq. (4) applies to particles of spin $\frac{1}{2}$.

From the remarks made above it follows that for all but very high energies ($\epsilon \gtrsim 200$) the range is proportional to the mass μ. Curves giving the rate of energy loss due to ionization for air, Fe and Pb up to $\epsilon = 100$ are given in Fig. 2 of reference 7. Range-momentum curves are given in Fig. 3 of the same reference.

In addition to the attenuation due to energy loss the intensity of the mesotron component of the cosmic radiation decreases as a result of decay.[12] If τ is the lifetime of the mesotron measured in a frame of reference moving with the particle, the fractional decrease of intensity due to decay in traversing a distance dx is

$$-\frac{dI}{I} = \frac{dx}{v\tau}. \tag{6}$$

In terms of the lifetime τ_0 measured in the laboratory frame of reference this becomes

$$-\frac{dI}{I} = \frac{dx}{v\tau_0}\left(1 - \frac{v^2}{c^2}\right)^{1/2} = \frac{dx}{cp\tau_0}, \tag{6a}$$

since $\tau = \tau_0(1 - v^2/c^2)^{-1/2}$. Here p is the momentum of the mesotron in units of μc. For the consideration of absorption in the atmosphere it will be desirable to express this attenuation due to decay in terms of lengths measured in g./cm.^{2} (cm. of water). Using the barometric formula

$$t = t_s e^{-x/x_s},$$

where t_s is the atmospheric thickness (10.3 meters water equivalent) and $x_s = t_s/\rho_s$, where ρ_s is the sea-level density of air at 15° C. and 76 cm. Hg. Then (6a) becomes

$$-\frac{dI}{I} = \frac{t_s}{t}\frac{dt}{\rho_s c\tau_0 p} \equiv \frac{\alpha dt}{tp}. \tag{7}$$

The numerical value of α depends on τ_0, the value of the lifetime of the mesotron at rest. The experimental determi-

[12] A partial summary of the ample evidence for decay is given by B. Rossi, *Rev. Mod. Phys.*, **11**, 296 (1939). More recently the lifetime has been measured by F. Rasetti, *Phys. Rev.*, **60**, 198 (1941), and G. Bernardini, B. N. Cacciapuotti, E. Pancini, O. Piccioni and G. C. Wick, *Phys. Rev.*, **60**, 910 (1941), which may be consulted for further references.

nations of τ_0 give values ranging from 1.3 to about 5×10^{-6} sec. The weight of the experimental evidence, however, points to a value lying between 2 and 3×10^{-6} sec. The procedure adopted here is to choose that value of τ_0 which gives the best fit between the observed and calculated energy distribution for vertically incident mesotrons at sea-level.

IV. SEA-LEVEL ENERGY DISTRIBUTION FOR VERTICAL INCIDENCE.[13]

On the assumption that the ordinary processes of energy loss due to electromagnetic interactions and the decay suffice to describe the behavior of mesotrons, the energy distribution of the particles at any depth below the formation layer may be determined with the following auxiliary assumptions:

(1) The specification of the primary energy distribution. Actually this is determined from the absorption of the mesotrons in thick layers of rock [19] and, properly speaking, the calculation of this absorption curve involves a knowledge of the sea-level distribution, which in turn depends on the primary distribution in energy. However, since those mesotrons with sufficient energy to penetrate thick rock layers do not undergo appreciable decay (Eqs. 6 and 7), it is permissible to replace the atmosphere by a layer of equivalent stopping power. The absorption is then entirely due to energy loss and it becomes a simple matter to determine the energy distribution which gives rise to the observed absorption (Sec. V). For that part of the primary spectrum which is of importance for the sea-level energy distribution we have for the number of particles formed per sec. per cm.^{2} with energy between ϵ and $\epsilon + d\epsilon$ with the direction of motion confined to the solid angle $d\omega$ at the zenith

$$F_0(\epsilon)d\epsilon d\omega = C_0\epsilon^{-\gamma}d\epsilon d\omega, \qquad (8)$$

where C_0 is a constant to be adjusted empirically and $\gamma = 2.90$. This result does not apply for very low energies, i.e., for $\epsilon < 20$ which is the minimum energy necessary to traverse

[13] The results presented in this section were also obtained by D. R. Hartree (cf. reference 12). Hartree's calculations are unpublished, and were repeated here for the purpose of an independent check. The details are presented for the purpose of illustrating the procedure used in this and in other parts of the work.

the atmosphere. Moreover, the distribution (8) does not apply for very large energies: $\epsilon \gtrsim 800$ (see Eq. 17). For such energies the primary intensity and the intensity at sea-level are too small to observe, and in fact, beyond the range of curvature measurements. Thus (8) applies to such energies as are of pertinence for the sea-level distribution.

(2) The foregoing implies that the mesotrons are observed at sea-level only after having traversed a large part of the atmosphere. This is true for most of the mesotrons detected at low elevations and, in accordance with the discussion of Section II, we assume that all the observed mesotrons originate in a thin layer near the top of the homogeneous atmosphere. We thereby overestimate the decay due to particles produced at lower elevations and underestimate the decay effect for particles originating above the assumed position of the formation layer. The effect of the assumption of a production layer in the upper atmosphere on ionization loss is not serious since most of the energy loss must take place at very low elevation where the atmospheric density is greatest. The height of the production layer will be taken at 10 per cent. below the top of the homogeneous atmosphere, that is, the layer at which the atmospheric pressure is 76 mm. Hg.

(3) Finally, we assume that scattering may be neglected so that the mesotrons observed in vertical incidence, for example, have described a vertical path from the point of origin to the point of observation. This assumption should be valid (on account of the strong forward scattering) for all but the very low energies ($\epsilon \lesssim 1$), and these low energy particles do not contribute greatly to the total intensity. An estimate of the effect of scattering may be made and it is concluded that the maximum error caused by its neglect is about one percent.

With these assumptions we may proceed to the calculation of the energy distribution at sea-level. The considerations of this section will be confined to mesotrons incident vertically. The case of oblique incidence is considered in Section VI. The number of mesotrons incident per cm.^{2} per sec. in the unit solid angle at the zenith with energy between ϵ and $\epsilon + d\epsilon$ at a point t cm. water (g./cm.^{2}) below the top of the homogeneous atmosphere will be denoted by $F(\epsilon, t)d\epsilon$. With

the origin of t at the top of the homogeneous atmosphere we have $t = t_s = 1033$ g./cm.^{2} at sea-level and $t = t_0 = 103.3$ g./cm.^{2} at the formation layer.

Consider first the case in which decay is neglected and the absorption is entirely due to stopping by energy loss. By virtue of the assumption of straight line paths (see (3) above), the energy loss from the point of production is known. Denoting the energy loss in units of μc^2 by $\Delta\epsilon$ we have

$$t_s = \int_{\epsilon}^{\epsilon+\Delta\epsilon} \frac{d\epsilon}{B(\epsilon)}. \tag{9}$$

Thus, for the atmospheric layer between the point of production and sea-level, or for any other layer of absorbing material, we may define a pair of corresponding energies: the energy ϵ at the bottom of the layer (point of observation) and the energy $\epsilon' = \epsilon + \Delta\epsilon$ at the top of the layer. The loss $\Delta\epsilon$, and therefore ϵ', is a slowly varying function of ϵ.

It is now clear that the number of mesotrons whose energy lies in any interval $(\epsilon, \epsilon + d\epsilon)$ at sea-level is equal to the number of mesotrons whose energy lies in the *corresponding* interval $(\epsilon', \epsilon' + d\epsilon')$ at the position of the production layer. Hence the distribution at sea-level $F(\epsilon, t_s)d\epsilon$ is obtained by shifting the distribution in the production layer $F_0(\epsilon')d\epsilon'$ towards smaller energies by the amount $\Delta\epsilon$, and taking into account the change in the energy interval $d\epsilon' \to d\epsilon$:

$$F(\epsilon, t_s)d\epsilon = F_0(\epsilon')d\epsilon', \tag{10}$$

or, from (9),

$$F(\epsilon, t_s) = \frac{d\epsilon'}{d\epsilon} F_0(\epsilon') = \frac{B(\epsilon')}{B(\epsilon)} F_0(\epsilon').$$

Then from (8) we have

$$F(\epsilon, t_s) = C_0 \frac{B(\epsilon + \Delta\epsilon)}{B(\epsilon)} (\epsilon + \Delta\epsilon)^{-\gamma}, \tag{11}$$

where B is given by (3), (4) and (5).

The effect of decay is now to introduce an attenuation factor which is readily obtained from (7). Taking into consideration the energy dependence of the probability for decay and the fact that the energy is changing during the traversal through the atmosphere, we find for the energy

distribution at sea-level:

$$F(\epsilon, t_s) = C_0 \frac{B(\epsilon + \Delta\epsilon)}{B(\epsilon)} (\epsilon + \Delta\epsilon)^{-\gamma} e^{-\alpha D}, \qquad (12)$$

where

$$D(\epsilon) = \int_{R_s}^{R_0} \frac{dR}{tp(R)}, \qquad \alpha = \frac{t_s}{\rho_s c \tau_0}. \qquad (12a)$$

In (12a) we have introduced the residual range R as the variable of integration. The limits of integration R_0 and R_s are the ranges in air (of normal density) for the corresponding energies $\epsilon' = \epsilon_0$ and ϵ_s respectively (cf. 5a). Obviously, we have

$$R + t = R_0 + t_0 = R_s + t_s. \qquad (12b)$$

It is evident that the result (12), aside from the trivial normalizing constant C_0, completely defines the energy distribution at sea-level for the vertical rays. However, it may be readily appreciated that specific results are obtainable only by a rather tedious numerical procedure. The decay integral (12a), which depends on the momentum-range relationship—Eq. 5a, cannot be evaluated analytically without simplifying assumptions; moreover, a separate numerical integration must be carried out for each value of ϵ. A great part of the labor involved may be eliminated if one adopts the simplification introduced by Euler and Heisenberg.[14] Here one assumes a constant rate of energy loss and this allows an exact expression for the momentum-range relationship and an analytic evaluation of the decay integral. The assumption of a constant energy loss, however, while fairly suitable for intermediate energies is a poor approximation for small energies ($\epsilon \lesssim 1$). As is evident from (3) or from the figure referred to above,[7] the rate of energy loss increases very rapidly for energies just below the rest energy. Hence the Euler-Heisenberg approximation cannot be expected to provide a valid description for such phenomena as decay, which depend primarily on slow particles. While it is true that accurate measurements of the intensity of slow particles, such as could be provided by the cloud chamber or proportional

[14] H. Euler and W. Heisenberg, *Ergeb. d. Exakt. Naturwiss.*, **17**, 41 (1938). See especially pp. 39–44.

counter, are very difficult and, in fact, are not yet at hand, the importance of the decay phenomenon makes it worth while to consider a more accurate solution of the problem. In addition, it is of interest to compare the observed results with a theoretical analysis based on as few assumptions as possible in order to obtain a better indication of the importance of the assumptions concerning the primary distribution of mesotrons which forms the basis of the present calculations. Therefore, the simplification of constant energy loss will be avoided and the results are to be obtained by a rigorous calculation.

In carrying out the calculations it is, of course, necessary to specify the numerical value of the constants which enter. Of these the mass and lifetime, μ and τ_0, are uncertain with the experimental uncertainty in the case of μ (about 20 per cent.) being considerably smaller than that of τ_0. In the procedure adopted here the mass was taken as $\mu = 200m$[8] and the lifetime τ_0 was adjusted so as to obtain as good agreement as possible with the observed energy distribution at sea-level. It is therefore pertinent to consider in what manner the results may be changed if another value of the mass were adopted. For this purpose in the energy distribution (12) we consider separately the factors directly due to energy loss and the exponential factor arising from the decay. In the factors arising from the energy loss the mass enters in the $\Delta\epsilon$ which is essentially inversely proportional to the mass (cf. remarks preceding Eq. 5a). Since the energy loss $\Delta\epsilon$ is a very slowly varying function of ϵ, a decrease in mass μ would mean, *cet par.* a distribution function varying less rapidly with energy. This will be more noticeable at energies for which $\Delta\epsilon \gtrsim \epsilon$; i.e., $\epsilon \lesssim 20$. In addition, the maximum of the energy distribution, see Fig. 1 below, arising from the rapid decrease of the energy loss factors in (12) and the increase in the decay exponential factor with ϵ, would shift toward slightly higher energy, provided the decay factor were unaltered. Since the effect of a small change in mass (from $200m$ to $180m$ for example) would have a rather unimportant effect on the energy loss factors we may conclude that the results given below will apply for other masses in the neighborhood of the chosen value if, as before, the decay factor remains

unchanged. The decay factor, as may be seen from (12a), is essentially proportional to μ/τ_0. Hence if the values given in the following for the lifetime are changed in proportion to the change of mass, the energy distribution will be relatively insensitive to the uncertain mass.

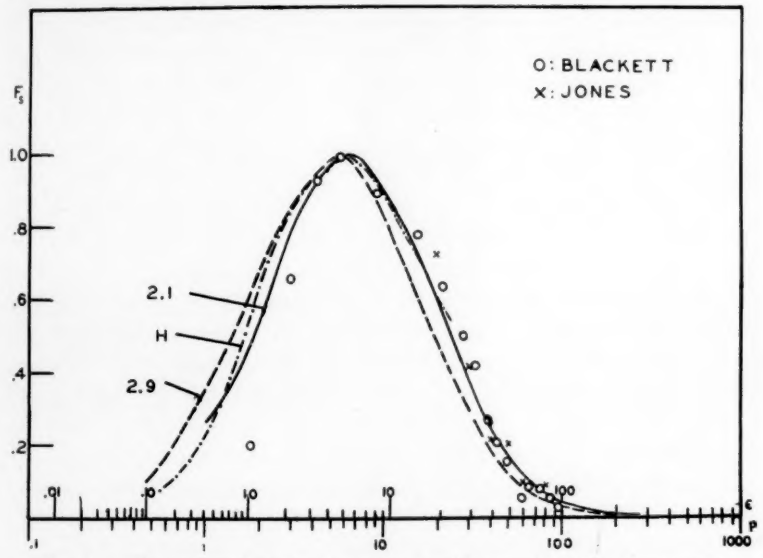

FIG. 1. The energy distribution at sea-level for vertically incident mesotrons as a function of momentum (in units μc) plotted on a logarithmic scale (lower scale). The upper abscissa scale gives the corresponding values of ϵ, the energy in units μc^2. The circles and crosses give the experimental points. The calculated distribution for $\tau_0 = 2.1 \times 10^{-6}$ sec. and 2.9×10^{-6} sec. are given by the full and dashed curves, respectively. The curve marked H was calculated by Hartree [13] with $\tau_0 = 2.7 \times 10^{-6}$ sec. and an initial distribution proportional to $p^{-2.9}$. All curves normalized to a maximum value of unity.

The method adopted in carrying out the numerical integration in (12) is described in the appendix. The results obtained for the energy distribution are given in Fig. 1. Both the experimental points and the calculated curves have been normalized to a maximum value of unity.[15] The full

[15] For $\tau_0 = 2.1 \times 10^{-6}$ sec., see below, the normalization constant C_0 has the value 7.4×10^4 with this normalization. With this choice of the normalization constant the total intensity in the zenith is 32.8 mesotrons per cm.^{2} per sec. per unit solid angle. The transition to other normalizations is obvious and needs no comment.

curve ($\tau_0 = 2.1 \times 10^{-6}$ sec.) is seen to agree quite well with the experimental points of Blackett [16] and of Jones,[17] except at low energies. It is to be remembered that the data for small energies are very uncertain and subject to large statistical errors due to the comparatively low intensity of slow particles. We may exclude the possibility that the discrepancy between observations and the calculated form of the distribution is due to an appreciable number of mesotrons which originate below the assumed position of the formation layer. For such mesotrons there would be relatively less attenuation due to decay and, since the decay affects the intensity of the slow particles to the greatest extent, the calculated distribution would then decrease less rapidly for low energies. This would increase the discrepancy rather than improve the agreement. While it is difficult to explain the deviation at low energies except in terms of the experimental uncertainty, the considerations of the following sections, which are based on the form of the sea-level distribution, are to a large degree independent of this part of the spectrum.

The theoretical curves have been calculated for several values of the lifetime and two curves are shown in Fig. 1: 2.1 and 2.9 $\times 10^{-6}$ sec. The normalization factors for various values of the lifetime differ considerably. However, the important point is that the shape of the distribution is not very sensitive to the lifetime and any τ_0 between the two values cited above would account for the observed results almost equally well. The insensitivity of the distribution function to the value of the lifetime may be regarded as unfortunate if it is desired to use these measurements to determine τ_0. However, in view of the indirect nature of such a determination of the lifetime, this procedure could not be expected to yield a reliable value. Thus, accepting the calculations and measurements at their face value, a lifetime of as much as 5×10^{-6} sec. would appear to be ruled out. But the discrepancy between the calculated curve and the observations in this case is perhaps even within the uncertainties involved in both, and it is not possible to definitely exclude such a large value of τ_0. Therefore, so far

[16] P. M. S. Blackett, *Proc. Roy. Soc.*, **A159**, 1 (1937).
[17] H. Jones, *Rev. Mod. Phys.*, **11**, 235 (1939).

as the energy distribution at sea-level is concerned, it seems safe to say that the observations are compatible with any value of the lifetime in the range reported in more direct experiments.[12]

From the sea-level energy distribution one readily obtains the integral energy distribution, that is, the number of mesotrons with energy greater than ϵ:

$$N_s(\epsilon) = \int_{\epsilon}^{\infty} F(\epsilon, t_s)d\epsilon. \qquad (13)$$

Here and in the following calculations the sea-level distribution corresponding to a lifetime of 2.1×10^{-6} sec. will be used. The integration (13) is then carried out numerically using the

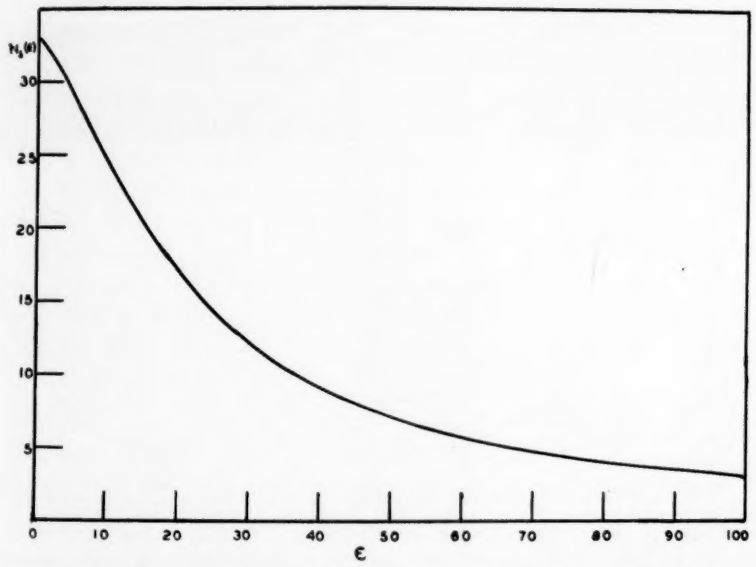

FIG. 2. The integral energy distribution at sea-level for vertically incident mesotrons. With the adopted normalization (see caption to Fig. 1), the total number of mesotrons per cm.^{2} per sec., per unit solid angle at the zenith is $N_s(0) = 32.8$.

curve given in Fig. 1. The result is given in Fig. 2. The total intensity (within a constant factor) of vertically incident mesotrons at sea-level is thus obtained from this curve when

ϵ is the minimum energy required to penetrate the walls of the counter or other device used as a detecting instrument.

V. ABSORPTION BELOW SEA-LEVEL IN LIGHT MATERIALS.

As was discussed above, the energy spectrum of the mesotrons in the formation layer can be determined from the results of absorption measurements of the particles under thick layers of dense materials such as rock. This conclusion is based on two facts. First, the energy necessary to penetrate 30 meters of rock (about 100 meters water equivalent) or more is at least 3×10^{10} e.v. The energy at the formation layer is then about 10 per cent. greater. For such energies the attenuation due to decay in traversing the atmosphere is unimportant. The exponential factor (cf. Eq. 12a), whose departure from unity is a measure of the effect of decay, is 0.92 for an energy at sea-level of 3×10^{10} e.v. The second basic fact is the following: in dense materials the effect of decay is negligible in all cases. Thus, only stopping by energy loss need be considered and the atmosphere could be regarded as an additional thickness of dense material whose thickness is given by the 10.3 meters water equivalent of the air layer. The absorption of the mesotrons is then directly determined by the primary energy spectrum since the number stopped in a thin layer dt at a certain depth t is just the number of particles in the formation layer whose energy lies between E and $E + dE$, where E and $E + dE$ are the energies necessary to just penetrate the layers of thickness t and $t + dt$ respectively. The primary spectrum is thus defined by the observed absorption and the given energy-range relationship.

The conclusion that decay in dense materials is always negligible may appear surprising at first sight. It may be argued that the intensity of the slow particles emerging from a thick layer should be very much dependent on decay. Moreover, it may further be supposed that the energy below which decay is appreciable is greater the greater the thickness of the material. This would appear plausible since greater thickness means greater path length and more time spent in traversing the layer. Both of these arguments are misleading. It is true that the slower the particle the greater the attenua-

tion due to decay. However, when the energy is reduced much below the rest energy, the rate of energy loss increases so rapidly that the particles will be stopped before appreciable numbers disintegrate. Thus even for a final energy which vanishes, the decay factor is very little different from unity (cf. below).[18] Again, increasing the thickness of the material does very little to enhance the effect of decay since the increased thickness requires a greater energy at the top of the layer in order that the mesotron may emerge. Thus, one simply adds to the path a portion in which the velocity is increasingly larger and the added effect of decay becomes increasingly smaller. In the limit of infinite thickness and vanishing energy of emergence the decay factor for light materials such as rock becomes $\exp(-4.4\ 10^{-3}/\rho)$ where ρ is the density of the material. This is virtually unity for all non-gaseous materials.

Since only energy loss is of importance in dense materials, the energy distribution for vertically incident mesotrons at a depth t cm. water below sea-level is

$$F(\epsilon, t)d\epsilon = \frac{B(\epsilon')}{B(\epsilon)} F_s(\epsilon')d\epsilon, \tag{14}$$

where ϵ' is the energy of the mesotron at sea-level and $F_s(\epsilon')$ is the energy distribution at sea-level for vertical incidence. The functions B refer, of course, to the dense material. For the comparison with the measurements to be considered in this section we are concerned with the energy loss in rock, whose heterogeneous chemical composition cannot be known exactly. However, the constituents of the absorbing material are almost entirely composed of light materials for which

[18] For materials of uniform density the decay factor becomes $\exp(-D')$, where

$$D' = 1/(\rho\tau_0 c)\int_R^{R'} dR/p(R).$$

Here ρ is the density of the material and R', R are the ranges at the top and bottom of the layer. The idea that decay should be important for very low energies amounts to the supposition that the integral D' will diverge for vanishing energy (lower limit = 0). Actually the integral converges because the range vanishes with decreasing energy more rapidly than does the momentum. E.g., if for small energy we have $R \sim E^n$, then $n > 1$. The integrand of D' then behaves as $R^{-1/2n}$ which gives a convergent result.

$Z/A \approx \frac{1}{2}$, cf. Eq. 3. The dependence of B on the nature of the material is then contained in the average ionization energy $I(Z)$ which enters only logarithmically. It is then permissible to assume for this ionization energy a value corresponding to an average Z. We take $Z = 13$ and $I(Z) = 175$ e.v. (Eq. 3a). The small error thereby incurred is of the same order as the uncertainty in the numerical factor in (3a). The same value of Z (and $A = 2Z$) is used in computing the radiation energy loss, Eq. 4. In this case the uncertainty in Z is of greater importance so far as the radiative rate of energy loss, B_r, is concerned. On the other hand radiative losses play a very minor role in determining the absorption in light materials for energies less than 5×10^{11} e.v. which constitutes practically an upper energy limit for our considerations.

The number of mesotrons transmitted through a thickness t is given by

$$N(\epsilon_1, t) = \int_{\epsilon_1}^{\infty} F(\epsilon, t)d\epsilon = \int_{\epsilon_1}^{\infty} \frac{B(\epsilon')}{B(\epsilon)} F_s(\epsilon')d\epsilon, \qquad (15)$$

where ϵ_1 is the energy required to penetrate the walls of the detecting instrument, counter telescope. For a given ϵ_1 the absorption could be calculated by first determining the energy distribution from (14) for various thicknesses t and then carrying out the integration (15) numerically for each thickness. However, a much simpler procedure is the following.

First of all we note that with the usual experimental arrangements, $\epsilon_1 \sim 0.1$. Since the energy distribution below a layer of dense material will not differ greatly from that at sea-level so far as shape is concerned, we may conclude that the number of particles stopped by the counter walls, etc., is negligible and the number of transmitted particles may be written as

$$N(t) \approx \int_0^{\infty} \frac{B(\epsilon')}{B(\epsilon)} F_s(\epsilon')d\epsilon \qquad (16)$$

$$= \int_{\epsilon_0}^{\infty} F_s(\epsilon')d\epsilon' = N_s(\epsilon_0).$$

Here ϵ_0 is the energy at the top of the layer corresponding to zero energy at the bottom and $N_s(\epsilon_0)$ is the number of meso-

trons at sea-level with energy greater than ϵ_0, that is, the number with range equal to or greater than the thickness of the rock. Thus the absorption is directly obtained from the results of Fig. 2.

Dividing by $N_s(0)$, the total number of particles at sea-level, we obtain the absorption curve normalized to unity at zero thickness. For all but the smaller thicknesses ($t \lesssim 40$ m. water) the sea-level energy distribution for $E > 10^{10}$ e.v. becomes of importance. Since the observations do not extend beyond this energy, the absorption was first calculated by extrapolating the $\epsilon^{-2.9}$ distribution. The result is shown in Fig. 3 by the curve drawn in full up to 280 m. water equivalent and by the dashed curve for greater thicknesses. The disagreement between this calculated curve and the experimental points due to Wilson [19] indicates a larger absorption coefficient at greater thicknesses. This was, in fact, originally pointed out by Wilson. While some attempt has been made to explain the rather abrupt change in absorption near 280 m. water in terms of some additional process of absorption or by postulating some change in the nature of the hard component, it does not seem possible at this time to arrive at a consistent interpretation of the observations in this manner. Instead, one may assume that the extrapolation of the primary energy distribution as given by (8) is unjustified, as it certainly is, and the behavior of the spectrum in the formation layer for energies above 8×10^{10} e.v., which is necessary for the penetration of 280 m. water, is deduced from the observed absorption for the larger rock thicknesses. The full curve in Fig. 3 gives the calculated absorption when it is assumed that for $\epsilon > 800$, the energy distribution in the formation layer is proportional to $\epsilon^{-3.4}$. When the multiplicative constant is chosen so as to make the distribution continuous, the primary energy spectrum is as follows:

$$F_0(\epsilon)d\epsilon = \begin{cases} 7.4 \times 10^4 \epsilon^{-2.9} d\epsilon, & \epsilon \leqslant 800, \\ 2.1 \times 10^7 \epsilon^{-3.4} d\epsilon, & \epsilon > 800. \end{cases} \qquad (17)$$

While the observed absorption may in this way be used to determine the primary energy distribution up to very large

[19] V. Wilson, *Phys. Rev.*, **53**, 337 (1938).

energies, it must be admitted that the adopted procedure is decidedly *ad hoc*. Thus the increase in absorption may be only partly due to a modification in the primary energy dis-

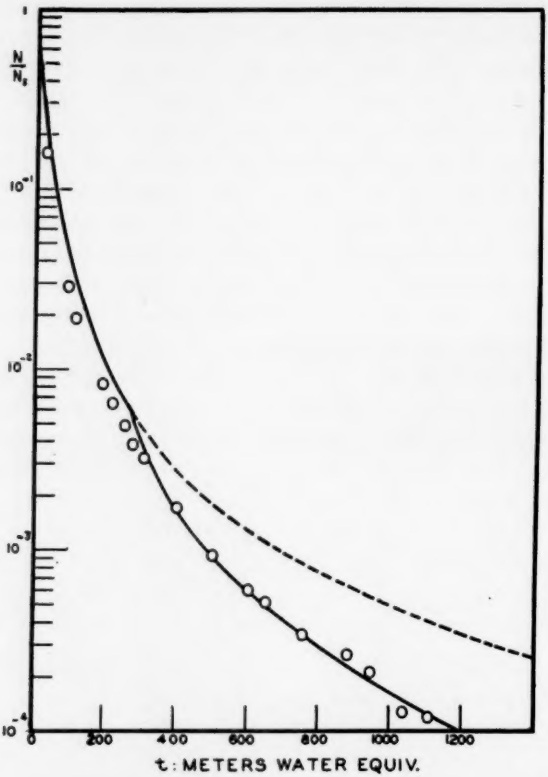

FIG. 3. The absorption in light materials for vertically incident mesotrons. The unit of thickness is 100 g./cm.^{2} = 1 meter water. The circles are the experimental points of Wilson [19] and the full curve is the calculated absorption with the primary energy distribution (17). The dashed curve results when the distribution (8) is extrapolated to high energies. Both calculated and experimental intensities normalized to unity at sea-level.

tribution and some as yet unspecified mechanism of additional absorption may still be involved. This question is best decided when further independent evidence concerning the primary spectrum is at hand.

VI. ANGULAR DISTRIBUTION AT SEA-LEVEL.

The energy distribution at sea-level for vertically incident mesotrons and the absorption in rock essentially serve to fix certain parameters; mainly, the primary energy distribution above the energy required to reach sea-level. Therefore, from the comparison of calculated results and those observed in experiments of these two types it is hardly permissible to draw conclusions as to the validity of the postulated absorption mechanisms. The validity of the assumed energy distribution, especially at higher energies than are important for vertical incidence at sea-level, can be tested by a comparison between observed and theoretical angular distributions at sea-level. For the inclined rays the path through the atmosphere, measured both in usual geometric units as well as mass units, is increased by a factor *sec* ϑ, where ϑ is the zenith angle. Therefore the decay and ionization loss are enhanced corresponding to the longer path. The number of mesotrons then depends more directly on the intensity in the formation layer at the higher energies.

Before the angular distribution at sea-level may be determined some decision in regard to the angular distribution in the formation layer must be made. In the absence of any information about the primary distribution in angle a calculation such as the following would only serve to obtain this information empirically. Fortunately, such *a priori* knowledge of the initial angular distribution is not entirely lacking. Although the precise nature of the process by which mesotrons are produced is not known, it is fairly certain that the collisions responsible for such production are due to short range forces. It would follow then that the mesotrons are produced with an isotropic distribution in angle. We assume that this is the case. We also assume that the primary distribution in energy is independent of the initial direction of motion so that (17) applies to all mesotrons in the formation layer.

The calculation of the angular distribution involves first the determination of the sea-level energy distribution for each angle of incidence. The procedure is exactly as described in Section IV (and the appendix) except that in the decay factor, D is multiplied by sec ϑ and the energy loss is computed for a thickness $(t_s - t_0)$ sec ϑ. The total intensity for each angle

is obtained by integration over the corresponding energy distribution as in (13). The angular distribution, normalized to unity for vertical incidence, is then

$$\frac{I}{I_0} = \frac{\int_0^\infty F_s(\epsilon, \vartheta)d\epsilon}{\int_0^\infty F_s(\epsilon, 0)d\epsilon}, \tag{18}$$

where now the second argument in F_s indicates the zenith angle.

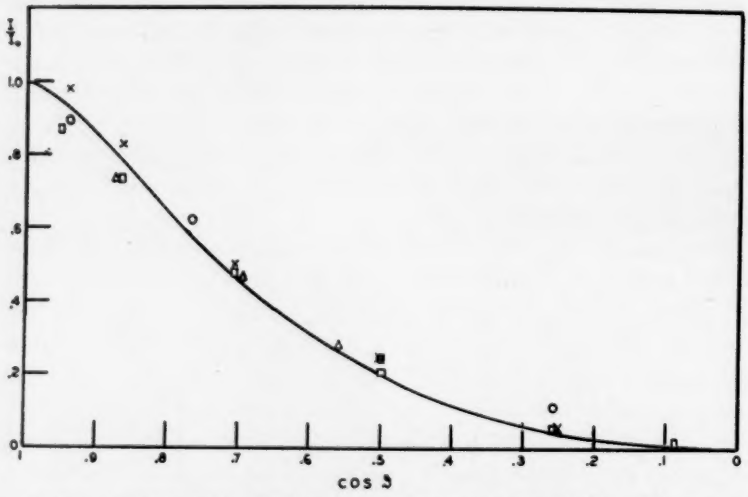

FIG. 4. The angular distribution for mesotrons at sea-level. The curve is the calculated distribution. The designation of the experimental points is as follows: ○, Bernardini, × Cocconi and Tongiorgi, □ Bernardini and Bocciarelli, △ Greisen. Both calculated and observed results are normalized to unity at zero zenith angle.

The computed angular distribution is shown in Fig. 4 together with the experimental points obtained from the observations due to Bernardini,[20] Cocconi and Tongiorgi,[21] Bernardini and Bociarelli [22] and Greisen.[23] It may be seen

[20] G. Bernardini, *Nat.*, **129**, 578 (1932).
[21] G. Cocconi and V. Tongiorgi, *Phys. Rev.*, **57**, 1180 (1940).
[22] G. Bernardini and D. Bocciarelli, *Ric. Sci.*, **1**, 3 (1935).
[23] K. Greisen, *Phys. Rev.*, **61**, 212 (1942).

that the agreement between the calculated curve and the data is as good as the agreement between the results of the various observers. In the absence of greater consistency in the experimental results one may only conclude that the theory is in accord with the measurements within the experimental error.

It may be noted that the theoretical angular distribution corresponds only roughly to a $\cos^2 \vartheta$ variation which is the form usually assumed. The distribution found conforms quite closely to the $\cos^2 \vartheta$ for intermediate angles (30°–40°) but decreases more rapidly for larger angles where it behaves as $\cos^{2.3} \vartheta$.

A further assumption may be verified by the above comparison. It has been supposed that the effect of scattering may be neglected. If an appreciable amount of scattering took place the angular distribution as observed would systematically deviate from the calculated one in the direction of greater isotropy. Since no systematic discrepancy of this kind is evident, the assumption of the negligible importance of scattering would seem to be justified.

From the calculated angular distribution one may obtain the integral angular distribution which may be of interest for certain experimental arrangements in which a limited solid angle is subtended by the apparatus. Thus,

$$\phi(\vartheta_0) = 2\pi \int_0^{\vartheta_0} (I/I_0) \sin \vartheta d\vartheta \qquad (19)$$

gives the total intensity at sea-level, in units of the vertical intensity, as determined by a detecting instrument which subtends the solid angle $2\pi(1 - \cos \vartheta_0)$. The result is shown in Fig. 5 where ϕ is given as a function of $\cos \vartheta_0$. No measurements are available for comparison.

VII. ABSORPTION IN LEAD AND OTHER MATERIALS.

The importance of the assumption of the absorption mechanism in dense materials, that is, energy loss by ordinary electromagnetic collisions, has been emphasized in the foregoing. The experiments designed to furnish some confirmation of this assumption are largely concerned with absolute measurements of the absorption coefficient in a given absorb-

ing material and with the comparison of the absorption in different materials.

The experiments in which we are interested are those involving the use of comparatively thin absorbers, that is, layers sufficiently thin so that the energy loss in the material is small compared to the energy at which radiative losses are of importance. For lead this restricts the consideration to thicknesses small compared to 10^3 meters water equivalent (100 meters Pb), and for absorber of atomic number 13 the

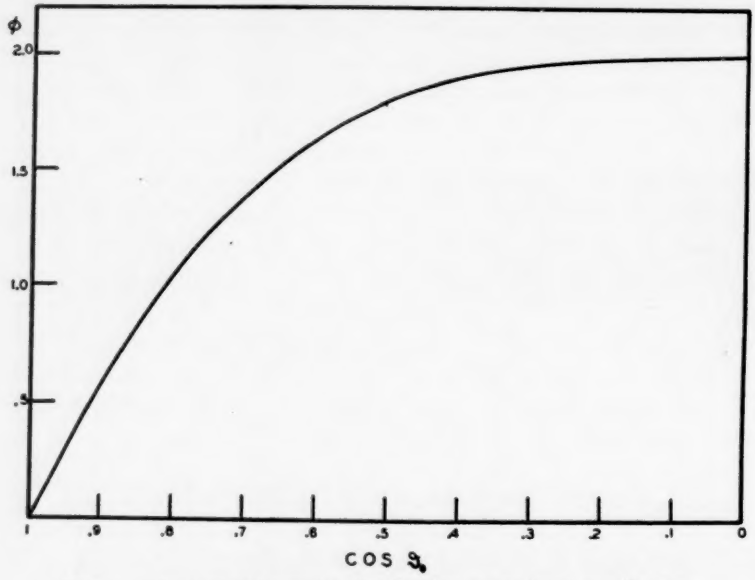

FIG. 5. The integral angular distribution at sea-level, see Eq. 19.

pertinent thicknesses must be small compared to 6,000 meters water equivalent. These thicknesses are well above those involved in the experiments. As a consequence, the intensity of the rays emerging from the absorber is mainly due to mesotrons which have suffered only ionization loss.

We consider first the comparative absorption data which evidently provides a measure of the dependence of ionization loss on atomic number. It is customary to present the data in the form of equivalent absorber thicknesses where the implication is equal absorber efficiency. More precisely, the

observed value of the ratio of absorption coefficients (measured in cm.$^{-1}$) in the two materials is compared with the calculated ratio of atomic electron densities, since according to (3) the rate of energy loss per cm. is, aside from the insensitive logarithmic factor, proportional to $\rho Z/A$, or the number of electrons per unit volume.[24] These ratios which are supposed to be identical within the experimental error, are identified with the inverse ratio of equivalent absorber thicknesses. An examination of the data, however, reveals what appears to be a discrepancy since materials of low atomic number absorb more strongly than is expected.

Against this method of analyzing the data two objections may be raised. First, the comparison of absorption coefficients and electron densities implies that the former is equal to the rate of energy loss, within a factor independent of the material, or very nearly so. Actually the absorption coefficient depends on the energy distribution of the mesotrons incident on the layer and, as will be shown below, for different materials the pertinent portion of the spectrum will be different. It must be admitted that this fact is due to the nonconstancy of the rate of energy loss but, while the energy loss varies slowly, the effect on the energy distribution and on the absorption coefficient due to this slow variation is in this case fairly important. The second objection is concerned with the definition of equivalent absorber thicknesses. The most useful definition is one based directly on what is measured. Thus, we define equivalent thicknesses of two materials as those thicknesses which will reduce the intensity of mesotrons at a given place by the same amount.[25] This definition would be equivalent to that used above according to which the thickness ratio is the reciprocal of the ratio of absorption coefficients, provided these coefficients were independent of thickness. Actually this is not the case.

In the following we consider mesotrons incident in the direction of the zenith and at first we shall consider the ab-

[24] E. G. Steinke and H. Tielsch, *Zeits. f. Physik*, **84**, 425 (1933); H. Tielsch, *ibid.*, **92**, 589 (1934); A. Sittkus, *ibid.*, **108**, 421 (1938).

[25] See, e.g., M. A. Pomerantz and T. H. Johnson, *Phys. Rev.*, **59**, 143 (1941). In the definition given it is essential to specify the incident energy distribution in terms of the amount and nature of material between the absorber and sea-level. Obviously, the angular distribution of the particles is of importance also.

sorption at sea-level. A total of N_s mesotrons are incident on the absorbing plate of thickness t and the number transmitted will be denoted by $N_1(t_1)$ or $N_2(t_2)$ to distinguish between two different materials. It will be convenient to introduce what may be called the attenuation coefficient k according to

$$k_i = -\frac{1}{N_s}\frac{dN_i}{dt_i}. \tag{20}$$

The absorption coefficient κ is then given by

$$\kappa_i = -\frac{d}{dt_i}\log N_i = \frac{N_s}{N_i}k_i. \tag{21}$$

For vanishing thickness the two coefficients become identical.

The number of transmitted mesotrons is, as before,

$$N_i = \int_{\epsilon_i}^{\infty} F_s(\epsilon)d\epsilon, \tag{22}$$

where ϵ_i is the minimum energy required to penetrate the thickness t_i (Eq. 5a). Then we have from (20)

$$k_i = B_i(\epsilon_i)F_s(\epsilon_i)/N_s \tag{23}$$

and from (23)

$$\kappa_i = k_i\left(1 - \int_0^{t_i} k_i dt\right)^{-1}. \tag{24}$$

The dependence of the attenuation and absorption coefficients on thickness is of interest. Since the energy ϵ_i is rougly proportional to the thickness it follows from the form of the sea-level distribution (Fig. 1), that at large thickness the attenuation coefficient k_i decreases rapidly (about as $t^{-\gamma}$). At small thicknesses the factor $F_s(\epsilon_i)$ increases while $B(\epsilon_i)$ decreases with increasing t. However, as may be seen from (12) and (3), F_s varies more rapidly and over a wider range. Thus for small t the attenuation coefficient increases and a maximum is attained for some intermediate thickness. This behavior is depicted in Fig. 6 where k for Pb and a light material (see Section V) is given as a function of thickness. Due to the decrease with thickness of the factor in the denominator of (24) the absorption coefficient κ, also given in

Fig. 6, decreases less rapidly than does k and the maximum is considerably flatter. Nevertheless, it is apparent that the assumption of constant absorption or attenuation coefficient is an extremely crude one.

According to the definition given above, the equivalent thicknesses, t_1 and t_2, of two materials are related by

$$\int_0^{t_1} k_1 dt = \int_0^{t_2} k_2 dt. \tag{25}$$

The thickness of light material t_L equivalent to a given thickness of Pb, t_{Pb}, is at once obtained by (25) using the attenuation coefficients given in Fig. 6. The results, when t_i is

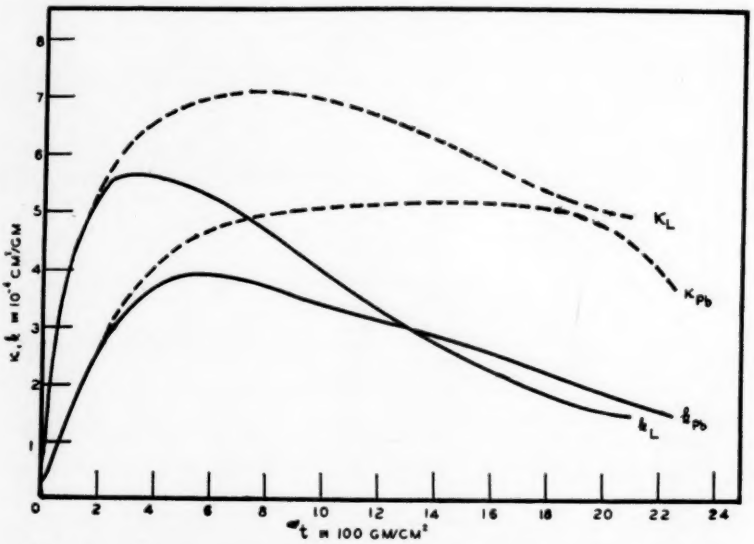

FIG. 6. The attenuation coefficient k and the absorption coefficient κ (Eqs. 20 and 21), for Pb and a light material ($Z/A \approx \frac{1}{2}$, $10 < Z < 15$). The ordinate gives the coefficients in units of 10^{-4} cm.²/g. while the abscissa gives the layer thickness in units of 100 g./cm.² or meters water equivalent.

expressed in g./cm.², are shown in Fig. 7. It is remarkable that despite a non-constant attenuation coefficient the ratio of equivalent thicknesses is constant (within the accuracy of calculation and certainly within the error of experiment). For all practical purposes the curve given in Fig. 7 may be

expressed by

$$t_L = 0.75 t_{Pb}. \tag{26}$$

This may be compared with the ratio of equivalent masses based on the ratio of absorption coefficients as given by Tielsch:[24] 0.78 for Fe/Pb, 0.78 for Al/Pb, 0.55 for H_2O/Pb and 0.65 for C/Pb.

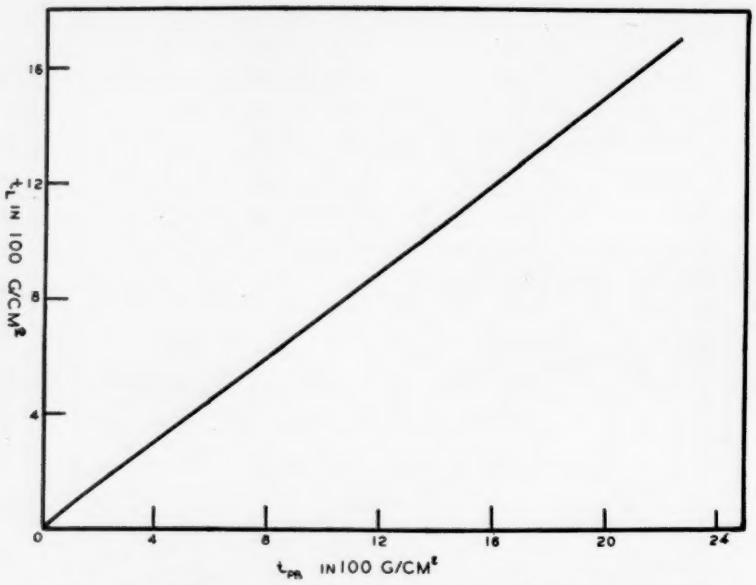

FIG. 7. The thickness of light material t_L equivalent in stopping power to a thickness t_{Pb} of lead. Both t_L and t_{Pb} are given in units of 100 g./cm.². The average slope of the curve is 0.75.

Having obtained the attenuation coefficient we may compare the calculated absorption with the observations for a given material. The relative intensity transmitted is

$$\frac{N}{N_s} = 1 - \int_0^t k dt. \tag{27}$$

Fig. 8 shows the theoretical absorption curve for Pb at sea-level (vertical incidence) and the experimental points taken from the measurements of Nielsen and Morgan,[26] Sittkus,[24]

[26] W. M. Nielsen and K. Z. Morgan, *Phys. Rev.*, **54**, 425 (1938).

Rossi [27] (for thicknesses up to 1 meter of Pb) and of Pomerantz [28] for larger thicknesses. While the experimental results usually indicate a linear absorption (constant k) it should be pointed out that over the range of observation (10–100 cm. Pb) the calculated curve is straight within the experimental uncertainty (of order 10 per cent.). However, a discrepancy of a somewhat more serious nature lies in the fact that the observed absorption coefficient is, in almost

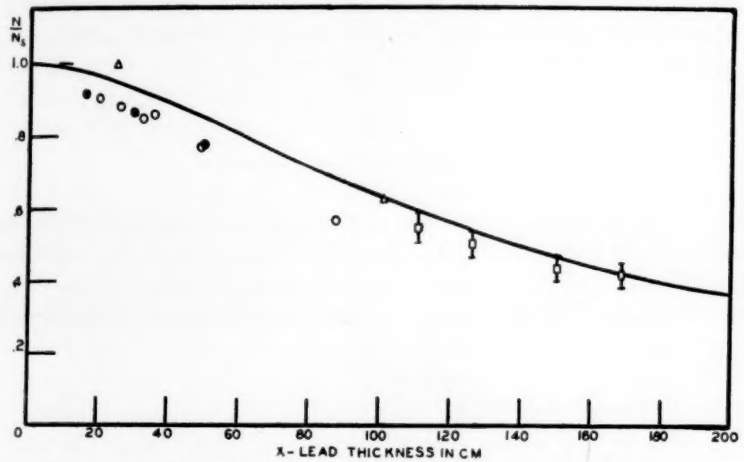

FIG. 8. The absorption of mesotrons in lead for vertical incidence at sea-level. The curve is calculated and the designation of the experimental points is as follows: ○ Sittkus, ● Nielsen and Morgan, △ Rossi, □ Pomerantz. The calculated curve is normalized to unity at zero Pb thickness as are the results of Sittkus and of Nielsen-Morgan. The data of Rossi and of Pomerantz are each fitted to the calculated curve at one point.

every case, larger than the calculated one. For the first meter of Pb the calculations give an average absorption coefficient of 3.9×10^{-3} cm.$^{-1}$ Pb. The data of Nielsen and Morgan give 4.5×10^{-3} cm.$^{-1}$, that of Sittkus 4.9×10^{-3} cm.$^{-1}$ and Rossi's data when fitted at the larger thickness give 5.0×10^{-3} cm.$^{-1}$ Pb. These deviations would seem to lie outside the limit of error of the measurements. At larger thicknesses the data of Pomerantz, when fitted at the point indicated in the figure, gives an absorption coefficient of

[27] B. Rossi, *Zeits. f. Physik*, **82**, 151 (1933).
[28] M. A. Pomerantz, *Phys. Rev.*, **57**, 3 (1940).

2.5×10^{-3} cm.$^{-1}$ Pb compared to the calculated coefficient, averaged over the range of thicknesses concerned, equal to 2.7×10^{-3} cm.$^{-1}$. The comparison in this case is more favorable and it is also satisfying that the theory accounts for the diminution of absorption with increasing thickness.

The absorption coefficient in Pb has also been measured at various depths below sea-level. Thus, for mesotrons incident in the zenith, the Pb absorption coefficient at 20 meters water below sea-level is 3.0×10^{-3} cm.$^{-1}$ (measurements from 10–100 cm. Pb).[29] At 60 meters water below sea-level the absorption coefficient is 2.3×10^{-3} cm.$^{-1}$ according to the measurements of Nielsen and Morgan.[26] This decrease of the absorption coefficient with depth can also be understood from the theory.

Suppose the depth of rock or other material at which the Pb absorption measurements are made is t_1 and the incident intensity is $N_1(t_1)$. The thickness of Pb is t_2 and the intensity at this thickness is $N_2(t_2)$. Let ϵ_2 be the minimum energy required to penetrate the Pb alone and ϵ_1 the corresponding energy at sea-level; that is, the energy required to just penetrate the rock and Pb together. Then if B_1 and B_2 denote the rate of energy loss in rock and Pb respectively, we find

$$k_2(t_1) = B_2(\epsilon_2) \frac{B_1(\epsilon_1)}{B_1(\epsilon_2)} \frac{F_s(\epsilon_1)}{N_1(t_1)}. \tag{28}$$

If the thickness t_1 is much greater than t_2, as is approximately the case, we can write

$$k_2 \approx \kappa_2(t_1) \approx -0.8 \frac{d}{dt_1} \log \frac{N_1}{N_s}, \tag{28a}$$

where we have used $B_2(\epsilon_2)/B_1(\epsilon_1) \approx 0.8$. Using the absorption measurements of Wilson [19] which can be expressed in the form

$$N_1/N_s = (1 + t_1/t_0)^{-\gamma'}, \tag{28b}$$

where $\gamma' \approx 1.8$ ($t_1 \leq 280$ meters water) and t_0 is the atmospheric thickness, we find

$$k_2 \approx \frac{0.8\gamma'}{t_0} \frac{1}{1 + t_1/t_0}. \tag{28c}$$

[29] V. Wilson, *Phys. Rev.*, **53**, 908 (1938).

The decrease of Pb absorption coefficient with depth is thus directly related to the decrease of the absorption coefficient in rock. The result (28c) is too rough to allow a significant quantitative comparison with the observed values.

The results obtained in this section are of interest in still another connection. Because of the prime importance of obtaining direct evidence for decay in the form of cloud chamber photographs of the disintegrating mesotron, it is essential to examine the way in which the number of slow particles depends on the thickness of absorber placed above the chamber. As is evident from the definition (20), the number of slow mesotrons is proportional to the product of the attenuation coefficient k and the range of these mesotrons. Since the range depends only on the definition of a "slow" mesotron (e.g. ionization equal to twice the normal value associated with fast particles), the dependence of the intensity on thickness is given by the attenuation factor. The number of slow mesotrons beneath a given thickness of lead is therefore proportional to k_{Pb}.[30] From Fig. 6 it is seen that the addition of Pb up to 50 cm results in a rapid increase in the number of slow mesotrons. However, for larger thicknesses the number of such mesotrons decreases so that the thickness given is an optimum value. While the existence of an optimum thickness is, perhaps, not obvious it is to be understood very simply: The number of slow mesotrons is essentially the number in a narrow energy band at the top of the absorber which have just enough energy to penetrate the layer. For increasing thickness this band is selected from a portion of the sea-level distribution which lies at ever-increasing energy and the number of mesotrons in this band (which is of practically constant width) varies with thickness essentially as the sea-level distribution varies with energy. The behavior here predicted is in qualitative agreement with preliminary observations obtained in this laboratory.[31]

[30] If account is taken of the fact that there is, in addition to the lead, usually some amount of light material (wood, concrete, etc.) above the chamber, the number of slow particles becomes proportional to the attenuation coefficient as given by (28). Since for large lead thicknesses this is proportional to the value of k for lead alone, the conclusions are qualitatively the same in this case as those given below.

[31] R. P. Shutt, unpublished.

VIII. ABSORPTION AT ELEVATIONS ABOVE SEA-LEVEL.

The procedure utilized to calculate the energy distribution and intensity of mesotrons at sea-level may be applied to obtain the intensity in the atmosphere as a function of elevation above sea-level. Retaining the assumption of a production layer at 1.0 meter water equivalent below the top of the homogeneous atmosphere, the results of the calculation should show how serious this assumption is. At the same time an indication of the importance of mesotron production at lower elevations may be obtained.

The energy distribution for vertically incident mesotrons has been calculated for the elevation of Mt. Evans, 6.2 meters water equivalent below the top of the homogeneous atmosphere. The procedure used is as given in Section IV and the appendix. From the energy distribution the intensity relative to that at sea-level is readily determined. With a lifetime of 2.1×10^{-6} sec. we find for the ratio of intensities at Mt. Evans to that at sea-level the value 1.98. The observed value [32] is 2.25. The difference is significant and cannot be explained by errors of calculation or experiment.

It is essential to note that the calculated ratio is based on the extrapolation of the $\epsilon^{-2.9}$ energy distribution in the formation layer down to $\epsilon = 12.8$ which is the minimum energy required for transmission through the 5.2 meters water from the assumed position of the formation layer to the Mt. Evans elevation. Of course, no evidence can be cited in support of this extrapolation and it is moreover rendered uncertain by the necessity of some modification of the energy distribution due to latitude effect. This arises from the exclusion of slow primary particles by the action of the magnetic field of the earth.[33] If anything, it is more plausible to assume that the extrapolation of the distribution (8) overestimates the number of slower mesotrons and therefore gives too large a value for the relative intensities at elevations above sea-level. Hence the source of the discrepancy noted above is to be sought elsewhere.

---

[32] B. Rossi, N. Hilberry and J. B. Hoag, *Phys. Rev.*, **57**, 461 (1940). See also reference 5.

[33] T. H. Johnson, reference 2.

By far the most plausible reason for the low value of the calculated intensity ratio is the possibility that mesotron production occurs much below the assumed position of the formation layer. It is readily seen that if this is the case the increase of intensity for the elevation of Mt. Evans, for instance, would be greater than that for sea-level. Consequently, the calculated ratio would be increased as the data demands. If the discrepancy between calculated and observed intensity ratios is to be entirely attributed to production of mesotrons at lower elevations, then the results presented above indicate appreciable mesotron production at elevations comparable with the 4,300 meters at Mt. Evans. Essentially the same arguments have been used by Greisen [23] to arrive at the same conclusion. Finally, this conclusion is in accord with the observations of Regener and Regener and Rossi.[34]

APPENDIX.

The decay integral, upon which the energy distribution depends, can be written in the form (cf. Eq. 12a)

$$D(R_s) = \int_{R_s}^{R_0} \frac{dR}{\eta - R} \frac{1}{p(R)}, \qquad (1A)$$

where $\eta = R + t$ is a constant for the integration (Eq. 12b). Obviously, the lower limit R_s may refer to the range at other elevations than sea-level. The integral can be evaluated numerically for each energy by some procedure as the method of trapezoids. However, since we are interested in the values of D over a wide energy range (from $\epsilon \leqq 0.1$ to about 500) it is necessary to compute the integral for many points in the energy scale. Again, the integrand varies rapidly, especially in the region where it has its largest values, and it is necessary to resort to a rather fine division of the range scale in order to obtain a reasonably accurate value for D. Finally, the results of a straightforward integration would apply for only one elevation and it would be necessary to repeat the process for other elevations. A method which avoids many of these objectionable features has been devised and is described below.

[34] V. H. Regener, *Phys. Rev.*, **61**, 105 (1942); V. H. Regener and B. Rossi, *Phys. Rev.*, **58**, 837 (1940).

It is clearly advantageous to carry out the integration in an analytical way so far as this is possible, and for this it is necessary to find an analytical representation of the range-momentum relationship. It is also essential that this representation be valid especially at low energies and that it be such as to permit the integration to be carried out in a not-overcomplicated manner. For this purpose it was found most suitable to introduce functions which vary slowly. First, we note that the momentum is roughly proportional to the range and therefore it is convenient to introduce R/p in (1A). This also suggests the introduction of $\log R$ instead of R as a variable of integration. This has the advantage that R/p is then a slowly varying function of the integration variable over the entire range of integration. We may therefore replace the integrand, or R/p, by a series of straight line segments.

$$R/p = a_\nu + b_\nu \log R, \qquad R_{\nu-1} \leq R \leq R_\nu, \tag{2A}$$

where the R_ν are selected points chosen so that the straight line segments give a good representation of the function R/p. In many cases only one or two such straight lines are necessary. It will be noted that once the representation (2A) is fixed it applies for all elevations.

We now introduce the function $G(R)$ according to

$$G(R) = \int_{R_m}^{R} \frac{dR}{\eta - R} \frac{1}{p(R)}, \tag{3A}$$

where R_m is smaller than the minimum value of the range for which the decay integral will be evaluated: $R_m = 1$ g./cm.^{2} is a suitable value. Evidently, we have

$$D(R_s) = G(R_0) - G(R_s), \tag{4A}$$

so that it is sufficient to evaluate $G(R)$. In view of (2A) this function will be expressed as a series of terms of the form

$$G_\nu(R) = \int_{R_{\nu-1}}^{R_\nu} \frac{dR}{R(\eta - R)} (a_\nu + b_\nu \log R), \tag{5A}$$

where the first R_ν is R_s and the last is R_0. The integration (5A) is readily carried out. We introduce y as an integration

variable where

$$y = \frac{R}{t}, \qquad \frac{\eta y}{1+y} = R, \qquad \frac{dR}{R(\eta - R)} = \frac{dy}{\eta y}.$$

Then the integral (5A) becomes

$$\begin{aligned} G_\nu(R) &= \frac{1}{\eta}\int_{y_{\nu-1}}^{y_\nu} \frac{dy}{y}\left(a_\nu + b_\nu \log \frac{\eta y}{1+y}\right) \\ &= \frac{1}{\eta}\left\{(a_\nu + b_\nu \log \eta)\log \frac{y_\nu}{y_{\nu-1}} \right. \\ &\qquad \left. + b_\nu[J(y_\nu) - J(y_{\nu-1})]\right\} \end{aligned} \tag{6A}$$

where

$$J(y) = \int_1^y \frac{dy}{y} \log \frac{y}{1+y}. \tag{7A}$$

$J(y)$ cannot be evaluated in closed form but is easily evaluated in terms of rapidly convergent series. We have

$$\begin{aligned} J(y) &= -\frac{\pi^2}{12} + \frac{1}{y} - \frac{1}{2^2y^2} + \frac{1}{3^2y^3} - \cdots, \qquad y > 1, \\ J(y) &= \tfrac{1}{2}(\log y)^2 + \frac{\pi^2}{12} - y + \frac{y^2}{2^2} - \frac{y^3}{3^2} + \cdots \\ &= \tfrac{1}{2}(\log y)^2 - (y-1) + \frac{(y^2-1)}{2^2} \\ &\qquad - \frac{(y^3-1)}{3^2} + \cdots, \qquad y < 1. \end{aligned} \tag{7'A}$$

The method of evaluating the decay integral D now consists in first computing R/p as a function of $\log R$. Then, having chosen a suitable representation of the form (2A) the values of a_ν, b_ν are fixed and for a given point of observation (t), the values of y_ν are prescribed. From the curve of $J(y)$ plotted against y (Eq. 7'A) the values of $J(y_\nu)$ can be read and $G_\nu(R)$ computed from (6A). In this way for each value of t it is not difficult to find the function $G(R)$ and hence the decay integral D at sea-level and at other elevations.

Bomb Shelters in Hudson Palisades Proposed.—(*Compressed Air Magazine*, Vol. 48, No. 2.) Mr. George C. Atwell, a prominent New York contractor, has made a suggestion for utilizing the Palisades, bordering the Hudson River directly across from New York City, for bomb shelters. The scheme embodies measures similar to those taken at Chungking, Dover, the Island of Malta, and Gibraltar, where underground galleries offer the citizenry and even some essential industries refuge from bombings. The topography and geological features of the Palisades are highly favorable to the plan. The cliffs rise sheer from the west side of the river to a height of 200 feet and more, extend for several miles along the stream and have a horizontal thickness of approximately 1½ miles throughout that section. They are composed of doleritic rocks which were intruded from subterranean lava reservoirs and spread out laterally between the horizontal beds of sedimentary deposits that formed the surficial covering. During the intervening centuries—geologists estimate the age of the Palisades at 150,000,000 years—the softer sedimentaries were worn away, exposing the igneous rocks. Along their eastern edge a deep gorge was cut by the Hudson River, and this was followed by a period of general subsidence, accompanied by filling of the stream bed with silt to its present level. Mr. Atwell, who says the plan was suggested to him by John C. Evans, chief engineer of the Port of New York Authority, proposes to drive a tunnel, 200 feet wide and 100 feet high, through the Palisades at a point just above the high water level of the river and emerging in the meadows of New Jersey to the westward. Within the depths of the sheltering rock he would enlarge this passageway to provide immense, pillar-supported rooms to serve as airplane hangars, depositories for national art treasures, sites for vital manufacturing plants, and havens during air raids for a large number of people living in the environs. All this, Mr. Atwell contends, could be accomplished with equipment and materials that are plentiful. As the rock, which is already penetrated by several transportation tunnels, is self supporting, no buttressing steel would be required.

R. H. O.

A QUANTITATIVE EVALUATION OF THE INFLUENCE OF THE LITHOSPHERE ON THE ANOMALIES OF GRAVITY.*

BY

ROSS GUNN,

Technical Adviser, U. S. Naval Research Laboratory, Washington, D. C.

ABSTRACT.

A quantitative investigation is made of the influence of a strong elastic lithosphere on departures from isostasy. Isostasy is shown to be a special case of a more general principle that may be called the principle of isobaric equilibrium. This principle which expresses the condition for vertical equilibrium is formulated quantitatively both in terms of the resultant vertical stresses in the lithosphere and in terms of measurable gravity anomalies. Employing the principle, a stress function may be determined that permits an estimate of the fraction of the uniform superposed load carried by the lithosphere. By applying this method, it is found that for the central region of a block to be in substantial isostatic adjustment (96 per cent.), the linear dimension of the load must approximate 330 Km., a value more than six times that often assumed. The basic constant characterizing the elastic deformations of the lithosphere is determined by appeal to geological data from deltas and regions near a thrust fault. The values so obtained suggest a value of 50 ± 15 Km. for the effective thickness of the lithosphere. The deformed figures of the lithosphere for certain special types of load have been worked out together with the stress function that measures both the gravity anomaly and the resultant vertical stress.

Modern ideas concerning the equilibrium of the lithosphere were introduced about 1855 when J. H. Pratt prepared, as a result of his studies in India, an extensive report on the figure of the earth. Measurements were made between two places in northern India separated by an angle of $5° 23' 42.294''$ as determined by a careful triangulation. Observations at the same stations by astronomical means led to a value which differed from that just mentioned by 5.236 seconds of arc. It was at first suggested that this discrepancy was due to the gravitational attraction of the Himalaya Mountains some 60 miles north of the point of observation, but Pratt showed that if the Himalayas had a density of 2.75, the discrepancy

* The opinions or assertions contained herein are the private ones of the writer and are not to be construed as official or reflecting the views of the Navy Department or the naval service at large.

should have been three times that observed. A year or so later George B. Airy discussed the discrepancy and advanced the idea that an unusually high mountain was analogous to a "log whose upper surface floats much higher than the upper surfaces of others." The original ideas proposed by Airy and Pratt have been examined in the light of numerous observational facts by many scientists and these have established the principle of isostasy, but only as applied to very large sections of the earth's crust. Wm. Bowie [1] writes, "According to the principle of isostasy, if the earth's crust were cut into prisms of the same cross-section by imaginary vertical planes, the prisms would have the same mass if the isostatic conditions were perfect." The principle of isostasy as developed within the last 30 years has thus been built upon the hypothesis of constant mass per unit area in these prisms which extend downward to some selected level where the strength of the crust in shear becomes quite negligible.

As a general rule, the difference between the calculated and the observed values of the acceleration due to gravity or the isostatic anomalies in undeformed and level country or over most of the ocean are satisfactorily low. However, in recent years as methods for correcting for elevation, density, and topography have become more accurate, and detailed data have become available, it has become increasingly clear that many regions of the earth are definitely not in isostatic adjustment. Misleading statements have frequently appeared in the literature of geology suggesting that these isostatic anomalies imply an unstable geological structure even though observational evidence is available showing that in such regions no actual geological activity is in progress. The basic concepts of isostasy, therefore, need review and modification so that known departures can be interpreted quantitatively in terms of fundamental physical laws. R. A. Daly [2] has well summarized the difficulties with present ideas concerning the term "isostasy" by writing ". . . its acceptability and its real value demand a certain vagueness in its definition." "Although phrased in terms of lithosphere and asthenosphere, an

[1] Wm. Bowie, Bull. No. 78, Nat. Res. Council, p. 103.

[2] R. A. Daly, "Strength and Structure of the Earth." Prentice-Hall, 1940, p. 340.

exact statement of thickness for either earth-shell is now out of the question." In this paper we will attempt to remove the "demanded vagueness" and answer, in part at least, fundamental questions regarding the strength and thickness of the lithosphere. It will be shown that in addition to isostatic forces, the vertical superposed stress in the lithosphere at any selected point must be considered and specified before any statement can be made as to the stability of any section of a continent or ocean bottom.

IDEAL ISOSTASY.

Consider a new born earth made up of rock material at such a temperature that its strength in shear is negligible. After circulation and mixing have acted for a few million years, such an earth will, except for a thin surface shell, approach the hydrostatic state characterized by: (*a*) a steadily increasing density toward the center; (*b*) the coincidence of surfaces of equal density, equal pressure and equal gravitational potential; and (*c*) a thin and probably floating surface layer of light rock.

Suppose that great prisms of continental rock are ultimately formed at the surface by selective crystallization or some other means and that these aggregates are systematically less dense than the underlying weak molten rock. Obviously they will be supported and, according to Archimedes' principle, will float in such a way that the weight of each prism will be exactly equal to the weight of the displaced underlying magma. Consider a number of prisms supported in the above manner, all of different but comparable density. Assume that each prism is self supported and *no friction whatever exists between the lateral faces.* Then if a reference prism is selected and if the acceleration due to gravity is measured on it, making suitable corrections for the distance of the observing station above some reference level, and for the figure of the earth, it will be found that the measured values on all prisms will not appreciably differ. This is a consequence of the laws of gravitational attraction and potential theory which show that to a sufficient approximation the vertical acceleration due to a horizontal plane plate of considerable extent is given by

$$\Delta g = 2\pi\gamma M, \qquad (1)$$

where Δg is the change in acceleration or the gravitational defect due to the plate, M is the mass per unit area of the plate, and γ is the gravitational constant. If the plate is not extensive, corrections must be applied, but Eq. (1) will represent the principal term. Since the mass per unit area of the floating block is on the average exactly equal to the mass per unit area of the displaced liquid, and since by Eq. (1) the gravitational defect depends on this quantity, it is clear that different thicknesses or densities of a floating block will not produce important changes in the measured value of the acceleration due to gravity. Because such a system of freely floating blocks will show a constant gravitational acceleration at some selected level, we may describe the state as one of ideal isostasy.

DEPARTURES FROM IDEAL ISOSTASY.

Suppose the separate prisms considered in describing ideal isostasy are brought into contact. Frictional and cohesive forces between the vertical faces of the prisms now prevent the individual adjustment of each. For example, select a central prism and assume that sediments are piled on it alone. If this prism were supported only by the weak asthenosphere, it would sink in the substratum and displace a weight of material exactly equal to that added. Due, however, to the assumed forces of friction acting on the prism, this cannot take place. The applied load attempts to force the prism down but now, because it is mechanically associated with the neighboring prisms, they are forced down while the original prism is supported by shearing stresses to exactly the same extent. Thus under the selected prism not enough mass is forced out laterally to support it from the bottom, and part of the support is supplied by vertical shearing stresses appearing on the vertical faces of the prism. Conversely, as a result of such stresses, considerable material is forced out from under the adjacent prisms even though no load of sediments is applied to them. Of course, considering the aggregate of prisms, just enough material is displaced to carry the superposed load of sediments on the original prism and a condition of regional isostasy is achieved.

The deficiency or excess of mass displaced from under any prism is readily calculated in terms of the applied force or the

vertical stress. For simplicity, consider a prism of unit cross-section supported ideally by the substratum. Suppose this prism is pushed down by an added load of sediments, by some arbitrary vertical force acting on unit area, or by shearing stress due to the finite strength of the lithosphere. This force per unit area is the vertical resultant stress S. This stress, acting on a freely moving prism, will displace substratum material of density d until a restoring stress equal to the weight of the displaced liquid restores equilibrium, or

$$S = M'g, \tag{2}$$

where M' is the mass per unit area of the displaced material. It is clear, therefore, that a downward or positive resultant stress from any source whatever results in a deficiency of mass under the prism, while an upward stress results in an excess of mass. If this change in mass is assumed to be a flat sheet, the principal term of the accompanying gravitational defect Δg by Eqs. (1) and (2) is

$$g\Delta g = -2\pi\gamma S, \tag{3}$$

where γ is the gravitational constant and g is the acceleration due to gravity in the region where the displaced substratum is forced out. Attention is directed to the fact that, due to the frictional forces or cohesive forces acting on the vertical faces of the prisms, these prisms are just as much in equilibrium as if they were supported ideally from the bottom. It follows from the above discussion that if the resultant vertical stress distribution can be determined for any arbitrary load on the lithosphere either by measurement or by calculation, then it is possible to evaluate the gravity anomalies associated therewith. Conversely, a knowledge of the space distribution of gravity anomaly and mass permits an estimate of the vertical superposed stresses and the resulting deformations of the lithosphere. Subsequent paragraphs consider two interesting cases in which the distribution of the vertical stress or the stress function can be determined.

ISOBARY, A CRITERION FOR THE STABILITY OF THE LITHOSPHERE.

Because the lithosphere is everywhere supported on a substratum having negligible strength, it is now possible to

establish the criterion for vertical equilibrium in any selected prism. In the asthenosphere below the lowest section of the lithosphere, we adopt some surface of equal pressure or equal gravitational potential as a reference. If an applied vertical load on the lithosphere should increase the pressure at this selected level, transient horizontal pressure gradients will be set up that force the weak rock outward more or less horizontally until the constancy of pressure over the selected equipotential surface is reëstablished. Calculations suggest that such transient states last only about 25,000 years and therefore are not of much geological interest. It is a property of the hydrostatic state that when constancy of pressure is reëstablished, the system is in equilibrium. Now the pressure at this selected level is made up of three components, namely: (*a*) the weight per unit area of the column of weak rock extending from the reference level up to the lithosphere; (*b*) the weight per unit area of the column that extends from the bottom of lithosphere to the surface; and (*c*) the vertical stress imposed on the column by the finite strength of the lithosphere or by some superposed load. The total pressure arising from (*a*) and (*b*) may be conveniently written $M\bar{g}$ where M is the average mass per unit area lying above the reference equipotential surface and $\bar{g}$ is the average gravitational acceleration in any selected prism.

The criterion for vertical stability therefore is

$$P = M\bar{g} + S = \text{Constant}, \qquad (4)$$

where P is the pressure at the selected equipotential or isobaric level and S is the superposed vertical stress. The relation is generally applicable even though each prism may be rigidly attached to its neighbors. S is taken to be positive when it acts in the direction of $\bar{g}$ or downward. This exact result, discussed by the author in an earlier paper,[3] may be stated in words as follows: For sections of the lithosphere to be in stable or isobaric equilibrium it is necessary and sufficient; in prisms reaching from a selected surface of equal

[3] R. Gunn, "Quantitative Study of Mountain Building," JOUR. FRANKLIN INST., **224**, 19, 1937.

T. A. Elkins, *Geophysics*, **7**, 45, 1942.

pressure in the asthenosphere to the actual surface, that the the average externally applied *vertical stress* added to the product of the mean *mass per unit area* and the average acceleration due to *gravity, shall be a constant.*

When the lithosphere is adjusted to this condition, one may conveniently say it is in isobaric equilibrium, since the word isobaric implies equal pressure. Isobary * is, therefore, the state of vertical mechanical equilibrium even though it permits real anomalies of gravity to exist. Obviously isobary reduces to isostasy as a special case in level regions where vertical stresses are negligible. It is convenient practically to pick some standard column as a reference. A suitable column might be like Heiskanen's [4] isostatic standard column except in most cases it would include a portion of the asthenosphere. It is important, however, to select the standard column near the center of a large undeformed region. At such a place one may be assured that the superposed vertical stresses usually due to deformation are small and the regional isostatic adjustment is nearly ideal, irrespective of the finite strength of the lithosphere. Now if gravitational measurements at other places are compared with those of such a reference point, it is clear that gravity anomalies will be an indication of vertical stress. Eq. (3) may be combined with Eq. (4) and the principle of isobaric equilibrium written in the approximate but useful form

$$P = M\bar{g} - \frac{g\Delta g}{2\pi\gamma} = \text{Constant.} \qquad (5)$$

This relation may be made exact if the geometrical distribution of stress, mass and topography is available in any given case. The principle of isobaric equilibrium as here expressed, together with observed numerical values for the gravity anomalies, provide a valuable tool for the study of lithospheric equilibrium, particularly special geological structures that are definite exceptions to the principle of isostasy as usually defined.

* C. E. Dutton considered the use of the term isobary to describe isostasy in 1889 but rejected it for reasons that now appear trivial.

[4] W. Heiskanen, *Gerlands Beiträge für Geophysik*, 36, 201, 1932.

DEFORMATIONS OF A HYDROSTATICALLY SUPPORTED ELASTIC LITHOSPHERE.

The lithosphere of the earth is the outer shell that is capable of maintaining relatively large shearing stresses for long periods of time. This outer layer is supported everywhere by the underlying asthenosphere that is assumed to have no such strength. The lithosphere, below about 10 Km. is subject to a vertical compressive stress that exceeds 3.10^9 dynes/cm.^{2} Such a stress can initiate plastic flow in any ordinary rock so that voids due to fracture probably cannot exist. Further Bridgeman's experiments [5] strongly suggest that fractures occurring under such circumstances will be self-healing. For this reason it seems logical to suppose that, except for the upper 5 or 10 Km. that may be traversed by many fractures, the lithosphere is usually a homogeneous sheet covering the earth, and one may discover its properties by considering the deformations produced by known loads superposed thereon. The mathematical complications imposed by three dimensional solutions make such investigations most laborious and impractical. However, several important two dimensional problems may be solved and these, because of the essentially linear nature of many earth features, are capable of giving an adequate description of the properties of the lithosphere. In the following discussions we consider the deformations of the lithosphere in sections taken at right angles to long linear blocks of sediments, long narrow oceanic deeps, and continental boundaries. On comparing these idealized sections with earth geology, a good quantitative idea of the fundamental physics involved in the production and maintenance of such surface features may be derived. It will be shown in this and succeeding papers that a lithosphere having uniform elastic properties and finite strength will explain in some detail most of the observed anomalous departures from isostasy. Moreover, a proper application of the principles of isobary as outlined above shows that many regions heretofore classed as questionable are, in fact, in definite mechanical equilibrium even though large gravity anomalies exist.

Exclude the upper 5 kilometers of the earth's crust and consider a section of a uniform lithosphere resting on magma

[5] P. W. Bridgeman, *Jour. Geology*, **44**, 666, 1936.

that supports it hydrostatically. For convenience assume that the section is of unit width, effective thickness T, its uniform elastic modulus is E, and its section moment of inertia is I. Reference to any good text on strength of materials will show that as such a section or beam is deformed, the radius of curvature r is given by

$$\frac{1}{r} = \frac{M_1}{EI}, \tag{6}$$

where M_1 is the magnitude of the bending moment at the point where r is measured. The product EI is called the flexural rigidity and is a fundamental constant of the lithosphere. Now if we ignore the square of small quantities in the factors which determine r and neglect the slight curvature of the earth, both of which are permissible, it follows that

$$EI\frac{d^2y}{dx^2} = -M_1, \tag{7}$$

where y refers to the vertical deflection of the neutral axis of the section, and x is the coördinate measured along its length. As a general thing, M_1 is an unknown factor in the case of the lithosphere so that Eq. (7) is differentiated twice, yielding the useful form

$$EI\frac{d^4y}{dx^4} = -\frac{dV}{dx} = -\sigma_v, \tag{8}$$

where V is the shear per unit width and σ_v is the resultant restoring stress applied to the section as a result of its deformation. If the neutral axis of the original undeformed section coincides with the x axis and if vertical displacements are produced by superposed loads or even by horizontal compression,[3] these vertical displacements will force out the underlying magma and produce a counter-stress

$$\sigma_1 = d_0 g y, \tag{9}$$

where d_0 is the density of the underlying magma and y is the downward displacement. It is clear that the deformation at the surface is substantially the same as that calculated for the neutral axis. Further, if the y displacement results from the loading of the section by sediments of density d washing

into the region, the resultant restoring stress is evidently

$$\sigma_2 = (d_0 - d)gy, \tag{10}$$

whence combining Eqs. (8) and (10)

$$-EI\frac{d^4y}{dx^4} = \sigma = (d_0 - d)gy \tag{11}$$

or, since I the sectional moment of inertia per unit width is $T^3/12$, one may write the basic equation that describes the deformation of the lithosphere as

$$\frac{ET^3}{12}\frac{d^4y}{dx^4} + (d_0 - d)gy = 0. \tag{12}$$

This expression may be compared with reference 3, Eq. (10), which contains another term involving the tangential compressional stress.

The solution of Eq. (12) is of the form

$$y = \epsilon^{-bx}(A\cos bx + B\sin bx) + \epsilon^{+bx}(C\cos bx + D\sin bx). \tag{13}$$

It is reasonable to suppose that the deformations of the crust are zero at great distances from any system of forces near the origin, so that one may set $C = D = 0$. The values of A and B depend on the boundary conditions of the particular problem under investigation.

Consider first the simplest case of a continuous section in which a downward force F is applied at the origin, and because the section is horizontal there, it is easily shown that $A = B$. The vertical deflection, therefore, is

$$y = \frac{3F\epsilon^{-bx}}{2ET^3b^3}(\cos bx + \sin bx), \tag{14}$$

where

$$b^4 = \frac{3(d_0 - d)g}{ET^3}. \tag{15}$$

Another useful solution of Eq. (13) corresponds to the case in which the lithosphere is vertically fractured. Select the origin to coincide with the fracture and suppose that a vertical force F and simultaneously a bending moment M_0

are there applied. The force F may be due to the overriding of an adjacent section, or it may be due to some externally applied force. The solution for this case is readily shown to be

$$y = \frac{6\epsilon^{-bx}}{b^3ET^3}[F\cos bx - bM_0\cos bx + bM_0\sin bx]. \quad (16)$$

Upon comparison with Eq. (14) it may be seen that the maximum deflection of a broken beam for a given vertical load is four times that of a continuous one. Thus, the most unusual geological characteristics of the lithosphere will appear in such regions of failure. The deflection of the lithosphere in all these cases is evidently wavelike in character, the wave-length λ being $2\pi/b$. For convenience and reference, Eqs. (14) and (16) have been plotted in Fig. 1, employing identical constants and taking $M_0 = 0$.

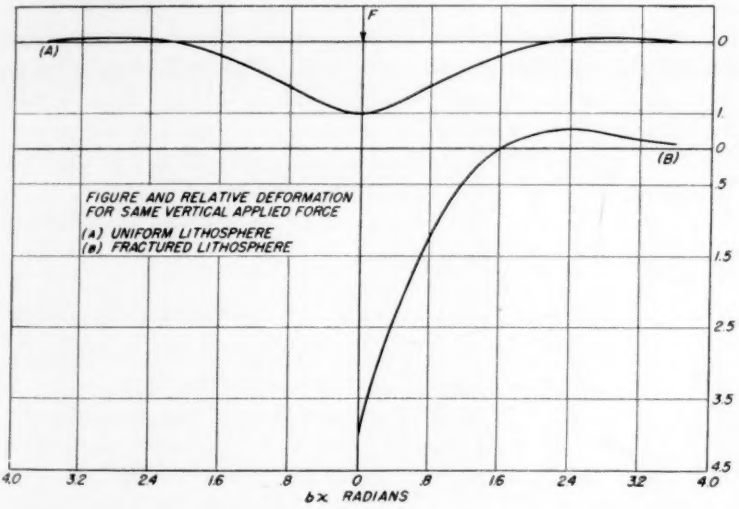

FIG. 1.

Because most loads on the earth are distributed over a considerable area, it is important to calculate with greater accuracy the deformation of the lithosphere due to any arbitrary linear distribution of load. Suppose that the section is continuous, uniform, of unit width, and that a load W per unit length is applied. The deflection dy due to

an element of this load Wdx is, by Eq. (14), obviously

$$dy = \frac{3W\epsilon^{-bx}}{2ET^3b^3}(\cos bx + \sin bx)dx, \tag{17}$$

where x is the distance from the point at which the elementary load Wdx is applied to the point where the beam is deflected a distance dy. Eq. (17) has been integrated for certain important load distributions but we here consider only uniform loading. Select the origin as the point at which the total deflection y is to be evaluated. Then if the superposed uniform load per unit area $h_0dg = W$ extends from $x = -L$ to $x = N$, Eq. (17) may be evaluated. The total deflection at the origin is found to be

$$y = \frac{h_0d}{4d_0}[4 - 2\epsilon^{-bN}\cos bN - 2\epsilon^{-bL}\cos bL], \tag{18}$$

where d is the density of the superposed block, d_0 that of the substratum, and h_0 is the height of the block. In this relation y may be expressed more conveniently as a function of a new variable x measured from the center of the block. Evidently then $N = m + x$ and $L = m - x$, where $m = (N + L)/2$, so that

$$y = \frac{h_0d}{d_0}[1 - \tfrac{1}{2}\epsilon^{-b(m+x)}\cos b(m + x) - \tfrac{1}{2}\epsilon^{-b(m-x)}\cos b(m - x)]. \tag{19}$$

Now if $m + x \gg 1/b$, that is, if the block has reasonably large dimensions compared to $1/b$, then Eq. (19) may be further reduced to a form most useful near the boundary of the block or

$$y = \frac{h_0d}{d_0}[1 - \tfrac{1}{2}\epsilon^{-bq}\cos bq], \tag{20}$$

where q is measured inward from the end of the block. Because the lithosphere just under the end of the block is a point of inflection and $M_1 = 0$ there, it is easy to show that for distances p measured away from the edge of the block

$$y = \frac{h_0d}{2d_0}\epsilon^{-bp}\cos bp. \tag{21}$$

It should be clear that in all of these relations the amplitude of any deformation decreases from its maximum value to zero in distances varying from $x = \pi/2b$ to $x = \pi/b$ so that b is evidently a most important lithospheric constant. Its value and significance will be discussed in a later section.

FRACTION OF SUPERPOSED LOAD CARRIED BY LITHOSPHERE AS A FUNCTION OF LOAD SIZE.

One of the important problems of isostasy is the determination of the size of the smallest superposed load that will be substantially in isostatic adjustment. This size is especially important in evaluating regional isostatic anomalies. The critical size may readily be calculated from the above relations and the principle of isobaric equilibrium. Let Z be the distance from the top of the originally undeformed lithosphere to the selected uniform pressure level in the asthenosphere and T be its thickness. Then $Z - T$ is the distance from the bottom of the lithosphere to the reference level. Further, let d be the density of a superposed block of sediments of height h_0, D be the density of the lithosphere, and d_0 be the density of the underlying magma. Without loss of generality, one may suppose that the acceleration due to gravity g is constant. At the assumed reference level the pressure outside the deformed region is

$$p_0 = [Z - T]d_0g + TDg \tag{22}$$

while the pressure at the same reference level under the deformation is

$$p_u = h_0dg + TDg + (Z - T - y)d_0g + S_v. \tag{23}$$

But by the principle of isobaric equilibrium and Eq. (4) these pressures are identical and may be equated to each other. Thus it is found that

$$S_v + h_0dg - yd_0g = 0. \tag{24}$$

This may be generalized and the *isobaric stress function* written as

$$S_v = yd_0g - Q, \tag{25}$$

where Q is the applied load per unit area at a selected point, y is the downward deformation of the lithosphere and S is

the vertical stress provided by the finite strength of the lithosphere at the same point. As before, a downward stress is taken to be positive. It will be noted that Eq. (25) is independent of the density of the lithosphere, and reduces to a statement describing isostasy if $S = 0$. This useful relation will be called the stress function and is invaluable in all discussions involving gravitational anomalies.

Employing Eqs. (19) and (25) one may write

$$-S_v = h_0 dg - y d_0 g = (y_{isos} - y) d_0 g$$
$$= \frac{h_0 dg}{2} \left[\epsilon^{-b(m+x)} \cos b(m+x) + \epsilon^{-b(m-x)} \cos b(m-x) \right] \quad (26)$$

where $y_{isos} = h_0 d / d_0$.

Now because erosion and sedimentation will round off any practical block of the assumed type and transfer material to the adjacent depressions, Eq. (26) can probably not be accurately applied to regions near its boundary. It is possible, however, through this relation to express in regions near the center of the block the ratio of the expected gravitational anomaly to that which would be observed were the load carried by a perfectly rigid lithosphere. This same ratio also is the fraction of the load carried by the lithosphere and will therefore be zero for a region in perfect isostatic adjustment. Employing Eq. (3) and taking $x = 0$ because regions near the edges may not be significant, it is found here that

$$\left(\frac{S_v}{h_0 dg} \right)_{x=0} = \left(\frac{\Delta g}{2\pi\gamma h_0 d} \right)_{x=0} = \epsilon^{-bm} \cos bm. \quad (27)$$

This ratio is plotted in Fig. 2 as a function of bm. It is interesting to note that small negative anomalies are possible even at the center of a large positive load of sediments, provided bm lies between $\pi/2$ and $\frac{3}{2}\pi$. This detail, however, may well be illusitory in geological structures if the erosion of the block edges is considerable. In any case, it is evident from Eq. (27) and Fig. 2 that a lithosphere having a finite strength in shear does not permit a superposed block load to be even in approximate (96 per cent.) isostatic adjustment unless its angular semidimension bm exceeds 1.4. The perfection of isostatic adjustment is measured, of course, by the

fraction of the superposed load carried by the immediately underlying magma, and this in turn is unity minus the fraction of the load carried by the lithosphere. For convenience, the *average* fractional load carried by the lithosphere for blocks of various semidimensions *bm* is also plotted in Fig. 2.

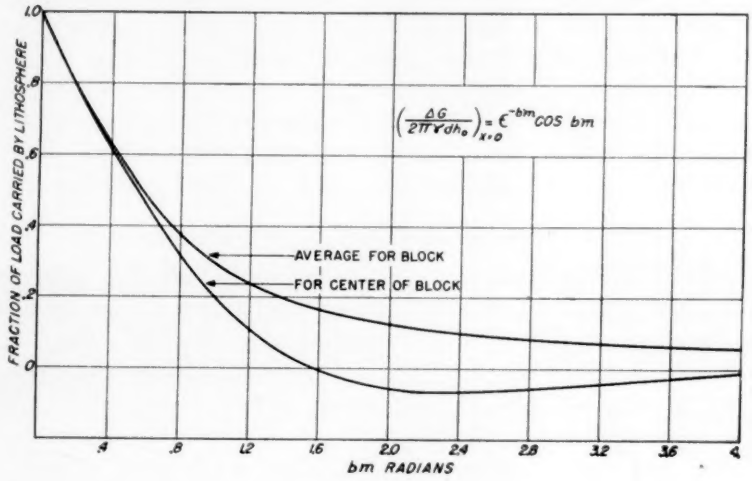

FIG. 2.

Now in order to calculate m the semi-linear dimension of the superposed load for any selected degree of approach to isostasy, it is necessary to know the value of b. Approximate values of b may be calculated immediately from Eq. (15) by assuming a value for the effective thickness of the lithosphere T. If in Eq. (15) one takes $E = 10^{12}$ dynes/cm.^{2}; $d_0 - d = 3$ gms./cm.^{3} (i.e., assume $d = 0$), $T = 10^7$ cm. and $g = 10^3$ cm./sec.^{2}, it is found that $b = 5.4 \cdot 10^{-8}$ cm.$^{-1}$, or if $T = 5.10^6$ cm., b is $8.4 \cdot 10^{-8}$ cm.$^{-1}$. Adopting this latter value as the most probable because of the values deduced in a later paragraph, it follows that a block of at least a semidimension $m = 167$ Km. will be necessary before even its center will approach 96 per cent. compensation or within 4 per cent. of perfect isostatic adjustment. A block of semidimension $m = 25$ Km., or total width of 50 Km., a value sometimes given as the extent of the block necessary to achieve isostatic adjustment, will only be 19 per cent. compensated, and

81 per cent. of the load will be carried by the lithosphere. This lithospheric load is passed on to the asthenosphere in regions outside the block for a distance approximating $1/b$ cm. It seems clear, therefore, that unless the values of the important lithospheric constants employed above are seriously in error, the areas necessary for the establishment of isostatic equilibrium must be at least three hundred kilometers square and the methods currently employed to estimate gravity anomalies are not valid. In a later section, the important constant b is calculated by two other independent methods not related to isostasy and a value approximating that adopted above is found.

GRAVITY ANOMALY AND DEFORMATION NEAR A THRUST FAULT.

We next investigate the distribution of the gravity anomalies that may be expected to result from a thrust fault if isobaric equilibrium is maintained. Assume that the horizontal compressive stress S_h in the lithosphere has been great enough to produce a thrust fault and that the plane of the fault makes an angle φ with the horizontal. Then the downward force at the origin due to the overriding section is $S_h T \cos \varphi \sin \varphi$ where T is the thickness of the section. The stress function acting on the depressed section from Eqs. (16) and (25) is evidently

$$S_v = (d_0 - d)gy = \frac{6(d_0 - d)gS_h \cos \varphi \sin \varphi \epsilon^{-bx} \cos bx}{Eb^3T^2}, \quad (28)$$

whence, from Eq. (3), the gravity anomaly in the depressed region approximates

$$\Delta g = \frac{-12\pi(d_0 - d)\gamma S_h \cos \varphi \sin \varphi \epsilon^{-bx} \cos bx}{Eb^3T^2}. \quad (29)$$

A nearly similar expression may be obtained for the positive anomalies in the overriding region by making allowance for the erosion after the original equilibrium is attained. Upon substitution of $b = 7 \cdot 10^{-8}$ cm.$^{-1}$, $d_0 - d = 2$ gm./cm.^{3} (because the depression is at first filled with water), $T = 5 \cdot 10^6$ cm. and $S = 10^9$ dynes/cm.^{2} it is found that

$$\Delta g = -0.280\epsilon^{-bx} \cos bx. \quad (30)$$

The actual tangential compressional stress acting on the thrust fault cannot be directly evaluated but because thrust fracture and the formation of arcuate mountains cannot take place without sufficient stress to induce considerable plastic deformation, the assumed stress seems reasonable. A value of 2×10^9 dynes/cm.^{2} may be equally probable so that one may only say that Eq. (30) is consistent with the known observational facts and that the maximum anomalies approximate from 200 to 500 milligals. Further, although Eq. (30) implies a sharp discontinuity in gravity anomaly coincident with the fracture, it is clear that erosion and sedimentation will always act to erase such rapid changes.

THE VALUE OF THE LITHOSPHERIC CONSTANT b.

Because the value of the lithospheric constant b is of first rate importance in all discussions of the stress and deformation of the lithosphere, it is of interest to examine various known geological formations to see how b changes under widely varying conditions. In general, one selects simple structures in which the acting forces are both known in position and localized in nature. For example, the downward force acting on a thrust fault is applied at the fault. Gravity anomalies near such a fault are given by Eq. (29) and in many cases may be observed. From Eq. (29) the width of the principal negative anomaly strip and the adjacent principal positive strip are both given by $bx = \pi/2$ whereas the secondary positive strip outside the principal negative region has a width $bx = \pi$. Upon comparison of these values with actual faults, b may readily be determined. There is considerable geological evidence showing that arcuate island or mountain chains result from great systems of tangential stresses in the lithosphere and that this opportunity for overthrusting frequently produces long linear geological features. One of the best examples is the East Indian chain, particularly south of Java, where the geometry of the deformation is remarkably simple and is suitable for comparison with the present calculations. It is assumed that this anomaly strip is a direct result of a long thrust fault.

The gravitational characteristics of the sea south of Java

have been well studied by V. Meinesz [6] and many facts are available that have been summarized in a well known map by van Bemmelen. Scaling from this map it is found that the negative anomaly strip varies in width from 150 to 185 Km. Adopting an average value of 170 Km. and setting this equal to $\pi/2b$ it is found that $b = 9.2 \times 10^{-8}$ cm.$^{-1}$. In the same manner the principal and secondary positive strips yield values for b of 9×10^{-8} cm.$^{-1}$ and 7.8×10^{-8} cm.$^{-1}$ respectively.

As another case of importance, consider the geological implications of Eq. (14) that represents the downward displacement of a continuous section of the lithosphere due to a localized load. The sediments initially deposited at the single mouth of a great river might represent such a great concentrated load, and instead of these sinking at the point of deposition establishing isostatic equilibrium, Eqs. (14) and (27) show that the first sediments deposited will be almost entirely supported by the lithosphere. Therefore, it will be bent down in a wide basin of half width $bx = 3\pi/4$. This wide basin of downwardly deformed ocean bottom encourages the deposition of sediments at a considerable distance from the original mouth, and a great symmetrical delta will be built up whose semidimension at right angles to the axis of its development is $3\pi/4b$. In general, sedimentation will proceed laterally until the downward deflection is filled, at least thinly, to the edge of the original depression. When such a delta is well developed, as in the case of the Nile and Niger Rivers,[7] the fact that no large gravity anomalies are observed guarantees that the piled up sediments on the ocean floor reflect the figure of the downward deformation of the lithosphere. Barrell's data indicate the semidimension $3\pi/4b$ for both of the above-mentioned deltas to be about 300 Km. Thus the characteristic constant for the lithosphere b is found to be $b = 7.85 \times 10^{-8}$ cm.$^{-1}$ or the characteristic distance $1/b = 127$ Km. The average of the four estimates above is $8.4 \cdot 10^{-8}$ cm.$^{-1}$. Perhaps real variations of thickness or modulus of elasticity exist, and one is therefore justified only

[6] V. Meinesz, "Gravity Expeditions at Sea," Vol. 2.

[7] J. Barrell, *Jour. Geology*, **22**, 1914.

in adopting

$$b = 8.4 \pm 2.0 \times 10^{-8} \text{ cm.}^{-1}.$$

Thus the characteristic relaxation distance of the lithosphere is $1/b$ or 120 ± 25 Km.

Further by aid of Eq. (15), one may estimate the effective thickness of the lithosphere by assuming $E = 10^{12}$ dynes/cm^2. and $d_0 - d = 2$ gms./cm.^{2}. From this it is found that $T = 50 \pm 15$ Km., a value that happens to be in fair agreement with that inferred from isostasy using the Airey hypothesis.

CONCLUDING REMARKS.

The foregoing analysis appears to show that the presumed approach of the earth's crust to exact isostatic adjustment has been somewhat exaggerated in the past and that some of the corrections applied to geodetic data have been carried to an accuracy beyond those values actually justified. Large sections of the earth do tend toward a precise regional isostatic equilibrium, but notable departures are necessary in special phases of geological evolution. The formation of great geosynclines, mountains, ocean deeps, and overthrusts at some time in their geological history were all characterized by departures from isostasy even though isobary was approximately preserved. Generally speaking, isostasy describes the equilibrium of the lithosphere to a sufficient approximation in level or undeformed regions but near mountains, continental boundaries, oceanic deeps, or fracture zones, the more general principle of isobary must be employed to account accurately for all the observed phenomena.

In a future paper the methods outlined above will be applied to the study of the Hawaiian mountain range and to continental boundaries.

Reclaiming Worn Files.—(*Iron Age*, Vol. 151, No. 6.) The useful life of an average file can be extended approximately three times its normal life by a reclaiming process used by the R.C.A. Mfg. Co.'s plant at Indianapolis. This process was suggested by Jason R. Harris, a plant employee, who received a W.P.B. certificate of individual production merit for the suggestion. Mr. Harris' suggestion was thoroughly investigated by the plant's engineering department and it was found to be very effective and applicable to files used on both non-ferrous and ferrous metal. At present all files used at the Indianapolis plant are being reclaimed by this method. The reclaiming process is as follows: (1) Clean the file with a wire brush wheel to remove deeply imbedded particles. (2) Clean and rinse file thoroughly, using ordinary degreasing solution. (3) Dip in solution made up of 800 c.c. water, 150 c.c. nitric acid, 100 c.c. sulfuric acid. (4) Cold water rinse. (5) Hot water rinse. (6) Cyanide dip to neutralize. (7) Cold water rinse. (8) Hot water rinse. (9) Dry thoroughly. The time of immersion in the solution (item number three) is dependent upon the condition of the files. Experiments will indicate the best time periods. The minimum dipping time is approximately 1 min. To save time, presorting of the files is recommended. Groups of files showing approximately the same wear should be dipped together. The files should be kept in an upright position while immersed so that the solution can act on both sides. R.C.A. engineers report that some of the rinse steps listed may be eliminated and fairly satisfactory results obtained. However, the steps listed here were found to give the best results. Using this procedure, the total handling time for 25 files is about 30 min.

R. H. O.

THE HORIZONTAL PATH ALONG THE EARTH'S SURFACE OF A PROJECTILE OR PLANE UNDER CONSTANT TANGENTIAL ACCELERATION.

BY

W. S. KIMBALL, Ph.D.,

Lt. Comdr. U.S.N.R., U. S. Naval Academy, Annapolis, Maryland.

OUTLINE.

The additional term in Coriolis' normal force due to the earth's rotation previously derived [1] by vector methods, and resulting from the increased rate of direction change that arises from tangential path acceleration along the surface of the rotating earth, is here derived again by the wedge method of showing normal path displacements. It is further shown that every tangential path acceleration along the surface of the earth rotating at constant angular velocity $\omega_L = \omega \sin \phi$ at latitude ϕ involves additional path curvature, $\frac{d\alpha}{ds} = \frac{3}{2}\frac{\omega_L}{v}$, where v is the velocity, and due to the earth's rotation; and when this curvature is multiplied by the velocity, v_r of the acceleration field, we obtain the extra rate of direction change, $\Delta\omega_L = \frac{3}{2}\omega_L \frac{v_r}{v}$, due to the earth's rotation where tangential acceleration occurs. Thus, Coriolis' force using the entire rate of direction change due to the earth's rotation becomes $2\theta' v = 2v\left(\omega_L + \frac{3}{2}\omega_L \frac{v_r}{v}\right) = 2v\omega_L + 3\omega_L v_r$ as previously derived, and the second term is now seen to arise from the extra path curvature that is due to and occurs with tangential acceleration along the surface of the constantly rotating earth, as well as to the effect itself of the earth's rotation.

A special study is made of the path of a body all of whose energy of motion is due to constant tangential acceleration, such as an ideal airplane of constantly increasing speed. The path is found to be the involute of a circle, and the rate of change of direction is constant and about a degree per

minute in middle latitudes. If 100 miles per hour per hour is taken as the constant tangential acceleration, the plane will completely reverse its direction in about three hours at a perpendicular distance of about 285 miles from the starting point of rest, and at a final speed of about 300 miles per hour. These results are shown to be in accord with the speed and distance requirements of elementary mechanics using only the familiar Coriolis' force term $C = 2\omega_L v$ for constant gradient velocity across a uniform parallel force field on the earth as previously [1] treated.

NO. 1. THE NORMAL FORCE DUE TO TANGENTIAL ACCELERATION FOR HORIZONTAL MOTION ON THE ROTATING EARTH.

We, here, treat the case of horizontal motion on the earth rotating at constant angular velocity $\omega_L = \omega \sin \phi$ at latitude ϕ. The acceleration with respect to fixed coördinates is given by the well-known vector experssion:

$$\frac{d^2s}{dt^2} = \frac{dv}{dt} + 2\omega_L \times v + \omega_L \times (\omega_L \times r), \qquad (1)$$

where v is the velocity relative to the moving earth, and r is the radial distance to an origin on the earth's surface about which a tangent plane rotates, and the Gibbs' notation for vector products is used. The extra term due to rate of change of ω_L is absent since ω_L = constant. Since we are dealing with horizontal motion v and ω_L are perpendicular and so (1) reduces to:

$$\frac{d^2s}{dt^2} = \frac{dv}{dt} + 2\omega_L v - \omega_L{}^2 r$$

Since we here consider motion along the earth's surface rather than out on the tangent plane away from it, we set $r = 0$ and consider the acceleration at the origin where the tangent plane touches the earth:

$$\frac{d^2s}{dt^2} = \frac{dv}{dt} u_r + 2\omega_L v u_\theta, \qquad (2)$$

where the unit vectors u_r and u_θ are taken along and normal, respectively, to the path, and the second term will be recognized as Coriolis' normal acceleration for the constant rate of direction change ω_L.

The present paper is concerned with departures from (2) arising from the fact that ω_L will not give the rate of direction change *due* to the *earth's rotation* where tangential acceleration occurs on a curved path. For example, the rate of direction change for constant speed on a circular path is not the same as when tangential acceleration occurs on the same path.

It was [1] shown by vector methods, such as above, that tangential acceleration along a horizontal path entails an extra rate of change of direction $\Delta\omega_L = \frac{3}{2}\omega_L \frac{v_r}{v}$ *due* to the earth's rotation and expressed in terms of the ratio of the velocity v_r of the acceleration field to the complete velocity v. Previously, v_r was $\sqrt{v^2 - 2H}$ where H is the energy of the harmonic field which is the straight line projection of energy stored at constant speed on the potential energy circle, where it is balanced by the effect of the earth's rotation, and hence contributes nothing to the tangential acceleration field energy with its velocity v_r. We treat now the more general case where the acceleration field energy, necessarily a part of the total energy of motion (relative to the earth's surface) is arbitrary and no longer restricted as above. This gives rise to a corresponding term of the Coriolis' force $K = 3\omega_L v_r$ which, where tangential accelerations exist, is essential to the complete treatment of the problem:

$$2\theta' v = 2\omega_L v + 3\omega_L v_r = C + K,$$

$$\theta' = \omega_L + \frac{3}{2}\omega_L \frac{v_r}{v}, \qquad (3)$$

where θ' is the complete time rate of change of direction due to the earth's rotation and $2\theta' v$ is the complete Coriolis force, given by replacing ω_L of (2) by θ' of (3).

For the case of unit mass going from rest to the steady state of constant gradient velocity across a uniform field, it was found that the work of path deflection was equally divided between the two normal forces C and K, showing that $K = 3\omega_L v_r$ was of the same order of magnitude as the familiar $C = 2\omega_L v$.

Its importance would thus seem to justify a second deri-

vation by the wedge method of showing normal displacements due to constant angular velocity ω_L in case of a given path velocity and acceleration according to Fig. 1. These displacements are shown for constant velocity v, and constant acceleration "a," where it is understood, as usual in calculus, that these are instantaneous velocity and acceleration at a given place and time, the velocity being the distance that would be covered in unit time if the rate of change of distance were kept constant over unit time interval, and similarly with

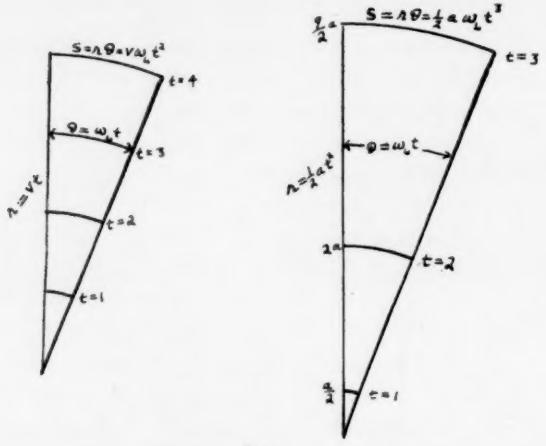

FIG. 1. The normal displacements due to the earth's rotation for constant velocity and constant acceleration along the path.

the acceleration. The normal displacement $s = r\theta$ is expressed in terms of the time t, using the constant angular velocity relation $\theta = \omega_L t$, and radial distances along the path are given by $r = vt$ and $r = \frac{1}{2}at^2$ as in Fig. 1. Thus:

$$s = r\theta = v\omega_L t^2 \text{ for velocity,}$$
$$s = r\theta = \tfrac{1}{2}a\omega_L t^3 \text{ for acceleration,}$$

and the second time derivative of these is:

$$\frac{d^2s}{dt^2} = 2v\omega_L = C,$$

$$\frac{d^2s}{dt^2} = 3at\omega_L = 3v_r\omega_L = K,$$

which are seen to be the same as expression (3) previously derived for the Coriolis' normal acceleration terms due to velocity and acceleration, and we note how v_r comes into the formula for K as the velocity due to tangential path acceleration. In the previous vector treatment the additive nature of C and K was demonstrated * by showing each to be an additive constant of integration obtained by the partial integration of (11)*, yielding K as the constant of integration for (10)* and C as the constant of integration for (13)*. In the present treatment, their additive nature is justified by the elementary fact that displacements due to acceleration may be separated from and superposed upon those due to velocity, to give the resultant effect. Thus for constant initial velocity v_0, and constant negative acceleration $-a$, we have $r = v_0 t - \frac{1}{2}at^2$, and the corresponding normal displacements, shown in Fig. 1, and their time derivatives above, will clearly be of opposite sign and additive (or subtractive) rates of change, and, in general, the resultant normal acceleration becomes:

$$a_N = 2v\omega_L + 3v_r\omega_L = 2v\omega_L\left(1 + \frac{3}{2}\frac{v_r}{v}\right) = C + K, \quad (3)$$

which is the same as (3) above. Here v is the actual velocity of the particle, and v_r is the part of the velocity due exclusively to the tangential acceleration field.

One or two special cases of interest may be noted. Suppose a particle has a constant initial velocity v_0 and negative tangential acceleration $-a$, then, we have for the time $t = 2v_0/5a$;

$$C = 2\omega_L v = 2\omega_L(v_0 - at) = 6/5\omega_L v_0,$$
$$K = 3\omega_L v_r = -3\omega_L at = -6/5\omega_L v_0.$$

This particular time is chosen because it shows a resultant zero value for the normal acceleration (3) since C and K are of opposite sign but equal magnitude.

Another simple case of interest is where a particle starts from rest and the actual velocity is entirely due to the acceleration along the field so that $v = v_r$; then (3) becomes:

$$a_N = 2\omega_L v + 3\omega_L v = 5\omega_L v. \quad (4)$$

* Referring to the corresponding equations in Reference 1.

NO. 2. THE PATH CURVATURE DUE TO TANGENTIAL ACCELERATION ON THE ROTATING EARTH.

The correction term $\Delta\omega_L = \frac{3}{2}\omega_L \frac{v_r}{v}$ to the rate of direction change for horizontal motion involving tangential acceleration on the rotating earth may be shown to be a direct consequence of the path curvature which always results where such motion exists in a tangent plane rotating at constant angular velocity ω_L. Thus, take constant radial acceleration "a." Then, the distance traversed and the angular displacement will be:

$$\begin{aligned} r &= \tfrac{1}{2}at^2, \\ \theta &= \omega_L t. \end{aligned} \tag{5}$$

Elimination of t between these gives the path equation in polar coördinates:

$$\begin{aligned} r &= \frac{a\theta^2}{2\omega_L{}^2}, \\ \frac{dr}{d\theta} &= \frac{a\theta}{\omega_L{}^2}. \end{aligned} \tag{6}$$

Divide the first of (6) by the second to obtain the tangent of the angle between curve and radius vector:

$$\tan\psi = \frac{rd\theta}{dr} = \frac{\theta}{2}. \tag{7}$$

Then the angle of inclination of the path will be:

$$\alpha = \theta + \psi = \theta + \text{arc tan}\frac{\theta}{2}.$$

Hence the curvature is:

$$\frac{d\alpha}{ds} = \frac{d\theta}{ds} + \frac{\frac{1}{2}\frac{d\theta}{ds}}{1 + \frac{\theta^2}{4}} = \frac{d\theta}{ds}\left(1 + \frac{1}{2\left(1 + \frac{r\omega_L{}^2}{2a}\right)}\right). \tag{8}$$

At the origin where the horizontal tangent plane shown in Fig. 2 touches the earth, $r = 0$ and (8) reduces to

$$\frac{d\alpha}{ds} = \frac{3}{2}\frac{d\theta}{ds} = \frac{3}{2}\frac{\omega_L}{v}, \tag{9}$$

where on the right we have introduced $d\theta = \omega_L dt$ and $ds = vdt$ whereby the curvature is restricted to the case in hand of

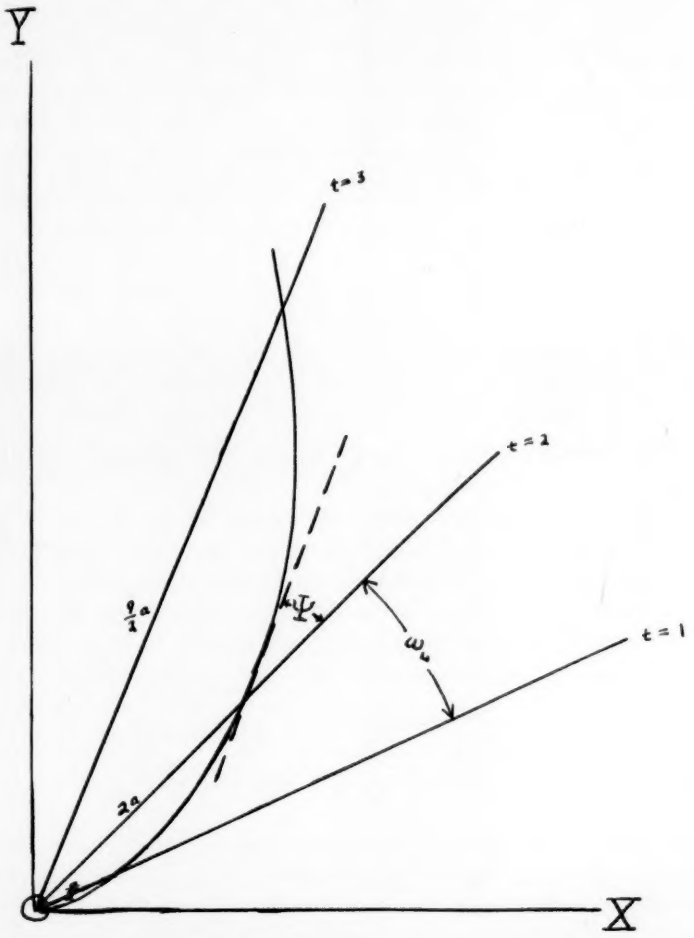

FIG. 2. The curved path where acceleration is along radii that are turning with the earth's constant rotation.

motion with velocity v in a frame rotating with angular velocity ω_L, being measurable physical quantities.

When the curvature (9) is multiplied by $v_r = at$, the velocity of the acceleration field, we have the corresponding

rate of direction change:

$$\Delta\omega_L = v_r \frac{d\alpha}{ds} = \frac{3}{2}\omega_L \frac{v_r}{v}. \tag{10}$$

If the $\overline{XY}$ plane of Fig. 2 were fixed, any particle of velocity v_r pursuing the path there shown will experience a rate of direction change given by (10). If in addition the $\overline{XY}$ plane rotates with angular velocity ω_L, its total rate of direction change will be given by the sum of these two rates:

$$\theta' = \omega_L + \frac{3}{2}\omega_L \frac{v_r}{v}. \tag{11}$$

The above results (9) to (11) are not restricted to the case of constant acceleration "a," but hold for any acceleration where the distance is given by a series instead of (5):

$$r = \tfrac{1}{2}at^2 + bt^3 + ct^4 \ldots, \tag{12}$$

with first and zero power terms absent since we treat only acceleration effect with zero initial velocity and displacement. The path is given as before by removing t by means of $\theta = \omega_L t$. The series expression for the path when divided by its derivative gives a series expression for $\tan\psi$, just as (7) is obtained from (6), and when this is used in (8), the curvature becomes:

$$\frac{d\alpha}{ds} = \frac{d\theta}{ds} + \frac{d\theta}{ds}\left(\frac{1}{2} - \frac{b\theta}{a\omega_L} \ldots\right)$$

for terms below second and higher powers of θ. At the origin where $r = 0$ and $\theta = 0$, this curvature becomes the same as (9), which is thus seen to apply to any acceleration law given by (12), provided only it occurs on the constantly rotating earth where $\theta = \omega_L t$.

We shall now apply the new expression (4) where constant horizontal tangential acceleration is completely responsible for all the motion with $v_r = v$, to obtain the corresponding path equation along the surface of the earth.

NO. 3. THE ROUTE OF AN AIRPLANE TRAVELLING AT CONSTANT HORIZONTAL ACCELERATION ALONG ITS PATH IS THE INVOLUTE OF A CIRCLE OF RADIUS $\epsilon = a/25\omega_L^2$.

It is well known that unit mass actuated by constant velocity on the earth's surface will follow the path of the inertia circle, in absence of outside forces, such as pressure gradient, etc., with the Coriolis force balancing the centrifugal force:

$$C = 2\omega_L v = v^2/r; r = v/2\omega_L, \tag{13}$$

where r, the radius of the inertia circle, is shown in terms of the velocity and the earth's constant rotation $\omega_L = \omega \sin \phi$ at latitude ϕ.

In this section we derive the path which will be followed by unit mass actuated by constant tangential acceleration along the earth's surface and in complete absence of all other outside forces, so that as with (13) the Coriolis force (4) due to the earth's rotation will balance the centrifugal force. No airplane or projectile is, of course, ever actuated by such exclusive acceleration, but if it were, then this is the path it would follow. We take zero initial velocity, so that the velocity of the tangential acceleration field is the same as v, the complete actual velocity, and all of the energy of the acceleration field goes into energy of motion along the path, none of it being lost in the form of energy stored on a potential energy circle, since there is no outside force field to balance it.

Thus instead of (13), we have, using (4):

$$C + K = 5\omega_L v = v^2/r = -v^2 d\alpha/ds, \tag{14}$$

where on the right the curvature is introduced using α for the angle of inclination of the path and s for the distance along the path. Since we have constant tangential acceleration, a, the energy and velocity are given by integration along the path:

$$\int_0^s a\,ds = as = \frac{v^2}{2}; v^2 = 2as. \tag{15}$$

Hence from (14):

$$d\alpha/ds = -5\omega_L/\sqrt{2as}, \tag{16}$$

which integrates to:

$$\frac{\pi}{2} - \alpha = \beta = 5\omega_L \sqrt{\frac{2s}{a}} \tag{17}$$

taking $\alpha = \frac{\pi}{2}$, at $s = 0$, as in Fig. 3, and β is the total angular range of the path. Then:

$$\sin(\pi/2 - \alpha) = \cos\alpha = dx/ds = \sin\left(5\omega_L\sqrt{\frac{2s}{a}}\right) = \sin\beta,$$

$$x = \int \sin 5\omega_L \sqrt{\frac{2s}{a}}\, ds$$

$$= \int \sin\sqrt{\frac{2s}{c}}\, ds = c\int \beta \sin\beta d\beta, \tag{18}$$

where $c = a/25\omega_L^2$, $\beta = \sqrt{\frac{2s}{c}}$ and $ds = c\beta d\beta$.

Upon integrating again, we have:

$$x = c(\sin\beta - \beta\cos\beta) \tag{19}$$

Again taking the cosine of $\pi/2 - \alpha$ as given by (17):

$$\cos(\pi/2 - \alpha) = \sin\alpha = dy/ds = \cos 5\omega_L\sqrt{\frac{2s}{a}} = \cos\beta, \tag{20}$$

and with the same substitution as in (18), we obtain by integration:

$$y + c = c(\beta\sin\beta + \cos\beta), \tag{21}$$

where the constant of integration, c, provides that $y = 0$ at the start where $\beta = 0$ according to Fig. 3. Note that the maxima and minima of y occur at $x = \pm c$ where (20) is zero, and the maxima and minima of x occur at $y = 0$ or $-2c$, and that $x = \pm\beta c$ at $y = 0$, as well as at its maxima on the line $y = -2c$. Equations (19) and (21) are well known as the parametric equations of the involute of the circle of radius c shown in Fig. 3, which is the locus of the centers of curvature of the involute.

Elementary mechanics affords a check on the path shown

in Fig. 3, as may be seen by comparing it with the path followed in a uniform force field on the rotating earth by unit mass starting from rest, as shown in Fig. 2 of the previous [1] article. In that case, the path extended distance $b = a/8\omega_L^2$ along the direction of the force field before attaining gradient

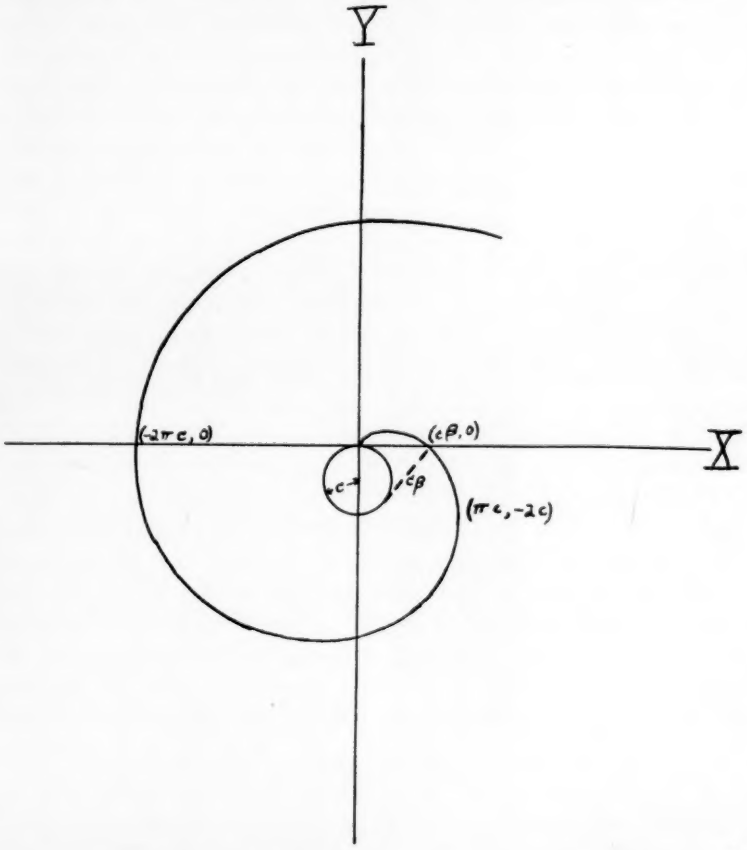

FIG. 3. The involute of the circle of radius $c = a/25\omega_L^2$ which is the path of a plane or projectile actuated by constant tangential acceleration "a" along the surface of the constantly rotating earth.

rectilinear velocity across the field after a 90° deflection. Compare this with the first maximum of x in Fig. 3 where the derivative of x given by (18) is zero, and hence β, the angular

path range is π and by (19) $x_m = \pi c = \pi a/25\omega_L^2$ after a 180° path deflection.

The notable thing about these two perpendicular distances, b and x_m, from the starting point of rest is that they are approximately equal (compare (22) and (25) below) with, for b, a 90° deflection and for x_m a 180° deflection, using the same acceleration, a. This shows that the deflecting force of the present case of Fig. 3 averages about twice as great as for the previous problem, since the angle is doubled for about the same normal distance to the starting point, a result which checks the mechanics of the situation. For, while the present problem involves no field acceleration to resist deflection, the previous case of a uniform parallel field, supplied a force squarely against the y component of the deflecting force due to just such a field resistance and extending over half the angular range in making a 90° turn. Thus for the uniform parallel field half the angular deflection is to be expected in about the same distance from the starting point. Moreover this distance, b, was seen to be independent of the path and entirely determined by the classical Coriolis term $C = 2\omega_L v$, so that when the deflection angle is doubled in the absence of a resisting field of acceleration as in the present case of Fig. 3, the result is seen to be consistent with and thus checked by this classical mechanics.

We may compute this first maximum of x given by (19) when its derivative (18) is zero. It occurs where the angle of path deflection $\beta = \pi$ (see Fig. 3) and we may take for middle latitudes $\phi = 53°$; $\sin\phi = .8$, so that $\omega_L = \omega \sin\phi$ becomes 4/5 the rate of the earth's rotation about its polar axis, i.e. $\omega_L = 12°/\text{hr} = \frac{\pi}{15}$ rad./hr. Thus using (19), we have

$$x_m = \pi c = \frac{\pi a}{25\omega_L^2} = \frac{225a}{25\pi} = \frac{900}{\pi} = 286 \text{ miles.} \qquad (22)$$

If we assume a small * but constant acceleration of 100 miles

* 100 miles/hr.^{2} $= \frac{4.4}{9}$ inches/sec.^{2} = about $\frac{1}{2}$ inch/sec.^{2} = about $1\frac{1}{4}$ thousandths of the acceleration of gravity. For large accelerations leading to distances comparable with changes in latitude, ω_L would not be constant and a corresponding modification of the present treatment would be required.

per hour [2], then (22) becomes about 286 miles as shown on the right.

From the distance formula for constantly accelerated motion and the relations between a, β, c and s given by (18) we have:

$$s = \tfrac{1}{2}at^2 = \tfrac{1}{2}c\beta^2 = \tfrac{1}{2}a\left(\frac{\beta}{5\omega_L}\right)^2 \text{ or } t = \beta/5\omega_L. \qquad (23)$$

Hence, we note that when we use $a = 100$, this first maximum, x_m occurs three hours after starting from rest, and at a velocity of 300 miles an hour:

$$t = \beta/5\omega_L = (\pi/5)(15/\pi) = 3 \text{ hours},$$
$$v = at = a\beta/5\omega_L = 300 \text{ miles per hr.},$$
$$d\beta/dt = 5\omega_L = \pi/3 \text{ radians/hr.} = 60^\circ/\text{hr.} = 1^\circ/\text{min.} \quad (24)$$

Thus an airplane actuated by this constant tangential acceleration of 100 miles per hour [2] will completely reverse its direction ($\beta = \pi$) in about 3 hours and at a perpendicular distance of almost 300 miles from its starting point of rest.

On the other hand for the uniform parallel field of acceleration previously discussed the gradient velocity at right angles to the field where the Coriolis force is (13) and equals the field we have, using the above data:

$$a = 2\omega_L v;\ v = a/2\omega_L = 100/2 \times 15/\pi = 240 \text{ miles/hr.}$$

and the perpendicular distance from the starting point is

$$b = a/8\omega_L{}^2 = 100(225)/8\pi^2 = 285 \text{ miles} \qquad (25)$$

for $\beta = \pi/2 = 90^\circ$ or half the angular deflection of (22).

REFERENCES.

[1] The Special Form of Coriolis' Compound Centripetal Acceleration Due to the Rotating Earth, by W. S. Kimball, Ph.D., U. S. Naval Academy, Annapolis, Maryland. JOURNAL OF THE FRANKLIN INSTITUTE, **234**, p. 453 (1942).

Glass Fiber.—Parachute flare shades woven of glass fibers are being used to shield Army bombing planes and the eyes of bombardiers from the glare of flares dropped to illuminate the target. Field telephone cable used by the Signal Corps is now made with a tension core of glass yarn to replace the metal formerly used for this purpose. Navy deck motors employ glass fiber insulation because of its resistance to dampness. These and other Army and Navy uses of glass fiber materials were described by Major Hubert D. Keiser, Services of Supply Resources and Production Division, United States Army, in an address at the 158th meeting of the American Institute of Mining and Metallurgical Engineers at the Engineering Societies Building, New York City. The glass cloth parachute flare shades are used in connection with brilliant magnesium flares of about one million candle power which are employed to illuminate the objective of a bombing attack with almost the brilliance of daylight. If the light of the flare were not shielded overhead the bombardiers could not see the ground because of the intense glare, and the attacking planes would be revealed to enemy anti-aircraft positions. A light flare shade is therefore required, just above the incandescent element. Glass cloth, darkened with a colloidal graphite finish, is able to meet the requirements because it is light in weight and can withstand the intense heat of the flare. Describing Navy uses of glass fiber materials, Major Keiser said, "The most important single property required of materials used in Navy ships is incombustibility or fire safety. Reliability under extreme conditions of service is the primary requisite of equipment, and reduction of weight is always desired to increase fire power, cruising radius, or speed. For these reasons fibrous glass is extensively used in Navy cables, motors, generators and fire controls." Aircraft uses of glass fiber materials, according to Major Keiser, include glass fiber blankets for heat and sound insulation in hull and cabin, according to type of ship.

R. H. O.

NOTES FROM THE NATIONAL BUREAU OF STANDARDS.*

CONGRESS OF PHYSICS AT PUEBLA, MEXICO.

The First National Congress of Physics was held under the auspices of the Governor of the State of Puebla, the Rector of the University of Puebla, and the Director of the National Astrophysical Observatory of Tonanzintla, at Puebla City, Mexico, on May 3 to 8, inclusive.

Approximately 50 members were present, including the following from the United States who received special invitations from the President of Mexico to attend the Congress: Dr. J. G. Baker, Harvard University; Dr. J. W. Beams, University of Virginia; Dr. P. W. Bridgman, Harvard University; Dr. L. J. Briggs, National Bureau of Standards; Dr. S. Chandrasekhar, University of Chicago; Watson Davis, Science Service; Dr. W. V. Houston, University of California; Dr. L. D. Leet, Harvard University; Dr. I. I. Rabi, Columbia University; Dr. Harlow Shapley, Harvard University; Dr. W. F. G. Swann, Bartol Foundation of the Franklin Institute; and Dr. O. R. Wulf, United States Weather Bureau.

The regular sessions were held at the University, with certain special lectures at the University and at two of the city's theatres. At the opening session, the delegates were welcomed by Dr. C. Gonzalo Bautista, Governor of the State of Puebla. After the president of the Congress, Dr. Manuel Vallarta (formerly professor at Massachusetts Institute of Technology), had taken the chair, Governor Bautista presented the Cross of Honor of the State of Puebla to Dr. Harlow Shapley in recognition of his achievements in galactic astronomy.

In addition to five special evening conferences, seven regular sessions were held at which 45 papers were presented. Many of the visiting American scientists reviewed fields of activity with which their names are closely associated. They were later given a special audience by the President of

* Communicated by the Director.

Mexico, and many other outstanding courtesies were extended.

A most interesting feature of the Congress was a visit to the new Mexican astrophysical observatory located near Puebla with Popocatepetl towering in the distance. Work in this observatory is devoted largely to the study of galaxies, and the observatory is equipped with a very fine Schmidt reflector for this purpose. Here also is located the new seismograph recently purchased by the Mexican Government. At present the seismological stations in our eastern States are able to get a good north-south range on seismological disturbances in the Caribbean, but an east-west range for this region has been lacking. The new seismological station will provide the much-needed intersecting range and thus fix the center of the disturbances.

Great interest was shown by the Mexican scientists in the progress of research in the United States. In his address on the relation between the Government and scientific investigation, Dr. Briggs referred to the fact that the International Bureau of Weights and Measures at Paris is at present isolated from the republics of the world. In recognition of this condition, the Secretary of Commerce had requested him to convey the message that "the National Bureau of Standards will be most happy to carry out for the Mexican Government, and for other American republics, without cost, any comparison of your standards with our own that you may deem desirable." This invitation was the subject of much favorable comment, and a special article on the work of the National Bureau of Standards was published in one of the leading newspapers.

EFFECT OF AERATION ON SOILS.

A number of investigators have studied the change in pH value of soils in passing from the moist field condition to the air-dried state. It is evident from these studies that drying of soils is occasionally accompanied by a slight change in reaction, generally in the direction of increased acidity. Since the air-dried soil offers a more uniform basis, the soil in this condition is generally used for determining the pH value.

Samples of a poorly-drained soil showed large differences in hydrogen-ion concentration between the fresh soil and the soil in the air-dried condition. By varying the degree of aeration, the soil was passed through a cycle—from neutrality, as found in the natural field condition, to high acidity, which occurs in the air-dried state. As a result, it has been concluded that pH measurements of very poorly-aerated soils should be made only on samples maintained in the field condition. The change in pH value observed has been associated with the activity of sulfate-reducing bacteria.

The conclusions reached in this study, which will be reported in detail by Melvin Romanoff in a forthcoming issue of the magazine *Gas*, have an important bearing on the location of soil areas which are corrosive because of the activity of sulfate-reducing organisms. As these bacteria function only within a narrow pH range, the reaction of the soil is considered to be an important criterion in identifying corrosive areas where these bacteria are active.

ULTRAVIOLET SOLAR RADIATION.

Sun bathing and the resulting burns from overexposure of the untanned skin attest to the importance of reliable information on the amount of biologically effective ultraviolet radiation from the sun and from the whole sky, under various weather conditions.

For some years W. W. Coblentz and R. Stair have investigated the instruments and methods of evaluating the biologically effective component of ultraviolet solar and sky radiation useful in heliotherapy; including instruments for measuring ultraviolet radiation incident on a surface exposed normal to the sun, and instruments exposed horizontally to receive the direct solar rays and also the rays incident from the whole sky. The latter instruments are useful to meteorologists in their studies of ultraviolet climatology.

The instruments (photoelectric cells) now used in making ultraviolet radiation measurements are highly selective in their spectral response. Moreover, thus far it has been impossible to reproduce photocells having exactly the same response, which should, preferably, cover only the biologically

effective ultraviolet of wave-lengths shorter than about 3200A. It is this radiation that produces vitamin D and is effective in preventing and curing rickets; also in curing lupus and other skin diseases.

In the June *Journal of Research* (RP1542), measurements of ultraviolet solar radiation are given, as obtained with photocells differing widely in spectral response. If and when manufacturers succeed in making photoelectric cells in which the response range is identical, and is preferably one that coincides with the band of wave-lengths that heals lupus, surgical tuberculosis and rickets, that produces vitamin D, etc., the whole procedure used in evaluating biologically effective ultraviolet solar and sky radiation will be greatly simplified.

The data in the present paper show marked variations in the spectral quality and total intensity of the biologically effective component of ultraviolet solar radiation caused by slight changes in turbidity of the atmosphere and by the well-known cyclonic and seasonal changes in ozone concentration in the stratosphere—ozone being very opaque to ultraviolet solar radiation. It is further shown that at a sea-level station in mid-latitude (Washington, D. C.) on the clearest days, the ultraviolet intensity at the noon-hour in midwinter is only about one-sixth that of midsummer.

A TUNGSTEN-IN-QUARTZ LAMP, AND ITS APPLICATIONS IN PHOTOELECTRIC RADIOMETRY.

A paper by R. Stair and W. O. Smith of the Bureau of Plant Industry (RP1543) in the June *Journal of Research* gives constructional data of a tungsten-filament-in-quartz lamp, and discusses its applications to precision filter radiometry. The lamp is adapted for use in calibrating phototubes for spectral and total radiation sensitivity. In its applications, it supplements the spectroradiometer for calibrating phototubes, while employing the tubes with the associated filters used in measuring the radiation under investigation.

The spectral output-radiation from such a lamp depends upon the temperature of the filament, the emissivity of

tungsten, and transmission of the fused quartz envelope. A table of relative black body radiation intensities has been calculated for the range of temperature from 2500° to 2900° K. in the wave-length interval 2,300 to 3,500 Angstroms.

FLASH POINTS OF HEAVY-BODIED PAINTS.

The Tagliabue (Tag) Closed Cup Method for determining flash points is prescribed in certain specifications for paints. The use of this method in tests of heavy-bodied paints, such as the camouflage paint covered by Specification T-1279 of the Corps of Engineers, U. S. Army, is open to question because no stirring device is used to maintain an even distribution of temperature, as is done in the Pensky-Martens tester.

In an article which has been submitted for publication in *American Paint Journal* and in the *Bulletin of the American Society for Testing Materials*, David Busker reports that during tests of heavy paints at the Bureau, wide differences were noted in the results obtained with the two types of tester. In the Pensky-Martens tester, the heat was uniformly distributed throughout the paint, whereas in the Tag Closed Cup tester, the temperatures were higher at the periphery than at the central point where the thermometer is inserted, and corresponded quite closely with the flash-point temperatures indicated in the Pensky-Martens tester.

COMMERCIAL STANDARD FOR MINERAL WOOL.

Commercial Standard CS105-43 for mineral wool, loose, granulated or felted, for use in low-temperature installations, is now available in printed form. It is designed to improve the quality of mineral wool and to set up installation requirements to be followed in insulating refrigerated compartments or cold areas.

Mineral wool is a substance composed of very fine interlaced mineral fiber, having the appearance of loose wool or cotton. It is a fibrous, glass-like material composed principally of silicates of calcium and aluminum and is manufactured from rock, slag, or glass in numerous localities throughout the United States.

This voluntary standard was proposed in April 1942 by the Industrial Mineral Wool Institute. Following several preliminary meetings a proposed commercial standard was prepared and submitted to manufacturers and to technical, distributor, and consumer organizations for their comment. The standard was then adjusted according to the composite recommendations of those concerned and circulated to the trade for written acceptance. It covers minimum physical and chemical requirements for mineral wool, as well as for auxiliary materials used in insulating cold areas. Detailed descriptions and diagrams are included in the pamphlet to illustrate the proper way to insulate various types of construction, as well as the minimum thickness of insulation required for various operating temperatures.

Printed copies of CS105-43 are obtainable from the Superintendent of Documents, Government Printing Office, Washington, D. C., at 5 cents each.

THE FRANKLIN INSTITUTE.

NEW MEMBERS OF THE FRANKLIN INSTITUTE ELECTED, DECEMBER 1, 1942, TO MAY 1, 1943.

HONORARY MEMBERS.

Dr. Carl Van Doren
Dr. George Washington Pierce
Dr. Harold C. Urey

ACTIVE LIFE MEMBER (NON-RESIDENT).

Mr. Sidney R. Lindboe

SUSTAINING MEMBERS.

Mr. Charles M. Alrich
Mr. Harry Alfred Eberhardt, Jr.
Mr. Lionel L. Jacobs
Mr. Frank Koons
Mr. Harry M. Pflager
Mr. Joseph P. Rainey
Mr. John S. Smith
Mr. Stanley Switlick
Mr. George C. Tatem
Mr. William F. Wagner, Sr.
Mr. C. J. Waterman

ACTIVE MEMBERS WITH FAMILY PRIVILEGES.

Mr. Edward A. Allison
Mr. Samuel B. Amsterdam
Mr. J. Paul Austin, Jr.
Mr. Louis Back
Mr. Albert Bailey
Mr. W. Heston Bailey
Mr. Somerville N. Baker
Mr. Aaron Batchelor
Mr. Joseph Earl Borton
Mr. Louis L. Borucki
Mr. David Brein
Mr. Bennett K. Burris
Mr. C. Jack Cohan
Mr. Edward Corner
Mr. Paul Chrstos, Jr.
Mr. Ralph Cornell
Mr. Jesse G. Croll
Mr. Lloyd H. Daub
Mr. Michael Donnelly
Mr. William H. Dorrance
Mr. Walter C. Eberhardt
Mr. Abraham Ehrlich
Mr. French McC. Emmons
Mr. Harold N. Ewertz
Mr. Samuel S. Feldgoise
Mr. Edward J. Fisher
Mr. Wilmot Fleming
Mr. William N. Force
Mr. Frederick W. Fox
Mr. Philip Frank
Mr. Alex A. Gettlin
Mr. Joseph M. Goldberg
Mr. N. R. Guilbert, Jr.
Mr. Walter F. Graham
Mr. W. Howard Green
Mr. Theodore C. Hammel
Mr. Robert S. Harrison, Jr.
Mr. Jesse G. Haydock
Mr. J. Albert Herz
Mr. Joseph P. Hoffner
Mr. Frank J. Hoguet
Mr. Oskar Huber
Mr. John F. Igoe
Mr. Fred Jessar
Mr. Nelson Kelley
Mr. W. O. Kellogg
Mr. John E. Kieffer
Mr. William K. Kimbel
Mr. Stanley C. Kirn
Mr. W. A. Kofke
Mr. Charles La Scala
Mr. Samuel Lashof
Mr. Horace M. Laurence
Mr. John W. Lewis
Mr. Albert E. Lipp, Jr.
Mr. William Lu
Mr. George A. Lyons
Mr. Patrick L. Mackey
Mr. Charles F. May
Mr. John J. McCarthy

Mr. J. A. McPeak
Mr. Charles A. Miller
Mr. William Moennig
Mr. J. G. Morris
Mr. Herbert S. Murphy
Mr. George F. Nelson
Mr. Carl F. Norberg
Mr. Robert Odlen
Mr. Harry K. Pape
Mr. Joevert G. Parks
Mr. Ernest Peacock
Mr. Henry J. Perazzoli
Mr. G. M. Pfundt
Mr. George K. Porter
Mr. Robert W. Radcliff
Mr. Albert L. Reidl
Mr. Philip F. Ries
Mr. D. Rosenberg
Mr. J. K. Rothman
Mr. H. W. Rudoler
Mr. John B. Rulon
Mr. William W. Rutherford
Mr. W. H. Sackman
Mr. Albert Schnyder
Mr. J. F. Scott
Mrs. Lucille Seelig
Mr. Carl J. Seydel
Mr. Herbert L. Shallcross
Mr. Franklin Sheble II
Mr. William M. Sheehan
Mr. Barton P. Sloane, Jr.
Mr. Benjamin Small
Mr. Dudley S. Smith
Mr. Victor C. Smith
Mr. Felix Spatola, Jr.
Mr. Samuel Spector
Mr. Benjamin J. Spotts, Sr.
Mr. R. C. Stearnes, Jr.
Mr. William Swan
Mr. David G. Swanson
Mr. Raymond E. Tarpley
Mr. William O. Tatcher
Mr. Clarence Tolan, Jr.
Mr. David M. Trilling
Mr. F. Addison Urie
Mr. Frank J. Valetti
Mr. Ludwig Weber
Mr. Albert W. Zackey
Mr. Francis G. Zeiser, Sr.

ACTIVE MEMBERS.

Miss Berte Abramson
Mr. G. N. Ackley
Mr. Robert Goss Adams
Mr. Grover C. Albright
Mr. Erwin H. Aldinger
Mr. J. F. Alexander
Mr. Frank B. Allen
Mr. Paul Angstadt
Mr. B. F. Antrim, Jr.
Mr. E. Hulings Antrim
Mr. J. Milton Armstrong
Mr. William Arthur
Miss Marguerite Aspinwall
Mr. Edward Austin
Mr. Joseph Axelrod
Mr. Julius Axelrod
Mr. Harry Bailis
Mr. Philip Bailis
Mr. Charles Bain
Mr. Hermann F. Ball
Mr. William H. Ballman
Mr. William H. Barnes
Mr. Harry Batt
Mr. J. J. Baylson
Mr. Charles B. Beck
Mr. Lloyd Bergeson
Mr. Joseph Berlin
Mr. Joseph Berliner
Mr. Benjamin P. Berman
Mr. George W. Berry
Mr. George E. Billings
Mr. William Black
Mr. Louis Bless
Mr. L. J. Bloche
Mr. Nathan Bloom
Mr. Harry Bodenschatz
Mr. Thomas J. Boerner
Mr. Ernest Boghosian
Mr. Harry H. Bonner
Mr. Elmer H. Booz
Mr. Ralph C. Borthwick
Mr. Howard A. Bradley, Jr.
Mr. Charles S. Brangan
Mr. A. Balfour Brehman
Mr. Charles W. Brelle
Mr. Morris Brenner
Miss Alice Brothers
Mr. Harry F. Brown
Mr. George M. Brunner
Mr. Albert A. Buck
Mr. Stephen R. Buck
Mr. George B. Bush
Mr. William J. Bush
Miss Louise Calloway
Mr. Charles Campbell
Mr. John J. Campbell
Mr. Joseph A. Carlin, Jr.
Mr. Thomas A. Cashin
Mr. Philip Cass
Mr. F. C. Castelli
Mr. Morris Chaikens
Mr. Walter W. Chamberlain
Mr. Rowland J. Cheney
Mr. Daniel R. Cianciulli
Mr. Ray S. Clarke
Mr. Lloyd G. Clift
Mr. John P. Coghlan
Mr. Raymon Coghlan
Mr. Samuel A. Cohan
Mr. Benjamin Cohen
Mr. Samuel Cohen
Mr. William Cohen
Mr. S. Z. Cole
Mr. Robert C. Collins, Jr.
Mr. Watson R. Collins
Mr. Robert R. Colsher
Mr. Joseph M. Comerford
Mr. Ira L. Conkling
Mr. T. A. Connelly
Mr. Frank C. Connolly
Mr. Michael Cortizas

Mr. James F. Couch
Mr. William F. Covolus
Mr. H. L. Cox
Mr. Maurice A. Crews
Mr. John P. Croasdale
Mr. William J. Cronin
Mr. Horace Cullen
Mr. James E. Currie
Mr. G. M. Curry
Mr. William B. Curry
Mr. Herman Z. Cutler
Mr. Clarence R. Daugherty
Mr. Charles M. Davis
Mr. R. N. Davis
Mr. William M. Davis
Mr. W. H. S. Deckard
Mr. John E. Deininger
Mr. J. Carroll Deisher
Mr. F. M. Delrose
Mr. Americo A. DeMartinis
Mr. Guido D'Emilio
Mr. John C. Dettra
Mr. Alexandro Di Bona
Mr. W. J. Diederichs
Mr. Harry A. Dieffenbach
Mr. John E. Diem
Mr. Joseph A. Dietrick
Mr. David Di Prespi
Mr. Stan J. Dirvin
Mr. H. E. Doughty
Mr. Orney E. Dunnum
Mr. Rudolph H. Durnell
Mr. Leon T. Eckell
Mr. Alfred K. Edwards
Mr. K. F. Ehmann
Mr. Elmer T. Erb
Mr. Attilio Esposito
Mr. George M. Ewing
Mr. James D. Faires
Mr. Harry M. Farber
Mr. James F. Feehery
Mr. John Thorpe Feidt
Mr. Samuel P. Felix
Mr. Harry J. Ferguson
Mr. Joseph Ferraro
Mr. Epentus L. Fetteroff
Mr. Frank Feuse
Mr. Thomas J. Finnerty
Mr. Arthur M. Fischman
Mr. Adam Fisher
Mr. Leo Fisher
Mr. Irvin J. Fishman
Mr. Charles Flachbarth
Mr. M. L. Flashman
Mr. Nathaniel R. Fleischer
Mr. David A. Fleming
Mr. Norton D. Fleu
Mr. H. G. Fliess
Mr. Oliver K. Follweiler
Mrs. Irene W. Ford
Mr. Aug. C. Frank
Mr. Edward Frank
Mr. H. B. Frazer
Mr. Frank J. Frei
Mr. George H. Frew, Jr.
Mr. G. William Friedrich
Mr. B. H. Frishmuth
Mr. Robert S. Fulton
Mr. Samuel E. Fulton
Mr. Joel Gahuse
Mr. Charles I. Gallagher
Mr. Hugh F. Gannon
Mr. Fred H. Ganther
Mr. Andrew S. Gardner
Mr. L. R. Garretson
Mr. William C. Gaskill
Mr. B. E. Gerhring
Mr. Charles Gerlach
Mr. Richard G. Gerlach
Mr. Elbridge F. Gerry
Mr. George D. Gideon
Mr. Julius D. Gilbert
Mr. Harry Gilmore
Mr. Joseph F. Glaser
Mr. Thomas R. Glynn
Mr. Samuel Goldberg
Mr. Solomon Goldman
Mr. Morris Goldstein
Mr. G. F. Goodman
Mr. Harry Gordon
Mr. William R. Govett
Mr. Arthur S. Graham
Mr. Mario Grasso
Mr. W. F. Grau
Mr. Rowland N. Grauch
Mr. R. A. Gravdahl
Mr. Alfred M. Green
Mr. Louis B. Greenstein
Mr. John Greenwood
Mr. George H. Greiss
Mr. Charles H. Greyer
Mr. Elwood F. Groom
Mr. Samuel Gross
Mr. Samuel P. Gross
Mr. David Guither
Mr. F. Eldridge Guither
Mr. Joseph Guss
Mr. Albert M. Haas
Mr. Harry L. Haeberle
Mr. Samuel Haftel
Mr. Daniel J. Haley
Mr. Edward C. Hall
Mr. George F. Hall
Mr. George Purdy Hall
Mr. Charles D. Hamburg
Mr. Albert J. Hamlin
Mr. Elisha Hammonds
Mr. J. Walter Hammonds
Mr. B. J. Hansner
Mr. Harry K. Hardcastle
Mr. Josiah P. Harmer
Mr. Charles S. Harper
Mr. Robert L. Harper
Mr. A. M. Harrington
Mr. Edson S. Harris
Mr. John H. Harrison
Mr. Frederick E. Hartweg
Mr. Herman Hassinger
Mr. C. E. Hastings
Mr. George K. Heebner
Mr. C. Oscar Hegardt
Mr. Alfred G. Heinemann
Mr. Ralph E. Hellmer
Mr. William M. Hendrickson
Mr. Harry T. Henning
Mr. John J. Henry
Mr. H. C. Henssler, Jr.
Mr. Robert S. Herbert
Mr. Wilmer J. Herrick
Mr. Joseph F. Hess

Mr. Michael Hibner
Mr. Newton Howard Holden
Mr. Charles A. Holm
Mr. Robert M. Holtzman
Mr. Frank P. Homer
Mr. Albert M. Hooven
Mr. Charles A. Hooven
Mr. Russell Hopkins
Mr. Clifford F. Howard
Mr. James Huey
Mr. Ernest N. Hyde
Mr. Theodore Irvin
Mr. Albert Jackalous
Mr. Leroy S. James
Mr. Casper G. Jay
Mr. John E. Johnson
Mr. J. Carroll Johnston
Mr. C. Walker Jones
Mr. Charles D. Jones
Miss D. E. Jones
Mr. Edward Worthington Jones
Mr. Whitney W. Jones
Mr. Yern Jorgenson
Mr. Alexander Kamens
Mr. Joseph Katz
Mr. William H. Kay
Mr. Alfred R. Kennedy
Mr. L. M. Kennedy
Mr. Matthew Kenney
Mr. Harry H. Kepley
Mr. Max Kersun
Mr. G. Walker Ketcham
Mr. Joseph D. Kevorkian
Mr. Carl Kirsch
Mr. Walter Kiwi
Mr. Charles Klause
Mr. William Kleimenhagen
Mr. J. Francis Kleinz
Mr. Maurice Kline
Mr. Harry N. Knauer
Mr. Charles Knox, Jr.
Mr. B. H. Brewster Koons
Mr. Lewis A. Kopp
Mr. Louis Korr
Mr. J. Kosoy
Mr. Abraham L. Krakovitz
Mr. William C. Kroberger
Mr. Alfred Kronschnable
Mr. Henry J. Kunzig
Mr. John M. Kupp
Mr. Claude Lachman
Mr. Charles Laessle, Jr.
Mr. G. Duke Lambert
Mr. Frederick William Lang
Mr. Percy L. Lanning, Jr.
Mr. Frederick B. Larsen
Mr. George F. Lawrence
Mr. Robert T. Lawson
Mr. Sandor Lederer
Mr. Stanley Lehmberg
Mr. Robert Paul Leopold
Mr. Robert T. Leopold
Mr. Aaron Levine
Mr. Benjamin Levy
Mr. Martin M. Levy
Mr. John Locke Lewis
Mr. Martin Lewis
Mr. Harry C. Lieberman
Mr. Arthur H. Lockhart
Mr. Isaac Lodge
Mr. Joseph Loeffler
Mr. Henry W. Long
Mr. Fred Lorber
Mrs. Ruth P. Loveland
Mr. William A. MacAvoy, Jr.
Mr. Robert MacMullen
Mr. David Maimin
Mr. Paul Maleson
Mr. Thomas D. Marino
Mr. Joseph Marziani
Mr. Earl L. Mason
Mr. Peter Masucci
Mr. Joseph Mayer
Mr. Robert McCurdy
Mr. James F. McCormick
Mr. Ralph D. Megee
Mr. Walter E. Michaelis
Mr. Samuel C. Milbourne
Mr. J. A. Mitchell
Mr. James H. Mitchell
Mr. Frank R. Moore
Mr. J.Frank Motson
Mr. J. N. Moyer
Mr. Frank A. Muenzenberger
Mr. A. P. Mynders
Mr. Charles R. Nalle
Mr. Martin Nebel
Mr. Palmer Nelsen
Mr. Walter A. Neuman
Mr. W. Herbert Newbold
Mr. Richard E. Newman
Mr. Russell E. Nittinger
Mr. William L. Noe
Mr. Richard T. Orth
Mr. F. C. Osterhout
Mr. Charles A. Paoli
Mr. Joseph W. Parkin, Jr.
Mr. R. A. Parkinson
Mrs. Robert W. Parkinson
Mr. George H. Pechin
Mr. H. F. Peirce
Mr. Nathan Perilstein
Mr. L. Franklin Peters
Mr. W. J. Pickwell
Mr. Arthur Platt
Mr. Harold W. Polin
Mr. Lawrence W. Post
Mr. Lynn F. Powell
Mr. Thomas J. Power, Jr.
Mr. Dana Pratt
Mr. F. V. Rais
Mr. Willard M. Rambo
Mr. Charles A. R. Rath
Mr. R. Stewart Rawlings
Mr. D. H. Redmond
Mr. D. E. Regan
Mr. Charles Reitzes
Mr. J. Walter Rex
Mr. Horace S. Rhoads
Mr. J. Cecil Rhodes
Mr. John H. Rice, 3rd
Mr. F. W. Riess
Mr. John P. Rife
Mr. Albert Riggall
Mr. John H. Ringe, 3rd
Mr. Joseph Roberts

Mr. Archie M. Robertson
Mr. David T. Robinson
Mr. Francis Churchill Rogers
Mr. Henry A. Romberger, Jr.
Commander W. P. Roop, U.S.N.
Mr. Benjamin Rose
Mr. Morton M. Rose
Mr. Charles Rosenthal
Mr. Edward J. Rosser
Mr. Howard T. Rossler
Mr. Louis Roth
Mr. Guy F. Rowlett
Mr. Karl Rugart
Mr. Warren E. Ruttle
Mr. Reginald Ryberg
Mr. Irvin Sachs
Mr. George Sachsenmaier
Mr. Ludwig Saha
Mr. Harold B. Saler
Mr. Samuel Saler
Mr. Julius Saltzman
Mr. Edgar M. Scattergood
Mr. Fred C. Schadrack
Mr. A. E. Schaffer
Mr. H. V. Schaffer
Mr. Irving Schaffer
Mr. Morris Scherb
Mr. John Schmidt
Mr. D. F. Schmit
Mr. Fred J. Schmitt
Mr. Joseph Schmitz, Jr.
Mr. Charles F. Schneider
Mr. E. Schneider
Mr. William L. Schneider
Mr. Charles Schoenfeld
Mr. W. Richison Schofield
Mr. Herman Schulty
Mr. David Schwartz
Mr. Frank S. Schwarz
Mr. Nicholas Sclufer
Mr. David Scott, Jr.
Mr. Donald C. Scott
Mr. G. Frank H. Senderling
Mr. Paul J. Seng
Mr. Milton C. Seib
Mr. C. J. Seibel
Mr. George Senn
Mr. Bernard Shapiro
Mr. M. M. Sharf
Mr. Edgar Y. Sharlip
Mr. F. Dickman Shaw
Mr. Nathan Sherman
Mr. L. H. Shingle
Mr. W. L. Shirley
Mrs. Stella D. Shober
Mr. D. F. Showell
Mr. Morris I. Shoyer
Mr. George Siegel
Mr. Charles Silver
Mr. Maurice A. Singer
Mr. William H. Simkins
Mr. James A. Simmons
Mr. Omer Simon
Mr. E. A. Skowbo
Mr. Albert J. Slap
Mr. H. Royer Smith
Mr. James J. Smith
Mr. Joseph A. Smith
Mr. Nicholas A. Smith
Mr. Parker M. Smith
Mr. Rudolph Smith
Mr. Joseph J. Smyth
Mr. Willard H. Snell
Mr. A. D. Snyder
Mr. Baer Soffe
Mr. Norwood R. Solly
Mr. K. Theodore Sorensen
Mr. Morris J. Sostmann
Mr. Meyer Sperber
Mr. Leo J. Spillane
Mr. William Spring
Mr. Cameron F. Stains
Mr. Howard B. Steigelman
Mr. Michael Stein
Mr. Seymour E. Steinbrook
Mr. G. H. Stevens
Mr. William H. Stilz
Mr. John H. Stortz
Mr. Joseph A. Stott
Mr. Albert H. Stover
Mr. Charles W. Strong
Mr. A. Fred Sturgis
Mr. Jacob Sucknow
Mr. W. E. Swanger
Mr. A. W. Swartz
Mr. L. H. Swind
Mr. Joseph H. Thomas
Mr. Eric E. Tinney
Mr. J. B. Tomlinson
Mr. J. Edward Topper
Mr. Lew Trenner
Mr. Julius J. Trumper
Mr. Peter Tursi
Mr. Paul S. Tyson
Mr. Alfred Paul Urban
Mr. Roland G. E. Ullman
Mr. Daniel M. Vail
Mr. J. T. Vallbrecht
Mr. C. K. Van Rensselaer
Mr. Edmond F. Venzie
Mr. Frederick C. Vieser
Mr. Joseph S. Vila
Mr. Morris Vinskin
Mr. Harry C. Viti
Mr. Thomas A. Voelker
Mr. John C. Vogtle
Mr. H. G. von Cullin
Mr. Conrad Wacker
Mr. Charles A. Wagner
Mr. Alfred S. Wall
Mr. Curtis C. Wallace, Jr.
Mr. William J. Walsh
Mr. Joseph H. Walter
Mr. Edgar S. Ward
Mr. Martin L. Wasserman
Mr. J. Hampton Webb
Mr. Franklin Wedge
Mr. David M. Weiner
Mr. Morris Weiner
Mr. Irvin I. Weinreich
Mr. Philip H. Weinreich
Mr. Morton B. Weinstein
Mr. F. W. Weir
Mr. Samuel Weisfield
Mr. Harry Weissinger

Mr. Frank A. Wellman
Mr. H. O. West
Mr. S. Rogers Wetherill
Mr. Clarence B. White
Mr. James J. White
Mr. R. R. Wiggins
Mr. G. Philip Wild
Mr. I. W. Wilenchik
Mr. Charles Wilhelm
Mr. James S. Wilkes
Mr. T. Carroll Willson, Jr.
Mr. T. Carroll Willson, Sr.
Mr. Alfred J. Williams
Mr. J. R. Williams
Mr. Charles D. Witman
Mr. Clarence W. Wood
Mr. Howard Woodward
Mr. Earl Wunderlich
Mr. Charles A. Yeager
Mr. Alexander Younger
Mr. Aram Zakian
Mr. Henry G. Zeiher
Mr. Edward E. Zimmerman
Mr. J. Milton Zimmerman
Mr. John Zimmermann, Jr.
Mr. George Zorn, Jr.
Mr. Nathan Zucker

ACTIVE NON-RESIDENT MEMBERS.

Mr. Donald P. Campbell
Mr. Randolph Church
Mr. Thomas Harley Davis
Mr. Frank S. Fawcett
Mr. A. A. Green
Mr. James G. Goodwillie
Mr. Isaac E. Johnson, 3rd
Mr. Arthur H. Jordon
Mr. Albert H. Klein
Mr. Richard Kravits
Mr. Joseph E. Mertle
Mr. Carl N. Martin
Mr. Wilbur E. Meserve
Mr. Allan W. Morton
Dr. Archie D. Power
Mr. Arthur L. Stern
Mr. L. E. Swedlund
Mr. Harry L. Winston
Mr. Howard Wright

NECROLOGY.

Active Life Members.

Mr. Charles Fearon
Mr. Robert Moran

Associate Life Members.

Mr. G. H. Blakely
Mr. William J. McCahan, Jr.
Mr. George W. Morris
Mrs. Arthur V. Morton
Mr. William L. Nevin
Mr. Frank A. Wills
Mr. Wilson S. Yerger

Active Members.

Mr. William H. Balls
Mr. George E. Deming
Mr. Thomas W. Evers
Mrs. Jennie M. Fels
Mr. Henry Reed Hatfield (Also Associate Life Member)
Mr. Edwards Kneass
Mr. Charles McDowell
Mr. Charles A. Schranz
Mr. Joseph F. Stockwell
Mr. Walter A. Sweeting
Mr. John P. Sykes
Rear Admiral J. G. Tawresey
Mr. Paul Thompson (also Associate Life Member)
Mr. Charles W. Werst

Active Non-Resident Members.

Mr. Frederick M. Becket
Dr. Alice G. Bryant
Dr. Charles E. Caspari
Mr. H. H. Vaughan

LIBRARY NOTES.

The Committee on Library desires to add to the collections any technical works that members would wish to contribute. Contributions will be gratefully acknowledged and placed in the library. Duplicates received will be transferred to other libraries as gifts of the donor.

Photostat prints of any material in the collections can be supplied on request. The average cost for a print 9 × 14 inches is thirty-five cents.

The library and the reading room are open on Mondays, Tuesdays, Wednesdays and Fridays from nine o'clock A.M. until five o'clock P.M., Thursdays from two until ten o'clock P.M. and Saturdays from nine until twelve o'clock noon.

RECENT ADDITIONS.

AERONAUTICS.

ADAMS, HAROLD W. Aircraft Hydraulics. 1943.
AUMENT, HUGH C., JR. Airplane Hydraulic Systems. 1943.
GLAUERT, H. The Elements of Aerofoil and Airscrew Theory. 1943.
JORCH, WILLIAM F. Aircraft Electrical Systems. 1943.
KINERT, REED. America's Fighting Planes in Action. 1943.
MILBANK, JEREMIAH, JR. The First Century of Flight in America. 1943.

AGRICULTURE.

BROWN, HARRY BATES. Cotton. Second Edition. 1938.

ASTRONOMY.

GOLDBERG, LEO, AND LAWRENCE H. ALLER. Atoms, Stars and Nebulæ. 1943.

BIOCHEMISTRY.

HARRIS, ROBERT S., AND KENNETH V. THIMANN, Editors. Vitamins and Hormones. Volume 1. 1943.
PETERSON, WILLIAM H., JOHN T. SKINNER AND FRANK M. STRONG. Elements of Food Biochemistry. 1943.

BIOGRAPHY.

HOLT, RACKHAM. George Washington Carver. 1943.
KELLY, FRED C. The Wright Brothers. 1943.

CHEMISTRY AND CHEMICAL TECHNOLOGY.

American Institute of Chemical Engineers. Transactions. Volume 38, 1942. 1943.
BENNETT, H., Editor-in-Chief. The Chemical Formulary. Volume 6. 1943.
BENNETT, H. Practical Emulsions. 1943.
Chemical Rubber Company. Handbook of Chemistry and Physics. Twenty-seventh Edition. 1943.
KALICHEVSKY, V. A. The Amazing Petroleum Industry. 1943.
KILLIAN, J. Crystals. 1941.
MIDLETON, ARTHUR R., AND JOHN W. WILLARD. Semimicro Qualitative Analysis. 1940.
OLNEY, LOUIS A. Textile Chemistry and Dyeing. Part 1: Chemical Technology of the Fibers. Eighth Edition. 1942.
Organic Syntheses. Volumes 22 and 23. Collective Volume 2. 1942–1943.
SMITH, PAUL I. Glue and Gelatine. 1943.

DICTIONARIES AND ENCYCLOPEDIAS.

Americana Annual. 1943.
CRISPIN, FREDERIC SWING. Dictionary of Technical Terms. Revised Edition. 1942.

ELECTRIC ENGINEERING.

FIELD, SAMUEL, AND A. DUDLEY WEILL. Electroplating. Fourth Edition. 1943.

HARVEY, A. F. High Frequency Thermionic Tubes. 1943.
LINCOLN, E. S., Lincoln's Industrial-Commercial Electrical Reference. First Edition. 1941.
MACLAREN, MALCOLM. The Rise of the Electrical Industry during the Nineteenth Century. 1943.
SCHELKUNOFF, S. A. Electromagnetic Waves. 1943.
SCHIEPE, EDWARD M. The Inductance Authority. 1942.

ENGINEERING.

BILLIG, KURT. Pre-stressed Reinforced Concrete. Part 1. 1943.
HOOL, GEORGE A., AND W. S. KINNE, Editors. Structural Members and Connections. Second Edition. 1943.
PARKER, HARRY. Simplified Design of Reinforced Concrete. 1943.

GEODESY.

SHARP, H. OAKLEY. Geodetic Control Surveys. Second Edition. 1943.

GEOLOGY.

GROVER, NATHAN CLIFFORD, AND ARTHUR WILLIAM HARRINGTON. Steam Flow Measurements, Records and their Uses. 1943.
SVERDRUP, H. U., MARTIN W. JOHNSON, AND RICHARD H. FLEMING. The Oceans. 1942.

INDUSTRIAL MANAGEMENT.

ALFORD, L. P. Cost and Production Handbook. 1942.

MANUFACTURES.

HUNT, ANTONY. Textile Design. No date.
LEE, RUTH WEBB. Sandwich Glass. Second Edition. 1939.
MONAGHAN, JAMES F. Processing and Finishing Cottons. Volumes 1–2. 1935.

MATHEMATICS.

American Society for Testing Materials. A.S.T.M. Manual on Presentation of Data. 1943.
CRAIG, HOMER VINCENT. Vector and Tensor Analysis. First Edition. 1943.
MARGENAU, HENRY, AND GEORGE MOSELEY MURPHY. The Mathematics of Physics and Chemistry. 1943.
TITCHMARSH, E. C. The Theory of Functions. Second Edition. 1939.

MECHANICAL ENGINEERING.

BILLINGS, J. HARLAND. Applied Kinematics. Second Edition. 1943.
New Jersey Zinc Company. Die Casting for Engineers. 1942.

METALLURGY.

HAYWARD, CARLE R. An Outline of Metallurgical Practice. Second Edition. 1940.
PAINTON, EDGAR T. The Working of Aluminium. 1927.
PORTEVIN, ALBERT. Introduction to the Study of Heat Treatment of Metallurgical Products. 1939.

NAVAL ARCHITECTURE.

CARMICHAEL, A. W. Practical Ship Production. Second Edition. 1941.
EDDINGTON, WALTER J. Glossary of Shipbuilding and Outfitting Terms. 1943.
HARMAN, F. WARD. Ship Models Illustrated. 1941.
RIMINGTON, CRITCHELL. Fighting Fleets. 1943 Edition.

PHYSICS.

DINGLE, HERBERT. Sub-Atomic Physics. 1943.
JAMESON, ALEX. H. An Introduction to Fluid Mechanics. 1942.
LEMON, HARVEY BRACE, AND MICHAEL FERENCE, JR. Analytical Experimental Physics. 1943.

RAILROAD ENGINEERING.

Railway Engineering and Maintenance Cyclopedia. Fifth Edition. 1942.
VAN NAME, WILLARD G. Collection of Photographs of Old Locomotives and Cars, Taken before the Year, 1898.

SANITARY ENGINEERING.

American Foundrymen's Association. Tentative Recommended Good Practice Code and Handbook on the Fundamentals of Design, Construction, Operation and Maintenance of Exhaust Systems. 1938.

NOTES FROM THE BARTOL RESEARCH FOUNDATION.

NOTE ON THE NATURE OF THE GAS MIXTURE IN SELF-QUENCHING GEIGER-MUELLER TUBES.*

BY

PAUL WEISZ

From studies on the breakdown of spark gaps, and from theoretical and experimental work on the discharge process of Geiger-Mueller tubes itself, we conclude that the intrinsic difference between self-quenching and non-self-quenching G-M (Geiger-Mueller) tubes lies in the particular nature of the action of ultraviolet photons in each case.

In the G-M tube which is not self-quenching, a great number of photons are emitted during the discharge process. In so-called self-quenching G-M tubes, no evidence has been found for the presence of photons at appreciable distances from the wire. Previous experimental evidence,[1] and a finding to be reported, seem to suggest that ultraviolet light quanta are still produced, but are quickly absorbed by the "quenching gas," probably within a distance of a few mean-free paths in the gas.

Thus it is the purpose of the quenching gas to absorb all ultraviolet quanta produced, or ultimately to make the probability of production of negative ions by way of photons and photoelectrons as nearly as possible equal to zero. Since this probability will depend on the density of the quenching gas, an investigation was made of the quenching properties as a function of the partial pressure of the quenching gas. This was accomplished by studying the width of the "plateau," for mixtures of argon as the "multiplication gas" and ethyl-ether as the quenching gas. The plateau is defined as

* Reprinted from an article published in full in *The Physical Review*, **62**, 477 (1942).

[1] W. E. Ramsey, *Phys. Rev.*, **61**, 96–97 (1942); H. G. Stever, *Phys. Rev.*, **59**, 765 (1941), and *Phys. Rev.*, **61**, 38–52 (1942).

that region of applied electrode potentials which lies between two limits A and B, such that beginning at the potential A all pulses are of a convenient pulse size (three volts in this case), and that the tube starts to show multiple discharges when the potential is increased beyond B, and the tube is operated with a normally small external resistance of 1 megohm. The appearance of such multiple pulses can be interpreted in the light of the picture of the mechanism as being evidence for the production of photoelectrons, their subsequent capture and release, and thereby the repetition of the discharge process.

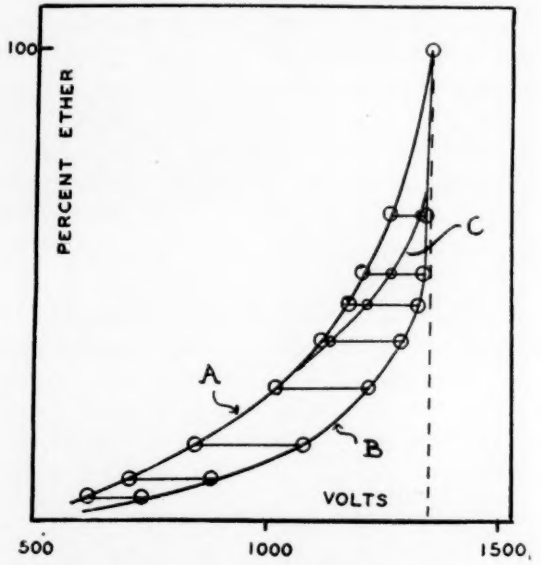

FIG. 1. The plateau region for the argon/ethyl-ether counter. The counter is $\frac{1}{2}'' \times 3''$. The central wire is 0.003", the total pressure, 6 cm of Hg.

Figure 1 shows the results of the plateau measurements for a tube containing argon/ethyl-ether at 6 cm. total pressure; the partial ether pressure is experssed in percentage of total pressure. It can be seen that for this total pressure, an ether content of about 20 to 25 per cent. yielded the optimum plateau. At relatively high ether contents, the pulses were no longer of equal amplitudes but showed appreciable dis-

tribution in size up to potentials indicated by curve *C*, although the average pulse size was still approximately 3 volts at *A*. In the light of the picture outlined the following explanation suggests itself: At great densities of the quenching gas the absorption of photons becomes so intense that even the propagation of the mechanism along the wire cannot always take place along its entire length. The pulse size, being proportional to the total amount of charge produced, may then be nearly proportional to the length along which each discharge is able to propagate before it fails in producing at least one more photoelectron. The pulse size may thus be subject to appreciable fluctuations.

Similar measurements concerning optimum plateau conditions were made at different total pressures, and the following data obtained:

Total pressure	Approx. % ether for opt. plateau
6 cm.	20 to 25%
15 cm.	7 to 10%
40 cm.	approx. 3%

It appears that the absolute pressure or density of the quenching gas alone determines the quenching characteristics regardless of what the total gas pressure may be, the partial ether pressure for optimum conditions being about 1.5 cm. of mercury. It seems noteworthy that this finding seems to favor the concept of photons being *absorbed* by the presence of a sufficient amount of the quenching gas, in preference to a picture of the mechanism involving the assumption of some action by which this gas prevents the creation of quanta during the ordinary discharge process.

NOTES FROM THE BIOCHEMICAL RESEARCH FOUNDATION.

Effect of Propionic Acid and of Na Propionate on Paramecia.—HUGH E. POTTS. Paramecium has been used as a test animal for various chemicals (Ferguson, Frederick F., Holmes, Jane R., and Lavor, Edward, *Journal of the Elisha Mitchell Scientific Society*, **58**: 53, 1942; Feiler, Marie, *Archiv fuer Protistenkunde*, **59**: 562, 1927; Mel'nikov, N. N., Avetesyan, A. M., and Rokitskaya, M. S., *Comptes rendus de l'académie des sciences de l'U. R. S. S.*, **31**: 123, 1941). It has the advantages of being large enough for observation of changes in size, shape, contractile vacuole activity, and of being easy to cultivate in large numbers.

Since propionic acid in minute traces (Miller, F. W., Jr., *Agricultural News Letter*, Public Relations Department, E. I. du Pont de Nemours and Co., **10**: 62, 1942) is capable of inhibiting growth of mold on bread, it was thought that it might prove to be of some value as a therapeutic agent. Therefore it was tested in different concentrations on *Paramecium caudatum*. Small watch glasses were used for the experiments. These measure about 20 mm. in diameter and can conveniently hold 1 cc. or a little more of fluid. The bottom of each glass is grooved and the upper rims are bevelled and ground so that they can be stacked one upon another, thus avoiding any great amount of evaporation.

Paramecia were cultured in small glass jars. The pH was kept at about 7.0 by addition of NaOH or $NaHCO_3$. An original inoculation of *Serratia marcescens* was made to the paramecia in aquarium water, and the organisms were fed on a few flakes of dried rolled oats per jar twice a week. Subcultures were made about once a month by putting several cc. from old cultures into clean jars and adding distilled water, a few cc. per day until the jars were filled.

For testing purposes paramecia were pipetted into the watch glasses and the desired amount of propionic acid added, proportions being reached by counting the number of drops of culture and of chemical, the same pipette being used for

both. Pipettes were rinsed thoroughly with distilled water whenever necessary.

The propionic acid used was acid propionic pure, purchased from The Coleman and Bell Co., Norwood, Ohio. This was titrated in our laboratory and found to be 13.13 normal. It was diluted into a series of stock solutions, each 1/10 the concentration of the previous one, down to 13.13×10^{-5} normal. From each stock solution 10, 8, 6, 4, 2 and 0 drops of the acid were added to 10, 12, 14, 16, 18 and 20 drops respectively of paramecium culture. After addition of the acid each watch glass was tilted and agitated to mix the acid evenly throughout the culture.

The paramecia were then examined under a magnification of 40×, through a dissecting microscope at half-hourly, hourly or greater intervals, as seemed advisable. The pH was approximated at the beginning or shortly after the beginning of each experiment by use of bromthymol blue.

All concentrations down to 2.63×10^{-3} N killed all paramecia in 3 hours. The pH on all these concentrations of propionic acid was 6.0 or less, the 2.63×10^{-3} N and 1.31×10^{-3} N being approximately 6.0. With dilutions beyond 1.31×10^{-3} N the pH rose gradually, being approximately 7.0 at 2.63×10^{-4} N, and none of these had any appreciable effect.

In order to determine whether or not it was merely the acid effect which killed the paramecia, the propionic acid was neutralized with normal NaOH, 2 cc. of the alkali being added to 10.5 cc. of acid. The resulting solution had a molarity of ca. 3×10^{-2}. 10, 8, 6, 4, 2 and 0 drops of the neutralized acid were added respectively to 10, 12, 14, 16, 18 and 20 drops of paramecia culture. The pH of all concentrations was about 7.1. 5.51×10^{-2} M killed all paramecia in 24 hours. 4.41 and 3.31×10^{-2} M killed a few in 24 hours. Greater dilutions had no noticeable effect.

These results indicate that both the acid and its sodium salt have an appreciable action on paramecia. The acid, however, is many times as active as its sodium salt. It is probable that the sudden drop in pH, on addition of propionic acid, is in itself capable of causing the death of paramecia.

BOOK REVIEWS.

ATOMS, STARS AND NEBULÆ, by Leo Goldberg and Lawrence H. Aller. (The Harvard Books on Astronomy.) 323 pages, 150 illustrations. Philadelphia, The Blakiston Company, 1943. Price $2.50.

The fifth of the Harvard Books on Astronomy has now appeared, and will soon find its place on the shelf of most-used books of astronomers and physicists. For while the book is intended for the serious non-professional reader, it has so summarized the present status of astronomical spectroscopy that astrophysicists will find it constantly useful.

The narrative style is maintained in excellent fashion through the whole work, and as in some of the other books of the series the photographs of contemporary contributors to advances in the field add a worthwhile touch. Tables summarizing the data on star temperatures, masses, densities and other characteristics are scattered liberally, and every other page contains an illuminating photograph of a spectrum, a graph, or a diagram.

Supplemented with readings in the current literature, this book fills the need for a modern introductory textbook in astrophysics, yet it can be read with pleasure by those who are merely inquisitive about the methods and findings of modern astronomical spectroscopy.

ROY K. MARSHALL.

AN INTRODUCTION TO FLUID MECHANICS, by Alexander H. Jameson, M.Sc., M. Inst. C. E., F. K. C. 245 pages, illustrations, 14 × 22 cms. New York, Longmans, Green and Company. 1942. Price $3.40.

Although the principles of fluid mechanics have been applied in various fields for a good many years, it has only been comparatively recently that applications have been multiplied to a great extent. Perhaps the most common peacetime use today is the stream-lined automobile and only a short time before the appeared, was there such broad application of fluid mechanics. The University of London decided that an elementary knowledge of this fundamental subject shall be required of all candidates in the Part I, B.Sc. (Engineering) Examination, and this book is intended for such second year students.

The treatment is, of course, of a rigorous mathematical nature. The method of presentation, the logical progression, and the somewhat unusual approach in the way of demonstrating the solution of examples in the text and the means indicated in the exercises at the end of chapters all make for a lightening and more impressive text. The book is divided into eight chapters. They begin with an explanation of liquids and gases, and follow through with pressures, the perfect fluid, motion of a perfect fluid and motion of a cylinder and sphere through a fluid, flow through orifices, flow in pipes, channels and notches, and the measurement of velocity. Appendixes contain Bernoulli's Theorem for Compressible Fluids, and alternative treatment in the method of dimensions, and the derivation of exponential flow formulae. A subject index is in the back.

R. H. OPPERMANN.

THE ELEMENTS OF AEROFOIL AND AIRSCREW THEORY, by H. Glauert. 228 pages, illustrations, 14 × 22 cms. New York, The Macmillan Company, 1943. Price $3.50.

The actions of an aerofoil are not new to those thousands who have been so fortunate as to have observed them in the museum of The Franklin Institute. That they are of importance is unquestioned as is the theory behind them. The main object of aerofoil theory is to explain and to predict the lift and drag experienced by an aerofoil. Much of this has been done, as is shown in the exhibition and in everyday practice. A satisfactory theory has been developed in recent years for the ordinary range below the critical angle. The determination of the maximum lift of an aerofoil and of the critical angle at which it occurs is not yet possible, although some insight has been obtained into the cause of the phenomenon.

This is an American edition of the British book. It aims to give an account of this mathematical subject in terms that may be understood by those not having previous knowledge of hydrodynamics and by minimizing complex mathematical analysis. After a brief introduction, Bernoulli's equation is discussed followed by an analysis in stream function which led to the determination of the theoretical flow past a cylinder in a uniform stream. Another type of flow in which the fluid circulates round the cylinder is next taken up and finally the velocity potential and the potential function. All this constitutes an introduction to those aspects of hydrodynamics which are required for the development of aerofoil theory. The following chapters deal successively with the lift of an aerofoil in two dimensional motion and an examination of the fundamental basis of this theory of flow governed by Joukowski's hypothesis, the aerofoil in three dimensions, the monoplane aerofoil, and biplane aerofoils. The last three chapters deal with the development of the airscrew theory. This treatment begins with the momentum theory and goes through an investigation of the forces experienced by airscrew blades regarding each blade as an aerofoil element moving in its appropriate manner, and then wind tunnel interference.

The book gives a rather complete treatment within its limitations. It forms a workable basis of knowledge of the subject.

R. H. OPPERMANN.

THE FIRST CENTURY OF FLIGHT IN AMERICA, by Jeremiah Milbank, Jr. 248 pages, illustrations, 15 × 22 cms. New Jersey, Princeton University Press, 1943. Price $2.75.

New industrial developments or inventions when presented for use or consumption by the public are seldom recognized as being the result of evolution over a long period. Without such a process there would be few of the many things available today that make up the tempo and ease of modern life. Aviation is certainly one of these and the book at hand is a means of bringing this realization. Mr. Milbank here reveals much that is generally unknown about flight in America for the nineteenth century. His account gives details of experiences of great inventors and aeronauts who provided most spectacular feats for early America, and at the same time laid the foundations for one of the greatest wonders of our present generation.

The first authenticated ascent in America was made June 24, 1784, by a boy of only 13 years, Edward Warren, in a balloon. Almost ten years later Jean Pierre Blanchard made the first actual aerial voyage in this country. George Washington was Blanchard's patron, and the voyage lasted 46 minutes from Philadelphia to Gloucester County, N. J. These and other events are vividly described by the author in more or less chronological order. Special attention is given to the events occasioned by outstanding men such as John Wise and others. An entire section is devoted to T. S. C. Lowe and the Civil War and it is interesting to note here that in 1859 Lowe had decided to attempt flight in a balloon over the Atlantic Ocean. The voyage was scheduled to start from New York but the New York Gas Company was unable to deliver hydrogen fast enough to effect full inflation of the balloon. Dr. John C. Cresson, President of the Franklin Institute and of the Point Breeze Gas Works, of Philadelphia, then invited Lowe to his city where he guaranteed sufficient speed of inflation. Weather conditions postponed the trip, however, temporarily and later postponement was made final due to the Civil War.

The Civil War offered the first demonstration of the military value of the balloon. Lowe organized a balloon division in the Union Army and did valuable work which was recognized by Federals and Confederates alike. Major General A. W. Greely, Chief of Army Signal Corps, stated "it may be safely claimed that the Union Army was saved from destruction at the battle of Fair Oaks, May 31 to June 1, 1862, by the frequent and accurate reports of Professor Lowe." Not only did the Confederates try to eliminate Lowe's aeronautical corps but they even tried to organize their own balloon outfit.

The book is a very interesting account that furnishes a background for those in aviation today and a fund of information for the layman.

R. H. OPPERMANN.

THE AMAZING PETROLEUM INDUSTRY, by V. A. Kalichevsky. 234 pages, diagrams, 13 × 19 cms. New York, Reinhold Publishing Corporation, 1943. Price $2.25.

There is a definite place in the literature for books of an informative character for general reading. Whenever a field of human endeavor becomes prominent enough to affect the lives of large numbers of people, there is a duty, educational if not otherwise, to make available to the people a means of understanding the processes involved. The petroleum industry is such a field. Its position as one of the foremost branches of chemistry is undisputed. Measured in tonnage it is probably the country's largest supply of chemical raw materials. Measured in achievement, it ranks second to no other branch of chemistry as a supporter of the war effort, both in its role as a motor fuel and lubricant source, and as the actual savior of military transport through its basic contribution to the synthetic rubber program. Dr. Kalichevsky's book, therefore, is timely.

The book embraces the entire industry including the production and nature of petroleum, its transportation and storage, and the processing of petroleum. Special sections are devoted to petroleum emulsions and natural gas, gasoline and crude oil distillations, cracking, hydrogenation and aviation gasolines, chemical treatment of light petroleum products, and chemicals from petroleum. The

book is a non-technical resumé—understandable by anyone. In the back there is a glossary of terms used in the industry.

Readers of all kinds can profit by reading this book. Coming from a man closely connected with the industry for many years it is an authoritative explanation. He rightly states that it "should be of assistance to college students, to young engineers beginning their careers in the petroleum industry, and to persons already connected with it but not directly engaged in production or refining of oil.

R. H. OPPERMANN.

VECTOR AND TENSOR ANALYSIS, by Homer Vincent Craig. 434 pages, diagrams, 16 × 23 cms. New York, McGraw-Hill Book Company, 1943. Price $3.50.

In the preface of this book the author refers to the economy of time in the training of engineers and physicists. While of course, this has been an important item before educators for years, it is refreshing to see it brought out so boldly when considering a subject for study, especially so fundamental a subject as concerns this book. Vector analysis is undoubtedly the best introduction to certain related branches of mathematics. Every student of theoretical physics, engineering, and differential geometry should have at least a reading knowledge of this subject. As to tensor analysis, this is a somewhat newer study and at present it can be said to be in a state of rapid expansion. The state of development is such that a broad and voluminous content is available. Nevertheless the book at hand undertakes to give an introduction to these subjects, sufficient to indicate their value as tools for the solution of practical problems and their flexibility of application.

The book is divided into three parts the first of which is devoted to a mathematical background necessary for the main and later divisions. Here reference is made to the calculus of functions of two variables, parameterized arcs, determinants, the ϵ-systems, and certain transformation equations. This takes up roughly, one-quarter of the content of the book and prepares the way for the study of elementary vector analysis which is the second division. It begins with a treatment on the algebra of vectors containing material basic for the examination of the simple N-dimensional space. Subsequently the differential calculus of vectors and integral transformations are taken up, followed by Stoke's theorem, proving for certain parameterized surfaces a modified form of the second of the two fundamental integral transformations.

The third division of the book is devoted to the introduction of tensors and the explanation of extensions and the differential calculus of tensors. Division number four provides some material for practice reading in vector notation and covers classical dynamics based on the notion of absolute space and time, special relativity characterized by a three-dimensional Euclidean space and other concepts, and concluding with a formulation of the most important assumptions of general relativity. To this division is appended a bibliography.

The construction of the book is one of logical progression with careful selection of topics. Within limitations it is thorough and provides a course of study for practical application.

R. H. OPPERMANN.

ANALYTICAL EXPERIMENTAL PHYSICS, by Harvey Brace Lemon and Michael Ference, Jr. 584 pages, plates and diagrams, 23 × 30 cms. Chicago, The University of Chicago Press. 1943. Price $7.00. Second Printing $5.75.

In view of the many textbooks on physics and laboratory manuals which are continually appearing, it seems strange that little mention is made of concentrated study of the subject of laboratory practice in a broad light. For instance, most of the laboratory procedures are in effect standardized, a routine performance without much attention directed to the training received compared to hours expended, and methods for improving this. Also, aside from the diagrams and tabulated results, there is little upon which can be based reflection of actions and functions during the experiment. A review and subsequent rearrangement of these as well as other details, incorporating any new devices, and coordination with an adequate text, will provide a course in physics which has outstanding merit. This is the thought behind the book at hand. Needless to say, it has many unusual features.

The presentation leans toward the narrative type wherever possible. The sequence of topics is mechanics, heat, electricity and magnetism, wave motion, sound and light. There is a mathematical appendix in the back which contains all the formulas needed. The story of each topic is so told that the experiment is woven into it, making it an integral part. The authors use the novel method of enlarged reproductions of strips of motion picture film of many of the experiments in action and under observation. These are photographed demonstration experiments. By running over the successive frames of the motion picture reproductions the student sees what is happening; he sees the measuring instruments as they are in position, making quantitative records. The readings of these instruments on the original films when too small for satisfactory reproduction by the half tone processes are set in type alongside the pictures, together with the necessary mathematical operations required to reveal the law that is dictated by the phenomenon. Insofar as possible, the experiments are set up in such a manner as to provide two methods of approach to the conclusion, and thus independent check of the results is available. Of course not all the work is susceptible to the photographic method and, too, all may not agree on the value in the method that should be weighed carefully by educators.

The text has been for nearly eight years at the University of Chicago in the sophomore sequence courses. It is stated that about twenty different instructors of a great variety of training and talent have been free to criticize, suggest alterations, and discuss results; and rewritings have been made to meet these suggestions.

R. H. OPPERMANN.

PUBLICATIONS RECEIVED.

Basic Physics for Pilots and Flight Crews, by E. J. Knapp, Ph.D. 118 pages, charts and diagrams, 13 × 19 cms. New York, Prentice-Hall, Inc., 1943. Price $1.25.

College Physics, Abridged, Revised Edition, by Henry A. Perkins, Sc.D. 593 pages, diagrams, 15 × 23 cms. New York, Prentice-Hall, Inc., 1943. Price $4.00.

The Rise of the Electrical Industry During the Nineteenth Century, by Malcolm MacLaren. 225 pages, illustrations, 16 × 24 cms. New Jersey, Princeton University Press, 1943. Price $3.75.

Basic Electricity for Communications, by William H. Timble. 603 pages, illustrations and diagrams, 15 × 22 cms. New York, John Wiley and Sons, Inc., 1943. Price $3.50.

The Chemistry of the Aliphatic Orthoesters, by Howard W. Post. 188 pages, tables, 16 × 23 cms. New York, Reinhold Publishing Corporation, 1943. Price $4.00.

Radio Troubleshooter's Handbook, by Alfred A. Ghirardi. 744 pages, illustrations, 22 × 29 cms. New York, Radio & Technical Publishing Co., 1943. Price $5.00.

CURRENT TOPICS.

Termite Research.—Research for the last 30 years—particularly since 1939—has enabled the Department of Agriculture's Research Administration to assist in developing and applying measures to protect buildings in military cantonments and in Federal housing projects against termites—among the worst insects hampering this country's war effort. Suggested improvements in plans for these projects include provision for adequate ventilation and clearance of wood debris beneath buildings. These measures have largely superseded the metal shields formerly used to protect buildings from termite damage. At the request of military authorities, Department entomologists also are seeking measures to prevent termite damage to military buildings and supplies in tropical and subtropical lands. Under way is a study to determine which of the many tropical woods are most resistant to termite attack. As facilities are not available for treating these woods with preservative chemicals in the areas where they are needed for construction, it is most important that the wood to be cut and used locally without treatment should have as much natural durability as possible. Research has shown that the life of most untreated woods used in contact with the soil, such as in temporary buildings and bridges, can be prolonged by poisoning the adjacent soil. Tests are in progress to determine which chemicals do this job best under tropical conditions. Creosote, pentachlorophenol, and some of the arsenical compounds are effective for the purpose in the United States. Department entomologists believe that tents, tarpaulins, clothing, and other materials that must be stored or used where they are subject to damage from termites, especially in the tropics, can be protected by chemical treatments at the time of their manufacture or use. Results of limited tests—the only ones yet made—indicate that some of the chemicals that prevent mildewing and decay of many fabrics may also prevent termite damage.

R. H. O.

Largest Steel Chain Ever Made in Canada Now in Service.—(*Mining and Metallurgy*, Vol. 24, No. 437.) This was made by Sorel Steel Foundries Ltd. for use on a marine railway in a new ship building plant. This plant, situated on a comparatively narrow river, builds 10,000 ton ships which are winched into place on the launching platform of the railroad; the railroad is then slowly

lowered into the water, thus floating the ship's hull. The chain, which was to be used as the restraining medium in lowering the platform with the 10,000 ton hull upon it, was of course an important factor in the plant. The job required $1\frac{1}{4}$ miles of $2\frac{1}{4}$ in. chain, each link weighing 38 lb., and cast into 90 ft. lengths. One of the many difficulties encountered had to do with the proper testing of the chain to ensure that each length would properly meet the drag it would be subjected to when letting the 10,000 ton hull and launching platform down the inclined marine railway. An ingenious solution was devised by Sorel engineers, who had eight lugs welded around the sides of a 180 ton scow. Hawsers were run from each lug to the center of the scow and attached in turn to each individual 90 ft. length of chain, the other end of which was hooked to a shear leg. The shear leg was then operated, lifting against the scow, a total dead weight of 125 tons, and the scow was raised a minimum of 27 in. on the draft line, which exerted a strain on the chain beyond the maximum called for in the specifications. Out of the 8400 links tested, only nine were rejected or less than $\frac{1}{10}$ of one per cent. of the total production, an outstanding record of foundry control under the circumstances.

R. H. O.

Dry Ice Kills Coal Pile Fires.—(*Heating and Ventilating*, Vol. 40, No. 4.) A new and ingenious use for dry ice as an extinguisher of coal fires has been developed recently. An estimated 80,000,000 tons of bituminous coal is now in storage throughout the country, a figure double the usual season's reserve. This likewise doubles the risk of loss through spontaneous combustion, notwithstanding the protective effect of modern methods of storage. The dry ice is applied directly at the seat of the fire, through 15 ft., 3 in., driven pipes fitted with perforated tips. Charges of 50 lbs. of the solid CO_2 are placed in the pipes. Heat liberates the gas to blanket the hot zone and smother the smoldering coal, while the chilling action of the dry ice reduces the local temperature, this effectively eliminating the hot spot. To locate such danger points in the pile a hot spot indicator, consisting of an iron pipe containing a spring loaded signal, held back by a chain with fusible links at one foot intervals has been made available by the same manufacturer. Only the hot test link lets go, permitting the signal to rise, and this occurs only when temperature rises to 150 deg. F. Thus the location and depth of the danger point are advertised 72 hours before combustion can take place, at the normal rate of temperature rise for the average coal composition.

R. H. O.

Two Traveling Tower Derricks Erect Timber Blimp Hangar.—(*Engineering News-Record*, Vol. 130, No. 11.) Steel Erector's tower-mounted derricks are used to raise pre-assembled timber hangar sections for blimp housing at the Lakehurst, N. J., Naval Air Station. The hangars have a span of 246 ft. and a height above the ground of more than 170 ft. The timber arch trusses are set 20 ft. C. to C., 51 of them being used to include a length of 1000 ft. Overall measurements of the hangar are 1058 ft. by 296.5 ft., the added length being taken up by door assemblies at both ends of the structure. Timbers are preassembled on the ground into four sections for each arch truss. Two similar sections are framed into a "brace-bay" 20 ft. wide that forms the unit to be handled. The bottom section of the truss is eight panels long and the top portion is the remaining ten panels to the center line of the structure. The bottom sections of the arches are set in place in braced pairs by the individual derricks. The top quarters are then joined on the ground by the two derricks working together and raised to a connection with the first erected part to form the complete ring. Timber members for the arches are accurately precut to template in mills on the West Coast and are given a pressure-cylinder impregnation with chemicals to fire-proof and preserve them. The fire-proofed wood is required to stand a $\frac{3}{4}$ hour exposure to a standard time-temperature test in which the wood is exposed to gas flames of 1300 deg. at $\frac{1}{4}$ hour, 1550 deg. at $\frac{1}{2}$ hour, and 1658 deg. at $\frac{3}{4}$ hour. The wood will char at these temperatures but will not support combustion. Progress of the work of erection when weather conditions have not been too adverse has been a complete 40 ft. advance in each working day. This requires that a braced-bay of the lower $\frac{1}{4}$ of the arch be set, followed by connection and erection of the two top quarters. Intermediate bracing then is immediately placed to stabilize the section just set. Winds with a 5 minute average velocity of 67 knots (80 m.p.h.) have been successfully withstood.

R. H. O.

Invisible "Raincoat" Waterproofs Many Kinds of Materials.—An invisible "raincoat" which can be formed on cloth, paper and many other materials by exposing them to chemical vapors, thereby making them water-repellent, has been developed in the General Electric Research Laboratory, Dr. William D. Coolidge, G. E. Vice President and Director of Research, has announced recently. Many possible uses of this new method of waterproofing are now being studied. One of the most important so far is the treatment of ceramic insulators for radio equipment used by the armed forces of the United States. Such insulators lose much of their electrical

resistance when exposed to high humidity. This causes formation of a thin film of moisture on their surfaces and allows the currents to leak away. It has been the practice to coat them with wax, but the new chemical treatment is about nine times as effective, and its results are permanent. The process was discovered by Dr. Winton I. Patnode, G. E. research chemist. Various chemicals are used, one class being known as methyl chlor silanes. In a closed cabinet, the articles to be treated are exposed for a few minutes to vapors from such a compound. Then they are taken out and, if necessary, are exposed to ammonia vapor. This is to neutralize corrosive acids which may collect during treatment. Dr. Patnode is not able to explain exactly what happens in the process, but the result is that an extremely thin film, which resists wetting, is formed on the surface. This "raincoat" is so thin that its structure cannot be determined by chemical analysis. It cannot be seen under a high powered microscope. But, whatever its nature, it prevents water from spreading to form a continuous film. If moisture does collect, it is in the form of small isolated drops. In the case of ceramic insulators, these do not allow electricity to pass because they are separated from each other. Another use is a laboratory one. The top of water in laboratory glassware, such as measuring cylinders and hydrometers, is ordinarily curved. Such a curved surface or "meniscus" is prevented if the inside of the apparatus is treated with the waterproofing vapors. Then the water surface is flat and its height may be read more easily.

R. H. O.